D-1

ARF

ARF 4132-6

ARMOUR RESEARCH FOUNDATION OF ILLINOIS INSTITUTE OF TECHNOLOGY

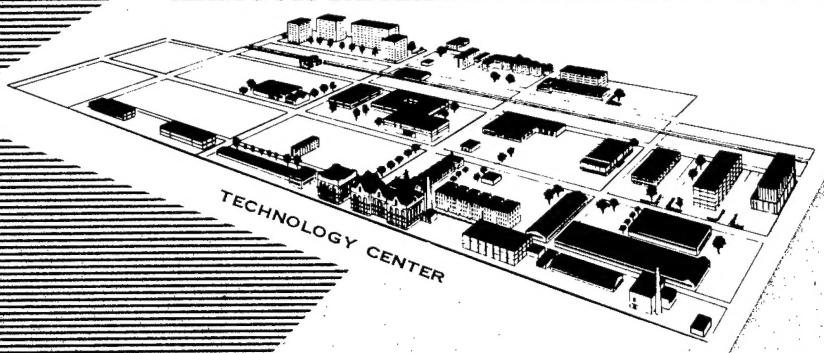

POINT SOURCE EXPLOSION IN A SOLID

T. A. Zaker

AEC Research and Development Report
Contract No. AT(11-1)-528

Index
(1) Ground shock (theory)
(2) Mechanics, Shocks in Solids and Liquids
(3) Weapon Effects, Ground Shock Theory

LEGAL NOTICE

This report was prepared as an account of Government sponsored work. Neither the United States, nor the Commission nor any person acting on behalf of the Commission:

A. Makes any warranty or representation, express or implied, with respect to the accuracy, completeness, or usefulness of the information contained in this report, or that the use of any information, apparatus, method, or process disclosed in this report may not infringe privately owned rights; or

B. Assumes any liabilities with respect to the use of, or for damages resulting from the use of any information, apparatus, method, or process disclosed in this report.

As used above, "person acting on behalf of the Commission" includes any employee or contractor of the Commission to the extent that such employee or contractor prepares, handles or distributes, or provides access to, any information pursuant to his employment or contract with the Commission.

Printed in USA. Price $2.50. Available from the Office of Technical Services, Department of Commerce
Washington 25, D.C.

ARF 4132-6
Reactors-General

ARMOUR RESEARCH FOUNDATION
of
ILLINOIS INSTITUTE OF TECHNOLOGY
Technology Center
Chicago 16, Illinois

POINT SOURCE EXPLOSION IN A SOLID

T. A. Zaker

United States Atomic Energy Commission
Contract No. AT(11-1)-528
ARF No. D132

November 1959

This is a report on a study of the point blast problem in a condensed medium performed by Armour Research Foundation for the United States Atomic Energy Commission under Contract No. AT(11-1)-528, "Studies of Reactor Containment", ARF Project No. D132. The work reported herein was performed between April 1957 and October 1958. Revisions were made in the period March 1959 to November 1959.

Foundation personnel who have contributed materially to this report include: D. C. Anderson, J. T. Cushing, F. B. Porzel, G. J. Tzantzos, A. H. Wiedermann, M. Wolf, and T. A. Zaker. R. W. Floyd of the Foundation's computer center performed the machine programming.

Respectfully submitted,

ARMOUR RESEARCH FOUNDATION OF
ILLINOIS INSTITUTE OF TECHNOLOGY

T. A. Zaker

T. A. Zaker, Project Engineer

T. H. Schiffman

T. H. Schiffman, Assistant Director of
Fluid Dynamics and Systems Research

APPROVED:

F. B. Porzel

F. B. Porzel, Senior Scientific Advisor
Fluid Dynamics and Systems Research

TAZ:mod

ABSTRACT

This report presents an approximate theory of the growth of a point source explosion in an infinite solid or liquid medium in the range of shock pressure below that required to induce a physical change of phase of the material, and above pressures at which the wave propagation can be considered acoustic. The analysis is based on the characterization of the shock state locus for the material by a general form containing three constants related to the compressibility of the material. Both porous and non-porous solids are considered.

Peak shock pressure and arrival time data obtained by machine calculation as functions of shock radius are presented graphically and numerically in dimensionless form for several values of the compressibility constants involved. Methods of deducing values of the constants from compressibility data for particular materials are presented. The results are applicable to estimates of shock attenuation in a variety of blast absorbing or shielding materials.

TABLE OF CONTENTS

TABLE OF CONTENTS (CONT'D)

LIST OF ILLUSTRATIONS

LIST OF TABLES

LIST OF SYMBOLS

Symbol		Definition
P	=	absolute pressure
V	=	specific volume
ρ	=	mass density
t	=	time
R	=	shock front radius
U	=	shock velocity
r	=	radial distance coordinate
u	=	particle velocity
c_o	=	sound speed
q	=	density wave form exponent
W	=	total energy release
Q	=	unavailable energy per unit volume
E_{HV}	=	recoverable energy per unit volume
E_{KV}	=	kinetic energy per unit volume
C, μ, n	=	shock compressibility constants
A, B	=	compressibility constants
p	=	$\frac{P_s}{C}$ = dimensionless absolute shock pressure
v	=	$\frac{V_o}{V_s}$ = shock density ratio
τ	=	$\sqrt{C\ V_o}\ (\frac{4\pi C}{3W})^{1/3} = t_s$ = dimensionless shock arrival time
λ	=	$(\frac{4\pi C}{3W})^{1/3} R$ = dimensionless shock front radius
ψ	=	dimensionless shock front velocity
T	=	absolute temperature

LIST OF SYMBOLS (CONT'D)

Symbol		Definition
γ	=	ratio of specific heats of gas
$c_{a,b}$	=	specific heats of gas and solid
a	=	volume fraction of gas

Subscript

o:	ambient or pre-shock conditions
s:	shock front conditions
1:	starting condition on integration
a:	quantities relating to gas fraction
b:	quantities relating to solid fraction

POINT SOURCE EXPLOSION IN A SOLID

I. INTRODUCTION

Recently interest has arisen in methods of reducing the mechanical or blast effects of a sudden, explosion-like release of energy. This interest has grown as a result of the need for defensive or protective measures against the high energy yield explosive weapons of modern warfare, and the need for the confinement and direction of large quantities of energy in peacetime applications of powerful energy sources. The concept of confinement or containment arises in explosion phenomenology itself, apart from any protective considerations, when a sudden release of energy takes place at a point in a confining medium such as soil or water. The propagation of a strong disturbance in a condensed medium is strongly controlled by the ability of the material to abstract mechanical energy from the disturbance as it progresses through the medium, and to degrade that energy to a non-destructive form through dissipative processes. These characteristics of certain solid materials and liquids can result in the rapid attenuation of the shock pressures due to an explosion in the medium.

There is limited information in existence on the type and magnitude of disturbance which can result from the serious malfunctioning of a nuclear reactor[1]. It is partly because of this element of uncertainty that stringent safety and precautionary measures are generally adopted, particularly in the cases of high-output thermal reactor power generators. Such power facilities will, at least eventually, be necessarily located in heavily populated areas, and this condition denies isolation as the sole safety provision.

[1] Superscript numerals refer to bibliography section.

Thus the concept of the complete containment of an incident within the confines of the facility arises as a prime safety provision.

The concept of explosion confinement has been applied to nuclear reactor safety through the placement of blast absorbing components, referred to as blast shields, surrounding the reactor core, which is considered as the potential origin of a catastrophic disturbance. Such shields possess the ability to reduce explosion pressures by several orders of magnitude and thus protect an enclosing gas-tight containment envelope. One suggested design for a blast shielding device is a sandwich type of construction of alternating rigid and compressible layers. The essential features of this design have been discussed elsewhere[2]; it suffices to note that its shielding characteristics are regarded as derived principally from the blast attenuating properties of the compressible solid material.

In order to place the concepts of blast absorption and blast shielding devices on a firm basis, a knowledge of the growth of explosions in condensed media is necessary. The purpose of this report is to present the results of a theory of explosion growth and shock propagation in a solid or liquid medium, in a form useful for application to reactor safety analyses and blast shield designs.

The present analysis attempts to predict at least the gross features of the mechanical output from a point-source explosion, i.e., the behavior of the flow variables within and on the explosion-engulfed sphere as the disturbance advances through the medium. Certain simplifying assumptions restrict the analysis to the region of strong shocks, where shock pressures are high enough to consider the material as fluid-like in behavior. The analysis rests to a certain extent on over-all energy considerations; no

attempt is made to predict in detail the history of conditions near the point of explosion. Fortunately, the more severe assumptions are applied in regard to behavior near the explosion source and involve only a small fraction of the explosion-engulfed spherical volume during most of the time history of the phenomena of interest. Thus the resulting peak shock pressure decays and arrival times are not strongly affected by these simplifications.

The techniques utilized in the present report have been developed in connection with research on the effects of underwater[3] and underground[4] explosions. Predictions which have been made regarding shock pressure decays and times of arrival using these techniques have met with substantial experimental verification in large-scale tests of nuclear weapons. The results presented here are only those directly of interest to the evaluation of blast absorbing materials.

One effect of the shock process on a particle of material is to make a certain fraction of the energy imparted to the engulfed particle unrecoverable as mechanical work. The analytical method involved here consists of evaluating this "waste heat" and abstracting it from the total available energy as the spherical shock front advances through the material. This permits the writing of a differential relation connecting the material compression to distance from the explosion source and to the explosion yield. The evaluation of the waste heat requires assumptions on the relationship of shock pressure to compression of the particular material considered and on the subsequent expansion experienced by the material. This set of relationships then admits solutions in non-dimensional form for shock pressure and shock arrival time as functions of distance from the explosion source for arbitrary values of parameters related to the compressibility of the condensed medium.

The solutions apply to regions in which the material, although crushed, does not undergo a physical change of phase. An assumption on the effects of the early history of the explosion permits the statement of initial conditions on the problem in the region where the formulation is applicable. No attempt is made to study in detail conditions at very early times, since the materials considered are of interest as blast absorbers reasonably distant from the explosion source. Methods are developed for determining the values of the constants describing the compressibility of the materials which are involved as parameters in the solutions from compressibility data. Thus, the rapid comparison of the effectiveness of a wide variety of specific materials as shock pressure reducers is possible.

Lastly, this report discusses the application of the results of the calculations to real materials. Although these results are for highly idealized physical situations, they provide information on the relative effectiveness of the materials as shock absorbers.

II. DISCUSSION OF THE PROBLEM

The present study concerns itself with the growth of a point source explosion in a solid or liquid medium in the range of shock pressure below that required to induce a change of phase of the material, and above pressures at which the propagation can be considered acoustic. As an initial state for the solution in this range, conditions are deduced from a grossly simplified representation of the behavior of the explosion durings its early history.

Of particular interest here are the readily crushable solids in which efficient acoustic shock transmission does not occur until the shock pressure decays to quite low values. Such materials are worth consideration as

blast absorbers, particularly those which are resistant to ignition at very high shock pressures. These requirements suggest that porous solids, such as foamed ceramic or siliceous materials, may be quite effective as blast shielding materials. Some of the assumptions of compressible fluid dynamics are therefore applicable in the range of interest of the present analysis, where the explosion-generated shock pressures are high enough relative to the strength of the medium to permit consideration of the material as behaving like a fluid. The limitations of the fluid dynamic model are discussed in Appendix A. The objective of design for explosion confinement itself would be to reduce shock pressures of this magnitude in solids to seismic levels, for which a large body of analysis is available.

In the present study, we consider the problem of the sudden introduction of energy at a point in an infinite medium, neglecting the effect of the mass of any reaction products. The spherical symmetry of the resulting wave propagation permits the description of phenomena in terms of radial distance from the explosion source, and time measured from the instant of explosion.

III. PROCEDURES AND ASSUMPTIONS

The usual approach to the problem of a point-source release of energy into a fluid medium employs the differential equations of motion, continuity, and some form of the statement of conservation of energy for the region engulfed by the advancing spherical shock. These equations can, in principle, be simultaneously integrated at least numerically by machine calculation, provided an appropriate equation of state for the material is given. The integration starts from a specified initial state, and is subject to the conditions at the moving boundary defined by the shock front. The shock front conditions are in turn established by the laws of conservation

of mass, momentum, and energy (Hugoniot conditions) across the shock front. There are a number of solutions to the point blast problem in air and water[5,6,7,8] all presuming equation-of-state data of some type for the medium.

A. Flow Variable Wave Forms

In the absence of adequate data for the formulation of a sufficiently general equation of state for the class of materials considered, we proceed directly to the application of the equations of motion and continuity for the engulfed region through an assumption for the distribution of material density at an arbitrary instant during the motion. The assumed density profile contains a time-dependent parameter, the value of which is determined by the shock front conditions through consideration of the conservation of mass over the entire shock-engulfed region.

The particle velocity and pressure profiles consistent with the assumed density distribution are obtained by direct integration of the continuity and motion equations. For the strong shock case in which the peak density varies relatively slowly with time, this process leads to relatively simple variations of particle velocity and pressure with distance from the explosion source.

B. Shock Compression Locus

The wave forms of density, particle velocity, and pressure contain the shock front values of the respective quantities. The relationship of particle velocity to pressure and density at the shock is established by Hugoniot conditions. We characterize the relationship of shock pressure to shock compression or density ratio (the Hugoniot relation) by a general form containing three constants related to the compressibility of the material. The form is sufficiently flexible to describe the properties of

a wide variety of materials under shock. Methods are subsequently given for deducing the values of the constants for specific materials from compressibility data.

C. Energy Partition

An equation is written describing the division of the total energy yield into two parts at any fixed instant during the motion. One part consists of kinetic and hydrodynamic energies available to perform destructive mechanical work on the material during later motion, and distributed over the entire explosion-engulfed sphere at the instant of time under consideration. The second part consists of energy made unavailable to do mechanical work at a later time by non-equilibrium processes, referred to as waste heat, and presumably evidenced as a temperature rise in the material. Now the shock process is considered as setting up conditions under which energy is degraded to waste heat; it remains to evaluate the quantity of energy committed to the unavailable fraction as the shock front advances through the material. This means that the waste heat term in the energy balance equation can be evaluated over the previous history of the shock front.

D. Expansion Process and Energy Dissipation

For the condensed media of interest in the present analysis, it is assumed for purposes of the waste heat calculation that the expansion undergone by shocked particles of material is equivalent to expansion to the pre-shock specific volume along the Hugoniot. The validity of this approximation is discussed in Appendix B. It is shown that, for the condensed materials of present interest, all changes of state are represented by nearly coincident traces in the pressure-specific volume when no change of phase occurs. The assumption on the expansion process permits (1)

calculation of the energy recoverable as mechanical work, and (2) calculation of the waste heat as the difference between the internal energy imparted to the material during shock and the recoverable mechanical energy.

E. Calculation of Pressures and Arrival Times

The energy balance equation is reduced to a differential equation involving only shock compression or density ratio, distance from the explosion source, and explosion yield which, in view of the Hugoniot relation, defines the correspondence between shock pressure and distance. The constants describing the compressibility of the material under shock appear as parameters in the equation. Integration was performed numerically on an IBM 650 digital computer. The results are presented graphically and tabularly in the form of a two-parameter family of pressure-distance curves, the parameters being two of those appearing in the assumed Hugoniot relation. Integration was performed from an arbitrarily selected starting condition, but it is shown that a change in the starting condition corresponds to a simple, one-directional translation of the pressure-distance curves on a logarithmic chart.

The non-dimensional time of arrival of the shock front as a function of distance from the explosion source is easily obtained as the result of integration of the reciprocal of the shock front velocity over the distance traversed by the shock front. This integration was also performed numerically on an IBM 650 digital computer; the results are again a two-parameter family of curves and are obtained for the arbitrarily selected starting condition. It is shown that a change in the starting condition corresponds to equal translation in two directions of the arrival time-distance curves on a logarithmic chart.

IV. CONDITIONS IN THE ENGULFED REGION

In this section conditions at the shock front are summarized. The velocity distribution and pressure profile consistent with an assumed density distribution in space at a fixed instant of time after the instant of explosion are deduced.

A. Shock Front Conditions

When a discontinuity in state variables exists in a continuous medium, the disturbance propagates into the region of lower pressure and density. In particular, if the discontinuity or shock moves into material at rest, application of conservation of mass across the shock front leads to a relation among the shock front velocity U, the particle velocity u_s following the shock front, and the densities ρ_o and ρ_s before and immediately following the shock:

$$\rho_o U = \rho_s (U - u_s). \tag{4.1}$$

The subscripts o and s refer to ambient and shock front conditions, respectively.

Application of conservation of momentum across the front leads to a relation between the absolute pressures P_o and P_s before and immediately following the shock, and the shock and particle velocities:

$$P_s - P_o = \rho_o U u_s . \tag{4.2}$$

Combination of Eqs. (4.1) and (4.2) leads alternatively to

$$\frac{U^2}{V_o^2} = \frac{P_s - P_o}{V_o - V_s} , \tag{4.3}$$

or to

$$u_s^2 = (P_s - P_o)(V_o - V_s) , \tag{4.4}$$

where the specific volume $V = 1/\rho$. The subscript s denotes conditions immediately following shock.

Equations (4.1) through (4.4) hold locally whether or not the shock front is a plane surface and irrespective of the properties of the medium, presuming only the existence of shock conditions.

The total energy input E_{Ts} to a unit mass of material during shock is easily obtained as

$$E_{Ts} = P_s (V_o - V_s) , \tag{4.5}$$

and since the unit mass acquires kinetic energy $E_{Ks} = u_s^2/2$, the internal energy increment per unit mass is obtained through Eqs. (4.4) and (4.5) as the difference between this total energy and the kinetic energy of net translation in the form

$$E_{Is} = \frac{1}{2} (P_s + P_o)(V_o - V_s) \tag{4.6}$$

In further work, we neglect the ambient pressure P_o in comparison to the strong shock pressure P_s. Inspection of Eqs. (4.4), (4.5), and (4.6) shows that the total energy is partitioned equally between internal and kinetic energy in the strong shock case.

Now if one could specify an equation of state connecting internal energy with pressure and specific volume or with other variables related through the laws of thermodynamics to pressure and specific volume, Eq. (4.6) would lead to a Hugoniot relation defining a locus of states in the P-V plane which can be reached by shock from the given ambient conditions. Instead, however, we assume a Hugoniot in the following form:

$$P_s - P_o = \frac{C\left[\left(\frac{V_o}{V_s}\right)^n - 1\right]}{\mu - \frac{V_o}{V_s}} \quad . \tag{4.7}$$

In this expression the constants C, μ, and n are regarded as characteristic of the medium. The form exhibits the properties of (1) decreasing compressibility with increasing density characteristic of a wide variety of materials, and (2) a limiting shock compression or density ratio μ at infinite shock pressures. The incorporation of three parameters related to the material allows a good deal of freedom in empirically describing the behavior of actual materials. In the discussion following, the ambient pressure P_o in Eq. (4.7) is neglected.

Interesting geometric interpretations of the energy partition and the shock and material velocities are afforded by the plot of Eq. (4.7) in Fig. 1:

1. The total shock energy input to a unit mass of material is numerically equal to the area of the rectangle of altitude P_s and base $V_o - V_s$.

2. The chord of the Hugoniot joining the points (P_s, V_s) and $(0, V_o)$ divides the rectangle into two equal triangles, each numerically equal in area to the kinetic and internal energies.

3. The square of the particle velocity is numerically equal to the area of the entire rectangle in view of Eq. (4.4) and the neglection of P_o.

4. Finally, Eq. (4.3) indicates that the square of the shock velocity is proportional to the negative slope of the chord of the Hugoniot.

If P_o is not neglected in comparison with P_s, observations (1) and (4) above still hold when the Hugoniot is constructed through the point (P_o, V_o). In particular, for small shock overpressures $(P_s - P_o)$ the chord of the Hugoniot approaches the tangent to the curve at (P_o, V_o), and the shock velocity approaches the acoustic velocity $c_o = -V_o (dP/dV)^{1/2}_{V=V_o}$, because the Hugoniot coincides locally with the adiabat through (P_o, V_o).

B. Density Profile

Following the discussion of Section III-A, we assume that the density ρ as a function of distance r at any time t after the instant of explosion is given by:

$$\rho = \rho_s \left(\frac{r}{R}\right)^q, \quad 0 \leq r \leq R, \tag{4.8}$$

where R is the radius of the spherical shock front and q is permitted to be a function of time. Neglecting the mass of any reaction products in comparison to the mass of the engulfed medium, we equate the total mass contained in the sphere of radius R before the explosion to that at the instant of time under consideration as follows:

$$\frac{4\pi}{3} \rho_o R^3 = 4\pi \int_o^R \rho r^2 dr. \tag{4.9}$$

Inserting the assumed density distribution into Eq. (4.9) and performing the indicated operation leads to:

$$q = 3 \left(\frac{V_o}{V_s} - 1\right), \tag{4.10}$$

and q is a function of time in view of the as yet unknown variation of V_s with time.

C. Particle Velocity Profile

Now consider the mass $(4\pi/3)\rho_o r_o^3$ enclosed initially by the sphere of radius r_o. After passage of the shock front and as a result of motion of the fluid particles, the same mass is enclosed in a sphere of radius r, where $r(t)$ is the trajectory of the particle initially at r_o (Fig. 2). Thus

$$\frac{4\pi}{3} r_o^3 \rho_o = 4\pi \int_o^r \rho r^2 dr. \tag{4.11}$$

Insertion of the density assumption, Eq. (4.8), and integration gives

$$\frac{\rho_o r_o^3}{3} = \frac{\rho r^3}{q+3}, \tag{4.12}$$

where use is made of Eq. (4.8) again after integration. Recognizing that r_o remains fixed during differentiation following the motion, we form the derivative of Eq. (4.12) with respect to time along a particle trajectory. The symbol D/Dt denotes the operator $\partial/\partial t + u\,\partial/\partial r$:

$$0 = \frac{r^3}{q+3} \frac{D\rho}{Dt} + \rho \left[\frac{3ur^2}{q+3} - \frac{r^3}{(q+3)^2} \frac{d}{dt}(q+3) \right],$$

from which

$$\frac{D\rho}{Dt} = \rho \frac{d \ln (q+3)}{dt} - \frac{3\rho u}{r}, \tag{4.13}$$

where the particle velocity $u = Dr/Dt$.

The equation of continuity for the fluid region engulfed by the explosion is

$$\frac{D\rho}{Dt} + \rho \frac{\partial u}{\partial r} + \frac{2\rho u}{r} = 0. \tag{4.14}$$

Inserting the result of Eq. (4.13) into Eq. (4.14), we obtain after rearranging terms

$$r \frac{\partial}{\partial r} \left(\frac{u}{r}\right) = - \frac{d \ln (q + 3)}{dt} . \qquad (4.15)$$

The right-hand side of Eq. (4.15) is a function of time only and integration can be performed with respect to distance at fixed time as follows:

$$\int_r^R \frac{\partial}{\partial r} \left(\frac{u}{r}\right) dr = - \frac{d \ln (q + 3)}{dt} \int_r^R \frac{dr}{r} ,$$

and since $u = u_s$ at $r = R$,

$$u = u_s \frac{r}{R} \left(1 - \alpha \ln \frac{r}{R}\right) , \qquad (4.16)$$

in which

$$\alpha (t) = \frac{R}{u_s} \frac{d \ln (q + 3)}{dt} = \frac{d \ln (\rho_s - \rho_o)}{d \ln R} ,$$

where dR/dt is the shock velocity U, and use has been made of Eqs. (4.1) and (4.10). Now the overdensity $\rho_s - \rho_o$ should be a slowly varying function of t (and hence R) in the strong shock region; we neglect $\alpha \ln r/R$ in comparison to unity in Eq. (4.16) to obtain approximately

$$u = u_s \frac{r}{R} , \quad 0 \leq r \leq R, \qquad (4.17)$$

and the velocity profile in the engulfed region is nearly linear.

D. Pressure Profile

The equation for radial motion of an ideal fluid in the absence of body forces is

$$\frac{\partial P}{\partial r} + \rho \frac{Du}{Dt} = 0, \qquad (4.18)$$

where $P(r, t)$ is the absolute pressure in the engulfed region $0 \le r \le R$. The derivative of Eq. (4.17) following the motion is

$$\frac{Du}{Dt} = \left[\frac{d\,u_s}{dt} - \frac{u_s U}{R} + \frac{u_s^2}{R}\right] \frac{r}{R} , \tag{4.19}$$

where use is made of Eq. (4.17) again after differentiation, and dR/dt is the shock velocity U.

Upon insertion of the density assumption and Eq. (4.19) into Eq. (4.18), integration can be performed with respect to distance at fixed time as follows:

$$\int_0^r \frac{\partial P}{\partial r}\, dr = \rho_s \left[\frac{u_s U}{R} - \frac{du_s}{dt} - \frac{u_s^2}{R}\right] \int_0^r \left(\frac{r}{R}\right)^{q+1} dr,$$

since the quantity in brackets is a function of time only. The result of integration is

$$P(r,t) - P(0,t) = \rho_s \left[\frac{u_s U}{R} - \frac{du_s}{dt} - \frac{u_s^2}{R}\right] \frac{R}{q+2} \left(\frac{r}{R}\right)^{q+2} . \tag{4.20}$$

Evaluating Eq. (4.20) at $r = R$ and noting that $P(R,t) = P_s(t)$, we obtain

$$P_s(t) - P(0,t) = \rho_s \left[\frac{u_s U}{R} - \frac{du_s}{dt} - \frac{u_s^2}{R}\right] \frac{R}{q+2} . \tag{4.21}$$

Dividing Eq. (4.20) by Eq. (4.21) results in

$$\frac{P(r,t) - P(0,t)}{P_s(t) - P(0,t)} = \left(\frac{r}{R}\right)^{q+2} . \tag{4.22}$$

From symmetry of the spherical explosion, the fluid at the origin must be stationary. In view of the assumption for density, Eq. (4.8), we assume $P(0,t) = 0$ and obtain from Eq. (4.22) the approximate pressure profile

$$P = P_s \left(\frac{r}{R}\right)^{q+2} , \quad 0 \le r \le R . \tag{4.23}$$

V. ENERGY BALANCE

We note a further geometric interpretation of the explosion energy partition in Fig. 1. The chord of the Hugoniot divides the rectangle representing the total shock energy input to a unit mass of material into two equal triangles, the upper one of which can be considered as representing the kinetic energy per unit mass at the shock front, $u_s^2/2$, in accordance with Eq. (4.4). The lower triangle then represents the internal energy increment. If, following the discussion of Section III-D, we consider the expansion of the shocked unit mass as being equivalent to expansion along the Hugoniot to pre-shock conditions, the recoverable fraction of the internal energy increment is given by the area under the Hugoniot in Fig. 1. Then the lens-shaped area between the Hugoniot and its chord may be regarded as waste heat, or energy per unit mass made unrecoverable as mechanical work as a result of the shock process.

A. Unavailable Energy

When an amount of energy W is released into the medium at a point, the division of energy into waste heat and kinetic and available mechanical (or hydrodynamic) energies when the spherical shock front has radius R is described by the equation

$$W - 4\pi \int_0^R Q R^2 \, dR = \frac{4\pi R^3}{3} (\overline{E}_{HV} + \overline{E}_{KV}). \qquad (5.1)$$

In this equation $\overline{E}_{HV}$ and $\overline{E}_{KV}$ represent average hydrodynamic and kinetic energies per unit volume, respectively, the averages being taken over the entire shock-engulfed volume. The waste heat per unit volume is denoted by Q. Following the discussion of Section III-C, the total

unavailable energy is calculated as an integral over the previous history of the shock front, since that energy is considered as commited to the unrecoverable state upon passage of the shock through the material. We note that after sufficient time all of the explosive energy must appear in the form of thermal energy as in a calorimeter experiment, so that

$$W = 4\pi \int_0^\infty Q R^2 \, dR. \qquad (5.2)$$

The quantity Q is evaluated as the lens-shaped area in Fig. 1 multiplied by the ambient density ρ_o, because a spherical shock wave of radius R must advance a distance numerically equal to $V_o/4\pi R^2$ in order to engulf an additional unit mass of material. Therefore

$$Q = \frac{1}{2} P_s \left(1 - \frac{V_s}{V_o}\right) - \frac{1}{V_o} \int_{V_s}^{V_o} P dV. \qquad (5.3)$$

B. Kinetic Energy Profile

The kinetic energy of radial motion per unit volume of the engulfed fluid, denoted by E_{KV}, can be written using the density and velocity distributions, Eqs. (4.8) and (4.17), as

$$E_{KV} = \frac{1}{2} \rho u^2 = \frac{1}{2} \rho_s u_s^2 \left(\frac{r}{R}\right)^{q+2} = E_{KVs} \left(\frac{r}{R}\right)^{q+2}, \qquad (5.4)$$

where E_{KVs} denotes the kinetic energy per unit volume at the shock front. The average kinetic energy density $\overline{E}_{KV}$ appearing in Eq. (5.1) is calculated from

$$\frac{4\pi R^3}{3} \overline{E}_{KV} = 4\pi E_{KVs} \int_0^R \left(\frac{r}{R}\right)^{q+2} r^2 \, dr,$$

and the result is

$$\overline{E}_{KV} = \frac{3E_{KVs}}{q+5} \,. \tag{5.5}$$

C. Hydrodynamic Energy Profile

The recoverable mechanical (or hydrodynamic) energy contained in a unit mass of material immediately following shock is, as shown in Appendix B,

$$E_{Hs} = \int_{V_s}^{V_o} PdV, \tag{5.6}$$

where the integral is understood to be taken along the Hugoniot. Then the hydrodynamic energy per unit volume at the shock front is given by

$$E_{HVs} = \rho_s \, E_{Hs} \,. \tag{5.7}$$

Assuming the expansion to take place along the Hugoniot, one could calculate the total recoverable energy in the engulfed volume from

$$\frac{4\pi R^3}{3} \overline{E}_{HV} = 4\pi \int_0^R \rho \left[\int_{V(r)}^{V_o} PdV \right] r^2 \, dr, \tag{5.8}$$

where $\overline{E}_{HV}$ is the average hydrodynamic energy density appearing in the energy balance, Eq. (5.1).

For computational purposes, it is desirable to express $\overline{E}_{HV}$ as the corresponding energy density at the shock front, E_{HVs}, multiplied by a form factor. We observe that $\overline{E}_{KV}$ is already given by Eq. (5.5) in such a form, but that this will not necessarily result for $\overline{E}_{HV}$ if the operations of Eq. (5.8) are carried out after insertion of the assumed Hugoniot, Eq. (4.7) and the density profile, Eq. (4.8), into the first integrand.

If the area under the Hugoniot in Fig. 1 is considered as a function of P_s and plotted on logarithmic coordinates for several values of the parameters μ and n, one observes that the relationship is quite closely approximated by

$$E_{Hs} = J P_s^j , \tag{5.9}$$

where j is constant or at most a slowly varying function of P_s (and hence of V_s). Then the coefficient J is correspondingly either constant or a slowly varying function of P_s.

Combining Eq. (5.7) with Eq. (5.9) results in

$$E_{HVs} = J P_s^j \rho_s . \tag{5.10}$$

Taking logarithms, one has

$$\ln E_{HVs} = j \ln P_s + \ln J + \ln \rho_s .$$

Differentiation yields

$$\frac{d \ln E_{HVs}}{d \ln P_s} = j + \ln P_s \frac{d j}{d \ln P_s} + \frac{d \ln J}{d \ln P_s} + \frac{d \ln \rho_s}{d \ln P_s} . \tag{5.11}$$

Because j and J are observed to be at most slowly varying functions of P_s and because ρ_s is also slowly varying with respect to P_s in the present problem, we have approximately

$$j = \frac{d \ln E_{HVs}}{d \ln P_s} . \tag{5.12}$$

Now it is assumed that throughout the engulfed region the hydrodynamic energy per unit volume is related to the pressure in the same manner as Eq. (5.10) for the shock front values. That is,

$$E_{HV} = J P^j \rho , \tag{5.13}$$

and j is calculated from Eq. (5.12). Thus, using the density and pressure profiles, Eqs. (4.8) and (4.23),

$$E_{HV} = J\, P_s^{\,j}\, \rho_s \left(\frac{r}{R}\right)^{j(q+2)+q} = E_{HVs} \left(\frac{r}{R}\right)^{j(q+2)+q} \qquad (5.14)$$

The average hydrodynamic energy density $\overline{E}_{HV}$ appearing in the energy balance, Eq. (5.1), is calculated from

$$\frac{4\pi R^3}{3}\, \overline{E}_{HV} = 4\pi\, E_{HVs} \int_0^R \left(\frac{r}{R}\right)^{j(q+2)+q} r^2\, dr,$$

and the result is

$$\overline{E}_{HV} = \frac{3E_{HVs}}{(j+1)(q+2)+1}, \qquad (5.15)$$

where E_{HVs} is to be obtained from the definitions of Eqs. (5.6) and (5.7).

D. Peak Pressure-Distance Relation

We momentarily regard all variable quantities appearing in Eq. (5.1) as functions of the single variable R (as they must be for any preassigned energy release W), and differentiate to obtain, after removing the common factor $4\pi R^2$,

$$-Q = \overline{E}_{HV} + \overline{E}_{KV} + \frac{R}{3} \frac{d}{dR} \left(\overline{E}_{HV} + \overline{E}_{KV}\right) .$$

Now adding and subtracting $(R/3)\, dQ/dR$ from the right-hand side and rearranging yields the differential form

$$3\, \frac{dR}{R} = \frac{-d(\overline{E}_{HV} + \overline{E}_{KV} + Q)}{(\overline{E}_{HV} + \overline{E}_{KV} + Q)} + \frac{dQ}{\overline{E}_{HV} + \overline{E}_{KV} + Q} . \qquad (5.16)$$

A partial integration can now be performed from a prespecified starting condition $R = R_1$ to an arbitrary upper limit. This results in

$$\ln \left(\frac{R}{R_1}\right)^3 = - \ln \frac{(\overline{E}_{HV} + \overline{E}_{KV} + Q)}{(\overline{E}_{HV} + \overline{E}_{KV} + Q)_1} + \int_{Q_1}^{Q} \frac{dQ}{\overline{E}_{HV} + \overline{E}_{KV} + Q}, \quad (5.17)$$

where the subscript 1 has been used to denote conditions when $R = R_1$.

All quantities on the right-hand side of Eq. (5.17) can be calculated in terms of V_s through Eqs. (4.4), (4.7), (4.10), (5.3), (5.5), (5.6), (5.12), and (5.15). We also write $dQ = [dQ(V)/dV]dV$, so that Eq. (5.17) can be rewritten

$$\left(\frac{R}{R_1}\right)^3 = \frac{(\overline{E}_{HV} + \overline{E}_{KV} + Q)_1}{(\overline{E}_{HV} + \overline{E}_{KV} + Q)} \exp \left[\int_{V_{s1}}^{V_s} \frac{(dQ/dV)dV}{\overline{E}_{HV} + \overline{E}_{KV} + Q} \right]. \quad (5.18)$$

Noting from Eq. (5.12) that

$$j = \frac{P_s}{E_{HVs}} \frac{d E_{HVs}}{d V_s} \frac{d V_s}{d P_s} = - \frac{P_s}{V_s} \frac{d V_s}{d P_s} \left[1 + \frac{P_s V_s}{\int_{V_s}^{V_o} PdV} \right],$$

we list the functions appearing on the right-hand side of Eq. (5.18) as follows:

$$\overline{E}_{HV} = \frac{\frac{3}{V_s} \int_{V_s}^{V_o} PdV}{\left[1 - \frac{P_s}{V_s} \frac{d V_s}{d P_s} \left(1 + \frac{P_s V_s}{\int_{V_s}^{V_o} PdV} \right) \right] \left(3 \frac{V_o}{V_s} - 1 \right) + 1}, \quad (5.19)$$

$$\overline{E}_{KV} = \frac{\frac{3P_s}{2} \left(\frac{V_o}{V_s} - 1 \right)}{3 \frac{V_o}{V_s} + 2}, \quad (5.20)$$

$$Q = \frac{P_s V_s}{V_o}\left[\frac{1}{2}\left(\frac{V_o}{V_s} - 1\right) - \frac{1}{P_s V_s}\int_{V_s}^{V_o} P\,dV\right], \qquad (5.21)$$

$$\frac{dQ(V)}{dV} = \frac{P}{2V_o}\left[\frac{V}{P}\frac{dP}{dV}\left(\frac{V_o}{V} - 1\right) + 1\right], \qquad (5.22)$$

where P_s is given by the assumed Hugoniot, Eq. (4.7), and

$$\frac{V_s}{P_s}\frac{dP_s}{dV_s} = -\frac{n\left(\frac{V_o}{V_s}\right)^n}{\left(\frac{V_o}{V_s}\right)^n - 1} - \frac{\frac{V_o}{V_s}}{\mu - \frac{V_o}{V_s}}, \qquad (5.23)$$

$$\frac{1}{P_s V_s}\int_{V_s}^{V_o} P\,dV = \frac{\mu - \frac{V_o}{V_s}}{V_s\left[\left(\frac{V_o}{V_s}\right)^n - 1\right]}\int_{V_s}^{V_o}\frac{\left[\left(\frac{V_o}{V}\right)^n - 1\right]}{\mu - \frac{V_o}{V}}\,dV. \qquad (5.24)$$

It will be noted that the integration indicated on the right-hand side of Eq. (5.24) can be performed analytically for integral values of n. Functions of V, which is now regarded as a variable of integration, appear in the integrand of Eq. (5.18), and are obtained by replacing V_s by V in the formulas of Eqs. (5.19) to (5.21).

E. Initial Conditions

To obtain starting conditions (denoted by the subscript 1) for the evaluation of Eq. (5.18), we consider the basic relation, Eq. (5.1), with the following simplified representation of the behavior at early times: Take R_1 such that the waste heat $Q_1 V_o$ per unit mass at this point (i.e., the energy per unit mass converted to thermal energy) is just sufficient to induce a change of phase when the material is decompressed to the pre-shock pressure.

For $R > R_1$, therefore, the material undergoes no change of phase and Eq. (5.18) is applicable. Now in $0 \leq R \leq R_1$ assume conservatively that the waste heat $Q V_o$ per unit mass is no higher than its value at $R = R_1$. With Q constant at the value Q_1 in $0 \leq R \leq R_1$, the basic relation, Eq. (5.1), can be integrated to yield

$$\frac{4\pi R_1^3}{3} (\overline{E}_{HV} + \overline{E}_{KV} + Q)_1 = W, \tag{5.25}$$

which gives a relation between the energy yield W and quantities with subscript 1 in Eq. (5.18). This is equivalent to replacing the point release of energy by a sphere of uniform temperature and radius R_1 containing the same energy. For condensed matter (so-called "water-like" substances) it is shown in Appendix B that $Q V_o = c (T - T_o)$, where c is the specific heat of the material and T is the absolute temperature. To obtain starting conditions for an explosion in water, therefore, one would find Q_1 from $Q_1 = \rho_o c (T_1 - T_o)$, where T_1 is the boiling temperature of water at normal pressure; from the Hugoniot curve, one would then find the pressure and specific volume at which the lens-shaped area is equal to the value of $Q_1 V_o$ so obtained.

Inserting Eq. (5.25) into Eq. (5.18) results in

$$\frac{4\pi R^3}{3W} = \frac{1}{\overline{E}_{HV} + \overline{E}_{KV} + Q} \exp\left[\int_{V_{s1}}^{V_s} \frac{(dQ/dV)\, dV}{\overline{E}_{HV} + \overline{E}_{KV} + Q} \right], \tag{5.26}$$

which can now be integrated numerically from the starting value of the specific volume V_{s1} to a series of values of V_s to yield a relationship between shock radius and specific volume for a particular material. In view of the

assumed Hugoniot, Eq. (4.7), this implies a relationship between radius and shock pressure which represents the pressure-distance decay.

F. Shock Arrival Time

When numerical results are obtained for the pressure- and volume-distance relationships, the time of arrival t_s of the shock as a function of shock radius R can be obtained by numerical integration of

$$t_s = \int_0^R \frac{dR}{U} \quad , \tag{5.27}$$

where U is obtained from Eq. (4.3). The shock velocity U will be quite large at $R = R_1$, so that its reciprocal can be considered as essentially zero at $R = 0$ and varying linearly in $0 \leq R \leq R_1$ for purposes of the calculation. This assumption cannot seriously affect the resulting arrival times, and is implicit in a numerical integration utilizing trapezoidal approximations.

VI. SOLUTIONS FOR PEAK PRESSURE AND ARRIVAL TIME

The operations indicated in the equations for shock pressure and arrival time developed in Section V represent for any set of values of C, μ, n, and V_{s1} corresponding to a particular material, and for a particular energy release W, a good deal of routine numerical or semigraphical computation. These equations, however, are readily adapted for machine calculation.

A. Non-Dimensional Forms

We introduce the non-dimensional notation

$$\left.\begin{aligned} p &= \frac{P_s}{C} \quad , \\ v &= \frac{V_o}{V_s} \quad , \end{aligned}\right\} \tag{6.1}$$

$$\left.\begin{aligned} \lambda &= \left(\frac{4\pi C}{3W}\right)^{1/3} R, \\ h &= \frac{\overline{E}_{HV}}{P_s}, \\ k &= \frac{\overline{E}_{KV}}{P_s}, \\ w &= \frac{Q}{P_s}, \\ x &= \frac{V_o}{P}\,\frac{dQ}{dV}. \end{aligned}\right\} \qquad (6.1)$$

Then Eq. (5.26) is written

$$\lambda^3 = \frac{1}{p(h + k + w)} \exp\left[- \int_{v}^{v_1} \frac{x}{v^2(h + k + w)}\, dv \right]. \qquad (6.2)$$

We also define

$$\left.\begin{aligned} y &= - \frac{V_s}{P_s}\,\frac{d P_s}{d V_s}, \\ z &= \frac{1}{P_s V_s} \int_{V_s}^{V_o} P dV, \end{aligned}\right\} \qquad (6.3)$$

so that

$$\left.\begin{aligned} h &= \frac{3z}{\left[1 + \frac{1}{y}\left(1 + \frac{1}{z}\right)\right](3v - 1) + 1}, \\ k &= \frac{\frac{3}{2}(v - 1)}{3v + 2}, \end{aligned}\right\} \qquad (6.4)$$

$$w = \frac{1}{v}\left[\frac{v-1}{2} - z\right], \qquad x = \frac{1}{2}\left[y(v-1) - 1\right]. \tag{6.4}$$

The Hugoniot relation, Eq. (4.7), becomes

$$p = \frac{v^n - 1}{\mu - v}, \tag{6.5}$$

from which

$$y = \frac{n v^n}{v^n - 1} + \frac{v}{\mu - v}. \tag{6.6}$$

After Eq. (5.24) is put in non-dimensional form, the indicated integration can be performed by standard methods to yield, for integral values of n,

$$z = \frac{(\mu-v)v}{\mu^2(v-1)}\left[(\mu-1)\ln\frac{(\mu-1)v}{\mu-v} - \mu\left(1-\frac{1}{v}\right)\right] \quad (n=1),$$

$$z = \frac{(\mu-v)v}{\mu^2(v^2-1)}\left[(\mu^2-1)\ln\frac{\mu-1}{\mu-v} - \ln v - \mu\left(1-\frac{1}{v}\right)\right] \quad (n=2), \tag{6.7}$$

$$z = \frac{(\mu-v)v}{\mu^2(v^n-1)}\left[(\mu^n-1)\ln\frac{\mu-1}{\mu-v} - \ln v - \mu\left(1-\frac{1}{v}\right) - \mu^n\sum_{i=1}^{n-2}\frac{1}{i\mu^i}(v^i-1)\right] \quad (n\geq 3).$$

These results make possible the numerical evaluation of Eq. (6.2) by machine calculation for selected values of μ and the integer n, once the upper limit $v_1 (= V_o/V_{s1})$ of the integral in Eq. (6.2) is specified. The results, in conjunction with the numerical evaluation of Eq. (6.5) for the same values of μ and n, constitute a two-parameter family of dimensionless pressure-distance data.

We now define the non-dimensional time of shock arrival

$$\tau = \sqrt{C\, V_o}\ \left(\frac{4\pi C}{3W}\right)^{1/3} t_s . \tag{6.8}$$

Then the arrival time definition, Eq. (5.27), can be written in the following dimensionless form using Eq. (4.3) and the non-dimensional notation of Eqs. (6.1):

$$\tau = \int_o^{\lambda} \sqrt{\frac{v - 1}{pv}}\, d\lambda . \tag{6.9}$$

The early time history $(0 \leq R \leq R_1)$ of the growth of the explosion is accounted for according to the assumption discussed in Section V-F. That is, $1/U$ and its non-dimensional equivalent $\sqrt{\frac{v - 1}{pv}}$ are taken as zero at $R = 0$ and varying linearly in $0 \leq R \leq R_1$. The numerical integration of Eq. (6.9) using the dimensionless pressure decay data obtained by evaluation of Eq. (6.2) is now straightforward, and can easily be performed by machine calculation.

B. Numerical Integration

Programs were written for the numerical evaluation of the specific volume-distance relation, Eq. (6.2), and the non-dimensional arrival time, Eq. (6.9), on an IBM 650 digital computer. As an initial condition for the integration of Eq. (6.2) the upper limit $v_1 = 7\mu/8$ was chosen. The evaluation was performed for the values $\mu = 4, 5, 6, 7,$ and 8, and for integral values of n from one to ten. This yielded a two-parameter family of 50 data curves each for pressure-distance decay and arrival time.

The upper limit $v_1 = 7\mu/8$ corresponds to a starting specific volume $V_{s1} = 8V_o/7\mu$, and was selected as a value sufficiently high so that all information desired in any application of the results is likely to be associated

with values of v less than v_1. Properties of the results discussed in a later section make this rather arbitrary selection unimportant, and the results turn out to be applicable with simple modification to any other starting condition.

The values of μ and n for which the calculations were performed were selected from experience with real materials as a set covering a wide range of possible values. The selection of μ and n for any real material of interest is discussed in Section VII of this report. In applications, pressure-distance and arrival time data for any specified values of μ and n lying within the range covered can be obtained by straightforward interpolation between the calculated curves. The parameter C is contained in the non-dimensional variables and does not appear explicitly in the calculations.

1. Pressure-Distance Solutions

The program for evaluation by machine calculation of the specific volume-distance relationship, Eq. (6.2), and the associated intermediate functions of v, was written in conventional computer language. The density ratio v was regarded as the independent variable for purposes of the stepwise calculation, a uniform increment of 0.1 in v being used for all cases.

Standard sub-routines were used for the evaluation of logarithms appearing in the expressions for z, Eqs. (6.7). The numerical integration of the exponent in Eq. (6.2) was performed using Simpson's rule to approximate the integrand over the increments of v. The integration proceeded downward from $v = 7\mu/8$, the terminal point being in the range $1.025 \leq v \leq 1.1$.

For each value of v, the quantities p, λ, ph, pk, and pw were printed out. The latter three are seen from their definitions in Eqs. (6.1)

to be the non-dimensional hydrodynamic, kinetic, and unavailable energies per unit volume. In addition, the values of the integrand, the integral, and the cube root of the coefficient of the exponential in Eq. (6. 2) were also printed out on computer data sheets.

2. Arrival Time Solutions

The machine program for calculation of the non-dimensional time of shock arrival by Eq. (6. 9) was also written in conventional language. The numerical integration was performed using a trapezoidal rule to approximate the integrand over the increments of λ. These increments were not uniform, but were determined by the uniform increment in v of 0. 1 and taken from the results of the preceding calculations.

In accordance with the discussion of Section V-F, the integrand was assumed to be zero for $\lambda = 0$, and the integration proceeded upward from $\lambda = 0$. Implicit in the integration by a trapezoidal rule is the linear approximation for the integrand in $0 \leq \lambda \leq \lambda_1$, where $\lambda = \lambda_1$ corresponds to $v = v_1$.

For each value of λ, the values of τ and the integrand were printed out on computer data sheets.

C. Graphical and Numerical Results

The shock pressure and arrival time data derived numerically by the procedures described earlier are summarized in Tables 1 through 20.

We define λ_e as the cube root of the coefficient of the integral in Eq. (6. 2):

$$\lambda_e = \left[p(h + k + w)\right]^{-1/3} \qquad (6.10)$$

This quantity is referred to as the "envelope radius". It is evident from inspection of Eq. (6. 2) that if an initial condition v other than v_1 is

assumed, the applicable pressure-distance data for some particular values of μ and n would begin at $\lambda = \lambda_e$ for those values of μ and n. Hence λ_e regarded as a function of v for given values of μ and n represents a locus of initial conditions on the pressure-distance data. The values of λ_e are included in Tables 1 through 20. The application of this information to account for the effect of an initial condition differing from that used in the machine calculations is discussed in the following section.

The non-dimensional shock pressure p is plotted in logarithmic coordinates as a function of the non-dimensional shock front radius λ for selected values of μ and n in Figs. 3 through 7. The values of λ_e are also plotted as the dash curves in these figures, and these curves of λ_e are referred to as "envelope" curves because each represents a locus of initial pressure-distance conditions.

The non-dimensional arrival time τ is plotted in logarithmic coordinates as a function of λ for selected values of μ and n in Figs. 8 through 12.

D. Properties of the Solutions

The solutions for shock pressure and arrival time as functions of distance from the explosion source have interesting properties with regard to the effect of the selection of initial conditions. Close in to the explosion source, the pressure decays are quite rapid with distance, these rates of decay decreasing rapidly beyond the region of effective shock absorption.

1. Variation of Initial Conditions

An arbitrary selection of the initial condition $v_1 = 7\mu/8$ has been made to permit solution in non-dimensional form of the equations governing shock pressure decay and arrival time. This corresponds to a starting

value of the specific volume which is in general not realized in an application to an actual situation. The effect of this difference is, however, easily accounted for.

Consider a material for which the starting value of the specific volume corresponds to a value of v other than v_1. Denote this value by v_2. The actual non-dimensional distance λ_a would be given in terms of v by Eq. (6.2) with the upper limit of integration v_2:

$$\lambda_a^3 = \frac{1}{p(h + k + w)} \exp\left[- \int_v^{v_2} \frac{x}{v^2(h + k + w)} \, dv \right]. \qquad (6.11)$$

We may compare the values λ and λ_a given by Eqs. (6.2) and (6.11), respectively, at the same dimensionless pressure p. Since p and v are uniquely related by Eq. (6.5) for fixed values of μ and n, this amounts to comparison at the same value of shock compression or density ratio v. The envelope radius $\lambda_e = \left[p(h + k + w)\right]^{-1/3}$ is thus the same in both cases. Dividing one equation by the other leads to

$$\lambda_a^3 = \lambda^3 \exp\left[\int_{v_2}^{v_1} \frac{x}{v^2(h + k + w)} \, dv \right]. \qquad (6.12)$$

The value of the exponential factor in this equation is a function of the limits of integration v_1 and v_2 only, and is thus fixed as far as the present comparison is concerned.

Taking the logarithm of Eq. (6.12), we obtain

$$\ln \lambda_a = \ln \lambda + \frac{1}{3} \int_{v_2}^{v_1} \frac{x}{v^2(h + k + w)} \, dv.$$

In logarithmic coordinates then, the effect of an initial condition differing from the value of v_1 used in the present calculations is represented by translation of the pressure-distance curve in the direction of the λ-axis. Each envelope curve represents a locus of initial conditions for given values of μ and n, and so the distance of translation is equal to the horizontal distance between the pressure-distance curve and its envelope at $p = p_2$ corresponding to $v = v_2$. The translation is to the right in Figs. 3 through 7 if $v_2 < v_1$, and the translated curve is meaningful only for $p \leq p_2$. The value $v_1 = 7\mu/8$ has been selected as a value high enough so that $v_2 < v_1$ in most cases of practical interest. In the event $v_2 > v_1$ for some application, both the curve and its envelope may be extrapolated in the direction of increasing pressure, and a translation to the left must then be performed.

The operation of translation is shown schematically in Fig. 13a. In general, the values of μ and n for any application will differ from the particular values for which the present calculations were performed. Strictly speaking, the necessary interpolations for both the curve and its envelope should be accomplished before the translation, although the order of operations makes little or no difference.

The effect of an initial condition v_2 differing from the value v_1 used in the present calculations is represented also by a translation of the arrival time curve. The actual non-dimensional time of shock arrival τ_a would be given by Eq. (6.9) with the integration following the shock front in the actual case:

$$\tau_a = \int_0^{\lambda_a} \sqrt{\frac{v-1}{pv}}\, d\lambda_a \,. \qquad (6.13)$$

A simplifying assumption on the early history of the explosion similar to that discussed in Section V-F is implied. Now define K such that

$$3K = \int_{v_2}^{v_1} \frac{x}{v^2(h+k+w)}\, dv. \qquad (6.14)$$

Then the pressure-distance curve on logarithmic coordinates is translated a distance K in the direction of the λ-axis. Thus $\lambda_a = \lambda\, e^K$. Recognizing that the values of p and v, and hence of the integrand of Eq. (6.13), remain unchanged during such a translation of the pressure-distance curve, we may write

$$\tau_a = \int_0^{\lambda e^K} \frac{d(\lambda e^K)}{\psi(\lambda)}, \qquad (6.15)$$

where the non-dimensional shock velocity ψ is given by

$$\psi = \frac{U}{\sqrt{C\, V_o}} = \sqrt{\frac{pv}{v-1}}. \qquad (6.16)$$

Changing the variable of integration to λ, we obtain from Eq. (6.15)

$$\tau_a = e^K \int_0^{\lambda} \frac{d\lambda}{\psi(\lambda)} = \tau e^K. \qquad (6.17)$$

Taking the logarithm of Eq. (6.17) results in

$$\ln \tau_a = \ln \tau + K,$$

which indicates that, at the same dimensionless pressure p, the logarithms of the actual and calculated arrival times differ by the constant K. On a logarithmic arrival time chart (Figs. 8 through 12), a point representing a given non-dimensional pressure p is also translated a distance K along

the non-dimensional distance scale. In logarithmic coordinates then, a time-of-arrival curve is translated a distance K in each direction, the translation being to the right and upward in Figs. 8 through 12 if $v_2 < v_1$; if $v_2 > v_1$, the translation is to the left and downward. The translated curve is meaningful only for $p \leq p_2$.

A family of envelopes to the time-of-arrival curves could be constructed with the non-dimensional envelope arrival time τ_e being given by $\tau_e = \lambda_e / 2\psi(\lambda_e)$ consistent with the assumption that $1/U$ varies linearly in $0 \leq R \leq R_1$. The information would however be redundant, since for any case of interest the translation distance K is already determined from translation of the pressure-distance curve.

The operation of translation of a time-of-arrival curve is shown schematically in Fig. 13b. Once again, any necessary interpolations on μ and n should be accomplished before the translation.

2. General Properties

From inspection of the pressure-distance curves, Figs. 3 through 7, it is evident that the pressure decays during the early portion of the explosion history are extremely rapid. The pressure in this range varies as $1/R^6$ or $1/R^7$. The corresponding arrival times in the same range (Figs. 8 through 12) appear to vary approximately as R^2.

Near $P/C = 0.1$, the rate of pressure decay slows quite rapidly, as is evidenced by the relatively rapid change in slope of the pressure-distance curves near this dimensionless pressure. At lower pressures, the shock energy transmission becomes progressively more efficient and the pressures appear to vary at rates approaching $1/R$. This is in agreement with acoustic theories of wave transmission from a point source.

An acoustic wave transmission solution should in fact be an asymptotic approximation to the present strong shock solution for large R. The present non-dimensional formulation, however, becomes highly indeterminate at $v = 1.0$, and numerical solution even by machine calculation becomes quite difficult for values of v close to 1.0.

VII. PROPERTIES OF MATERIALS

The present approximate theory of explosion growth in condensed media has been developed in such a way as to avoid the formulation of a general equation of state for these materials, and replace it by the assumption of a generalized Hugoniot, Eq. (4.7). This assumed form contains three arbitrary parameters, C, μ, and n, the determination of which, for any particular material of interest, permits application of the present generalized pressure and arrival time data.

The assumed form for the Hugoniot is such that $dP/dV < 0$ and $d^2P/dV^2 > 0$ for all values of $P \geq 0$. The corresponding model of the material is thus a solid or a liquid in which an increase in hydrostatic pressure results in a decrease in specific volume, and whose compressibility under shock decreases with increasing shock pressure. Nearly all real materials exhibit this kind of behavior at sufficiently high pressures. The conditions on the slope and curvature of the pressure-specific volume function are necessary for the formation of shocks from finite-amplitude compression waves.

The propagation of a large-amplitude hydrostatic pressure disturbance in a solid or a liquid has been studied in the present report. The material has been assumed to be fluid-like in behavior, or equivalently, its strength in shear has been assumed negligible in comparison to the pressures of

interest. A longitudinal wave of compression in a real solid will in general contain both dilational and distortional (or bulk and shear) components. When the amplitude of a longitudinal wave is sufficiently large so that its shear component cannot be supported by the material, at least a portion of the energy must be transmitted as a wave of hydrostatic pressure and a shock wave can form. In the material model which is used in the present theory, the passage of the wave is assumed to destroy the strength of the material in shear, so that the material is indeed fluid-like in behavior. Thus in the present model, no energy is transmitted by signals which could, under certain conditions in a real solid, run ahead of a trailing shock wave. The assumptions implicit in the fluid dynamic model are discussed further in Appendix A.

A. Non-Porous Materials

The best values of C, μ, and n for the present description of any given medium can be obtained by a process of fitting to an experimentally derived Hugoniot for the particular material of interest. Standard fitting criteria, such as that of the minimum sum of square deviations, can be applied to numerical laboratory data[9, 10, 11]. For example, for lead C = 2.86 kilobars, $\mu = 4$, and n = 4.64 provide an excellent fit of the data obtained by Walsh et al.[10]. For most metals the Walsh data indicate that the exponent n should be about 5; the exponent for water is close to 7.

Alternative to the use of conventional fitting criteria, one may choose to satisfy certain properties of compressibility, such as the limiting compression ratio and the initial rate of change of specific volume with pressure. The presence of the three parameters C, μ, and n permits,

in general, the satisfaction of three such conditions. In what follows, we present methods of deducing values of these parameters based on the satisfaction of general properties of compressibility data.

The quantity μ represents a limiting value of the density ratio V_o/V when the shock pressure P tends to infinity. As such, it plays the same role as the factor $(\gamma+1)/(\gamma-1)$ in the Hugoniot for a perfect gas, where γ is the ratio of specific heats. An appropriate value for this quantity in any given problem can readily be inferred from shock compression data. For most solids a value of μ about 4 appears applicable[10]; the influence of the exact value of μ on the final results is of course not particularly strong, since C and n remain to be selected so as to provide a best fit of compression data.

With an assumption for the value of μ, two further conditions on compressibility can be satisfied by proper choice of C and n. One scheme of presentation of experimental hydrostatic compressibility data at pressures up to 10^5 bars, at least for static results on relatively incompressible solids[12, 13], is in the form

$$-\frac{\Delta V}{V_o} = AP - BP^2 , \qquad (7.1)$$

where ΔV is defined as $V - V_o$, and the empirical constants A and B are tabulated for a number of solids.

The constants A and B can be related to C, μ, and n; C and n can then be written as functions of A, B, and the assumed value of μ. Dropping the subscript s on P and V for brevity in the assumed Hugoniot, Eq. (4.7), we define $\epsilon = \Delta V/V_o$ and write Eq. (4.7) in the form

$$\frac{P}{C} = \frac{\left(\frac{1}{1+\epsilon}\right)^n - 1}{\mu - \frac{1}{1+\epsilon}} . \qquad (7.2)$$

The right-hand side of Eq. (7.2) can be expressed as a Taylor's series in ϵ about $\epsilon = 0$:

$$\frac{\mu-1}{n} \frac{P}{C} = -\epsilon + \left[\frac{\mu(n+1) - (n-1)}{2(\mu-1)}\right] \epsilon^2 + \cdots \qquad (7.3)$$

From Eq. (7.3) we observe that the rate of change of P with ϵ at $\epsilon = 0$ is given by

$$-V_o \left(\frac{dP}{dV}\right)_{V=V_o} = \frac{Cn}{\mu-1} . \qquad (7.4)$$

Thus the reciprocal of the coefficient of P in Eq. (7.3) is in fact the bulk modulus of the material.

Now it is desired to obtain ϵ as a power series in P, so that the coefficients of the leading terms may be compared to A and B in Eq. (7.1). Defining $p = P/C$ as before, we have given $p = f(\epsilon)$ through Eq. (7.2), and it is required to find

$$\epsilon = \left(\frac{d\epsilon}{dp}\right)_o p + \frac{1}{2} \left(\frac{d^2\epsilon}{dp^2}\right)_o p^2 + \cdots \qquad (7.5)$$

Differentiating $p = f(\epsilon)$ repeatedly with respect to p, we have the identities

$$1 = f'(\epsilon) \frac{d\epsilon}{dp} ,$$

$$0 = f''(\epsilon) \left(\frac{d\epsilon}{dp}\right)^2 + f'(\epsilon) \frac{d^2\epsilon}{dp^2} ,$$

where primes on f denote differentiation with respect to its argument ϵ. These identities provide relations between the given Taylor coefficients of Eq. (7.3) and those of Eq. (7.5); the required inverse series is therefore

$$-\frac{\Delta V}{V_o} = \frac{\mu-1}{n}\,\frac{P}{C} - \left[\frac{\left[\mu(n+1) - (n-1)\right](\mu-1)}{2n^2}\right]\left(\frac{P}{C}\right)^2 + \cdots \qquad (7.6)$$

Now, by comparing the coefficients of like powers of P in Eqs. (7.1) and (7.6), we obtain C and n in terms of A, B, and μ as follows:

$$\left.\begin{aligned} C &= \frac{(\mu-1)^2 A}{2(\mu-1)B - (\mu+1)A^2}\,, \\ n &= \frac{2(\mu-1)B - (\mu+1)A^2}{(\mu-1)A^2}\,. \end{aligned}\right\} \qquad (7.7)$$

Typically, A is of the order of 10^{-6} bars^{-1} (1 bar = 10^6 dynes/cm^2) and B is of the order of 10^{-12} bars^{-2} for the less compressible homogeneous solids[12]. Assuming $\mu = 4.0$, C is of the order of 10^6 bars and n is of the order of unity.

When limited compressibility data is available in numerical form, a satisfactory procedure for the determination of C and n for a non-porous solid essentially consists of a numerical fitting process. The product Cn is related to the bulk modulus of the material through Eq. (7.4); hence

$$Cn = (\mu-1)\,\frac{c_o^2}{V_o}\,, \qquad (7.8)$$

where c_o is the velocity of sound in the medium. Equation (7.8) thus provides one condition on C and n if the value of μ is assumed. A second condition on C and n for the assumed value of μ can then be obtained by inserting a pair of experimental values of P and V into the analytical expression for the Hugoniot, Eq. (4.7).

B. Porous Materials

As in the case of non-porous materials, the best values of C,

μ, and n for a given porous material would be obtained by a process of fitting to an experimentally derived Hugoniot.

1. The Hugoniot

In what follows, we present an approximate method for deducing the behavior of a porous solid under shock from considerations of the behavior of its gas and solid fractions. The method consists of

1. Describing the behavior of the solid fraction under shock by an equation of the same form as the assumed Hugoniot, Eq. (4.7), in which the constants C, μ, and n apply to the solid fraction alone.

2. Describing the behavior of the gas fraction under shock by the usual Hugoniot derived on the assumption of the perfect gas law. The ambient pressure is considered as being very small in comparison to the pressures of interest.

3. Considering the gas and solid fractions as being shocked independently, and permitting heat transfer from the gas to the solid at constant pressure. The temperature rise in the pure solid due to shock compression alone is assumed to be insignificant, and the gas fraction is again assumed to behave as a perfect gas. The change in volume of the solid due to a rise in temperature is neglected.

4. Characterizing the resulting composite shock pressure-specific volume function by the form of the assumed Hugoniot, Eq. (4.7), in which the constants C, μ, and n now refer to the mixture.

Let the subscripts a and b denote quantities relating to the gas and solid fractions, respectively, and denote ambient conditions by the subscript zero. For brevity we omit the subscript s on P and V in the assumed Hugoniot, Eq. (4.7). We introduce the following notation:

V_o = initial specific volume of porous material

a = initial volume fraction of gas

$V_{a0} = a\ V_o$ = initial volume of gas

$V_{b0} = (1 - a)\ V_o$ = initial volume of solid

V_{am} = volume of gas after shock and preceding heat exchange

V_a = volume of gas after shock and heat exchange

V_b = volume of solid after shock

ρ_{a0} = initial density of gas fraction

ρ_{b0} = initial density of solid fraction

T_o = absolute initial temperature of porous material

T_{am} = absolute temperature of gas after shock and preceding heat exchange

T = final absolute temperature of the shocked porous material

c_a = specific heat of gas fraction at constant pressure

c_b = specific heat of solid fraction at constant pressure

R_* = gas constant

We study a volume of the porous material equal to its specific volume, so that V_{a0} and V_{b0} do not represent specific volumes. We restate Eq. (4.7) as it applies to the solid fraction:

$$P = \frac{C_b \left[\left(\frac{V_{b0}}{V_b} \right)^{n_b} - 1 \right]}{\mu_b - \frac{V_{b0}}{V_b}} , \qquad (7.9)$$

where the constants C_b, μ_b, and n_b refer to the solid fraction alone.

If the gas fraction is shocked separately to the pressure P, the volume is given by the usual Hugoniot:

$$\frac{V_{a0}}{V_{am}} = \frac{\frac{\gamma + 1}{\gamma - 1} P + P_o}{P + \frac{\gamma + 1}{\gamma - 1} P_o} , \qquad (7.10)$$

where γ is the ratio of specific heats of the gas. We neglect the ambient pressure P_o in Eq. (7.10), and obtain approximately

$$\frac{V_{a0}}{V_{am}} = \frac{\gamma + 1}{\gamma - 1} . \qquad (7.11)$$

Assuming that the ideal gas equation of state holds for the gas fraction, we may write

$$P V_{am} = \rho_{a0} a V_o R_* (T_{am} - T_o),$$

after neglecting the product $P_o V_{a0}$ in comparison to the product PV_{am}. The factor $\rho_{a0} a V_o$ represents the total mass of gas involved and R_* is the difference of the specific heats of the gas at constant pressure and constant volume, respectively. The temperature of the gas fraction after shock and before mixing with the solid, T_{am}, is then approximately

$$T_{am} = T_o + \frac{1}{\rho_{a0} R_*} \frac{\gamma - 1}{\gamma + 1} P, \qquad (7.12)$$

where Eq. (7.11) and the definition $V_{a0} = aV_o$ have been used. The temperature of the solid fraction after shock and before mixing with the gas is assumed to be T_o.

We now consider the solid and gas as being mixed at the shock pressure P, and assume that the mixture reaches thermal equilibrium:

$$\rho_{a0} a V_o c_a (T_{am} - T) = \rho_{b0} (1 - a) V_o c_b (T - T_o). \qquad (7.13)$$

The factor $\rho_{b0} (1 - a) V_o$ represents the total mass of solid involved.

Substituting Eq. (7.12) and rearranging, we obtain

$$\frac{aV_o c_a}{R_*} \frac{\gamma - 1}{\gamma + 1} P = \left[\rho_{b0}(1 - a)V_o + \rho_{a0} aV_o \frac{c_a}{c_b}\right] c_b(T - T_o). \quad (7.13)$$

Now c_a and c_b can be expected to be of roughly the same order of magnitude, and the ratio ρ_{a0}/ρ_{b0} has values like 5×10^{-4} for typical mineral solids and air at atmospheric pressure. Consequently, the factor in brackets on the right-hand side of Eq. (7.13) is very nearly equal to the total mass of gas and solid enclosed in the volume V_o, or unity. The final temperature of the mixture is then given approximately by the expression

$$T = T_o + \frac{aV_o}{R_*} \frac{c_a}{c_b} \frac{\gamma - 1}{\gamma + 1} P. \quad (7.14)$$

If the volume of the gas fraction is taken to be proportional to the absolute temperature at constant pressure, we may write

$$\frac{V_a}{V_{am}} = \frac{T}{T_{am}}. \quad (7.15)$$

Hence, using Eqs. (7.11), (7.12), (7.14), and the definition $V_{a0} = aV_o$, we have

$$\frac{V_a}{V_o} = a \frac{\gamma - 1}{\gamma + 1} \frac{T_o + \frac{aV_o}{R_*} \frac{c_a}{c_b} \frac{\gamma - 1}{\gamma + 1} P}{T_o + \frac{1}{\rho_{a0} R_*} \frac{\gamma - 1}{\gamma + 1} P}. \quad (7.16)$$

We now write Eq. (7.9) describing the solid fraction using the definition $V_{b0} = (1 - a)\, V_o$:

$$\frac{P}{C_b} = \frac{(1 - a)^{n_b} \cdot \left(\frac{V_o}{V_b}\right)^{n_b} - 1}{\mu_b - (1 - a) \frac{V_o}{V_b}}, \quad (7.17)$$

where C_b, μ_b, and n_b can be obtained for the pure solid by methods suggested in the preceding section.

In accordance with the assumption that the volume of the solid is not affected by temperature changes, we write the ratio of specific volumes of the porous material before and after shock as

$$\frac{V}{V_o} = \frac{V_a}{V_o} + \frac{V_b}{V_o} , \qquad (7.18)$$

and each term on the right-hand side of Eq. (7.18) is determined as a function of shock pressure through Eqs. (7.16) and (7.17). The composite Hugoniot may now be obtained numerically or by graphical addition of the shock pressure-volume curves for the gas and solid components. Such a graphical addition is shown schematically in Fig. 14 for $a = 0.25$ and $\gamma = 1.4$. The neglection of P_o in the Hugoniot for the gas fraction is evidenced by the fact that the composite curve does not pass through the point $(0, V_o)$. The structure of the solid matrix containing the gas in voids has of course been assumed to have negligible strength, so that the material is converted to a mixture of gas and solid particles at pressures which are negligible in comparison to the shock pressure of interest. The resulting composite Hugoniot thus has a flat portion in the neighborhood of $(0, V_o)$.

The condition of thermal equilibrium in the mixture immediately following shock, which is assumed in writing Eq. (7.13), depends on the mixture being sufficiently finely divided so that the required transfer of heat can take place. The large heat capacity of the solid thus effectively causes the gas fraction to be adsorbed into the solid mass.

It remains now to determine the values of C, μ, and n in the general analytical form of the Hugoniot, Eq. (4.7), for a best fit of the composite curve. It may be noted that a requirement of matching the initial slope of

the composite curve through Eq. (7.4) is inapplicable because of the effect of the presence of a gas fraction as evidenced by the initial flat portion of the composite curve.

2. Compressibility Parameters

Consider the limit of V_a/V_o in Eq. (7.16) as the shock pressure P becomes infinite:

$$\lim_{P\to\infty} \frac{V_a}{V_o} = a \frac{\gamma - 1}{\gamma + 1} \frac{c_a}{c_b} \rho_{a0}{}^{a}V_o . \tag{7.19}$$

Similarly from Eq. (7.17),

$$\lim_{P\to\infty} \frac{V_b}{V_o} = \frac{1 - a}{\mu_b} . \tag{7.20}$$

The limit of the fraction V/V_o is then obtained as the sum of the limits for the gas and solid fractions, Eqs. (7.19) and (7.20) above. Now the factor $\rho_{a0}{}^{a}V_o$ represents the total mass of gas in the specific volume of the mixture. If c_a/c_b is of the order of unity, $\lim(V_a/V_o)$ is entirely negligible in comparison to $\lim(V_b/V_o)$ for gas fractions up to about 0.85.

For example, for $a = 0.85$, $c_a/c_b = 1.0$, $\gamma = 1.4$, $\rho_{a0}/\rho_{b0} = 5 \times 10^{-4}$, and $\mu_b = 4.0$, we have $\lim V_a/V_b = 0.011$. Thus we obtain the limiting density ratio for the porous material

$$\mu = \frac{\mu_b}{1 - a} . \tag{7.21}$$

The largest value of μ for which numerical results have been obtained is $\mu = 8$, which corresponds to a 50 per cent gas fraction if $\mu_b = 4$.

Values of C and n in a generalized Hugoniot for the porous material can now be obtained by a fitting process consisting of inserting two pairs of values of P and V from the curve obtained by graphical

addition of the gas and solid pressure-volume relationships (Fig. 14) into the generalized Hugoniot, Eq. (4.7), with μ given by Eq. (7.21).

VIII. APPLICATIONS

The shock pressure decay and arrival time results presented in this report are intended for application to explosions in liquids and in porous and non-porous solids. The results are given in dimensionless form in order to accommodate a variety of materials having generally similar compressibility characteristics under shock. The techniques described herein have been successfully employed in predictions on the growth of high-yield explosions in water and soil. In these cases, values of the constants in the general form of the Hugoniot for the materials were obtained by fitting to experimentally obtained shock compressibility data. The table below gives values which have been used for water and a sandy soil.

	C(bars)	μ	n
Water	9,000	4	7
Sandy Soil	12,900	4	3

A. Behavior of Real Materials

Liquids and non-porous, non-crystalline solids under hydrostatic compression can be expected to exhibit continuously decreasing compressibility with increasing pressure. This is a characteristic of the assumed general Hugoniot, Eq. (4.7), and the behavior of such materials is readily represented by this form.

The porous solids under confined compression may show a distinct "crushing pressure" at which the structure of the solid matrix containing the gas in voids fails suddenly, and the porous material is converted to a mixture of solid and gas particles. This results in a rapid decrease of

specific volume with increasing pressure at crushing, followed by a slow decrease of specific volume with increasing pressure when crushing is complete. If results are desired in a shock pressure range well above the crushing strength of the solid matrix, the description of the porous solid as an idealized mixture is still adequate for the analysis of strong shock wave propagation. In this case the constants C, μ, and n must be obtained from a gross fit of compressibility data, disregarding details of the data at low pressures. In particular, one can no longer make use of the initial rate of change of pressure with specific volume as a condition on the constants, since this rate of change is related to the acoustic velocity, or speed of low-amplitude pressure waves in the material. The sound wave may be regarded as being transmitted as a low-amplitude stress wave through the solid matrix without inducing crushing of the matrix structure, and causing only negligible compression of the gas contained in the voids. One would find that the shock velocity, which is related to the slope of the chord of the actual Hugoniot, for the pressure range exceeding the crushing strength can in fact be considerably lower than the sound speed, which is related to the initial slope of the actual Hugoniot. This behavior gives rise to the possibility of an acoustic signal running ahead of a slower moving strong shock from an explosion in a porous material, but such an acoustic signal would carry a relatively small amount of energy compared to the trailing main shock. The crushing phenomenon is related to the initial flat portion of the composite Hugoniot of Fig. 14, where it has been assumed that ambient atmospheric pressure and the crushing strength of the material are negligible in magnitude.

B. The Ideal Absorber

Clearly, the ideal absorber would be one which maximizes the waste energy per unit volume. An upper limit on the waste heat QV_o per unit mass of material is, from Fig. 1, the total internal energy imparted to the unit mass by the shock. This would be realized by a material whose Hugoniot exhibited extreme upward concavity; it follows that in the ideal absorber, half the shock energy imparted to a unit mass of material is dissipated as waste heat. It is likely that a porous solid having proper characteristics of grain size and thermal conductivity could approach this sort of behavior. An increase in porosity is, however, accompanied by a decrease in average density, so that a unit mass of the material occupies an increasing volume. A large bulk of very low density porous material would thus be necessary to attenuate appreciably the shock pressure from an explosion. In design for explosion containment, therefore, it is necessary to effect a proper balance between porosity and total mass.

In general, it is desirable for efficient shock attenuation to use materials in a pressure range in which the rate of decrease of pressure with distance is extremely rapid, i.e., in the range in which the pressure-distance curves of Figs. 3 through 7 are very steep. Although the present results are for the case of a point-source explosion in an infinite medium, they make possible the evaluation of a wide variety of solids for their relative blast absorbing characteristics.

BIBLIOGRAPHY

1. BNL study team. Theoretical Possibilities of Major Accidents in Large Nuclear Power Plants, WASH-740, Brookhaven National Laboratory (March 1957) (U)

2. Porzel, F. B. Design Evaluation of BER (Boiling Experimental Reactor) in Regard to Internal Explosions, ANL-5651, ARF No. D090, Argonne National Laboratory Subcontract No. W31-109-eng-38-576, Armour Research Foundation (June 1956) (U)

3. Porzel, F. B. Study of Underwater Blast, ARF No. D079, Office of Naval Research Contract No. Nonr-1421(00), Armour Research Foundation (December 1956) (C)

4. Chaszeyka, M. A., and F. B. Porzel. Study of Blast Effects in Soil, ARF No. D119, U.S. Army Corps of Engineers Contract No. DA-44-009-ENG-3113, Armour Research Foundation (August 1958) (U)

5. Taylor, G. I. "The Formation of a Blast Wave by a Very Intense Explosion", Proc. Roy. Soc. A201, 159 (1950)

6. Taylor, J. L. "An Exact Solution of the Spherical Blast Wave Problem", Phil. Mag. 46, 317 (1955)

7. Gleyzal, A. N. An Analysis of Solutions of the Point Blast Problem, U.S. Naval Ordnance Laboratory No. 4183 (November 1957) (U)

8. Snay, H. G. A Theory of the Shockwave Produced by a Point Explosion, U.S. Naval Ordnance Laboratory No. 4182 (December 1957) (U)

9. Walsh, J. M., and R. H. Christian. "Equation of State of Metals From Shock Wave Measurements", Phys. Rev. 97, 1544 (1955)

10. Walsh, J. M., M. H. Rice, R. G. McQueen, and F. L. Yarger. "Shock Wave Compressions of Twenty-Seven Metals; Equation of State of Metals", Phys. Rev. 108, 196 (1957)

11. Rice, M. H., R. G. McQueen, and J. M. Walsh. "Compression of Solids by Strong Shock Waves", Solid State Physics 6, 1, F. Seitz and D. Turnbull, ed., Academic Press, Inc., New York (1958)

12. Bridgman, P. W. The Physics of High Pressure, George Bell and Sons, Ltd., London (1949)

13. Bridgman, P. W. "Recent Work in the Field of High Pressures", Rev. Mod. Phys. 18, 1 (1946)

14. Jeffreys, H. Cartesian Tensors, Cambridge University Press (1957)

15. Nadai, A. Plasticity, a Mechanics of the Plastic State of Matter, McGraw-Hill Book Co., Inc., New York (1931)

16. Lieberman, P. Shock Impingement Experiments on Crushable Solids, Report No. ARF 4132-10, U.S. Atomic Energy Commission Contract No. AT(11-1)-528, Armour Research Foundation (June 1959)

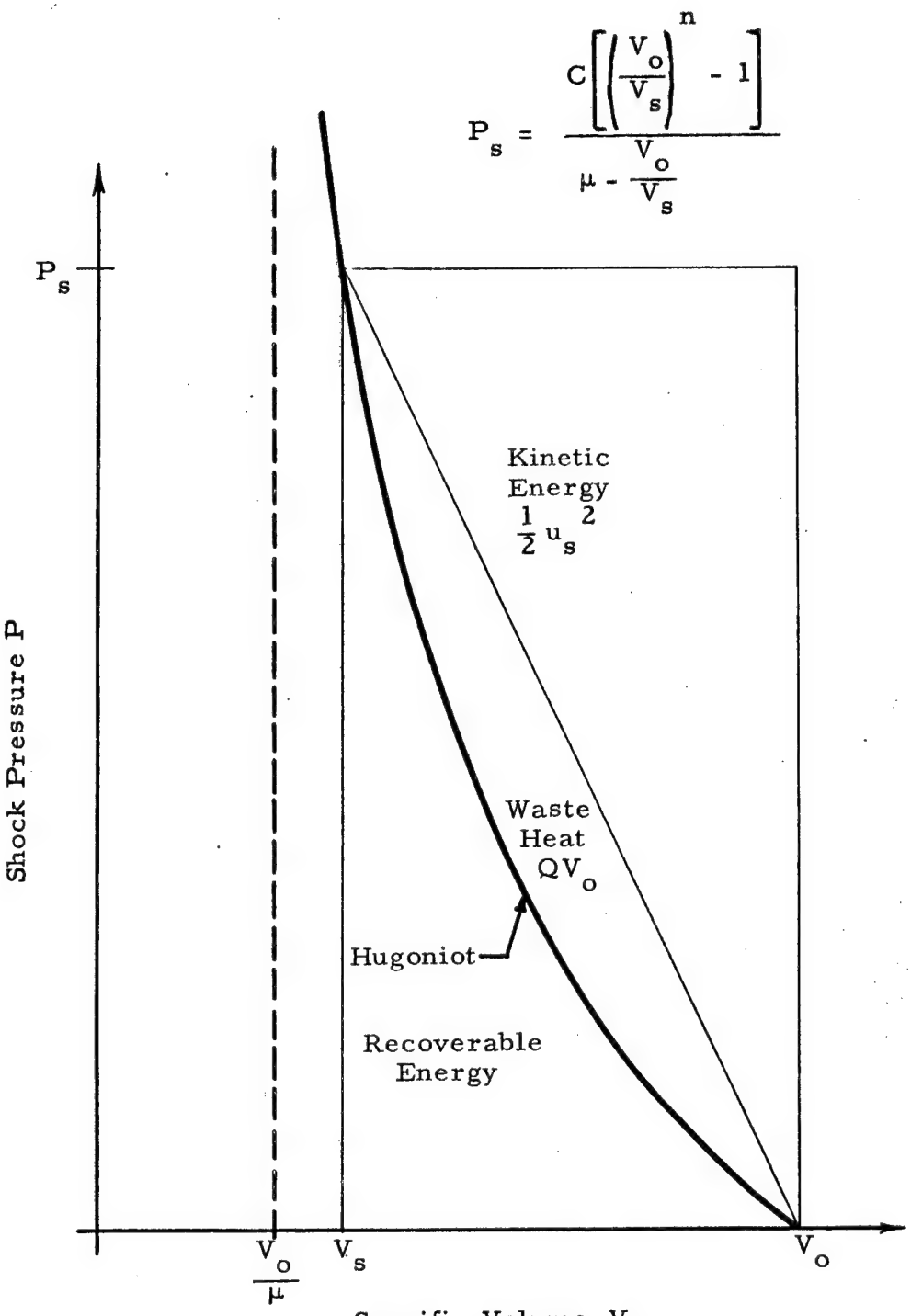

Fig. 1 SHOCK FRONT CONDITIONS

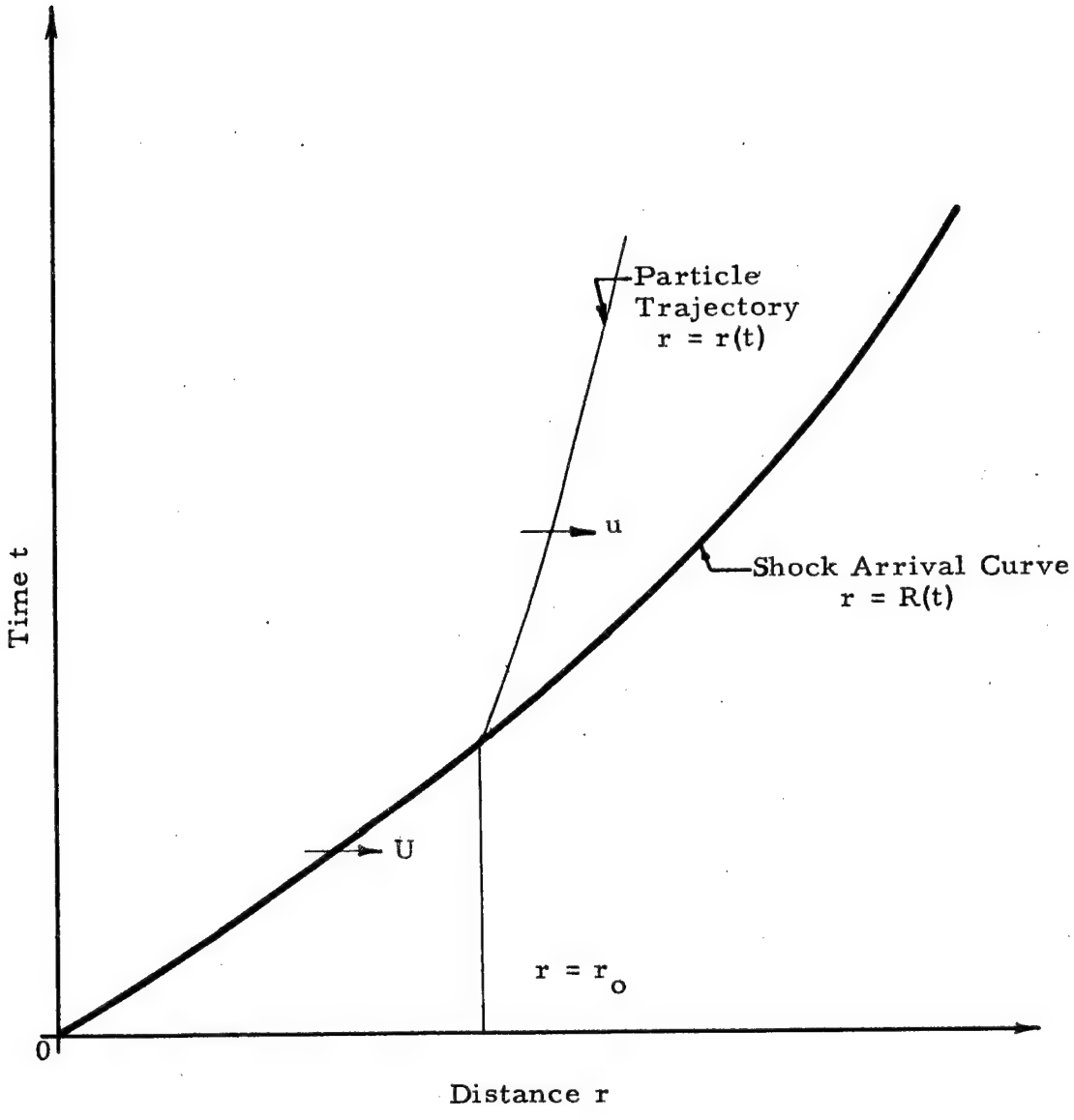

Fig. 2 DISTANCE-TIME RELATIONS

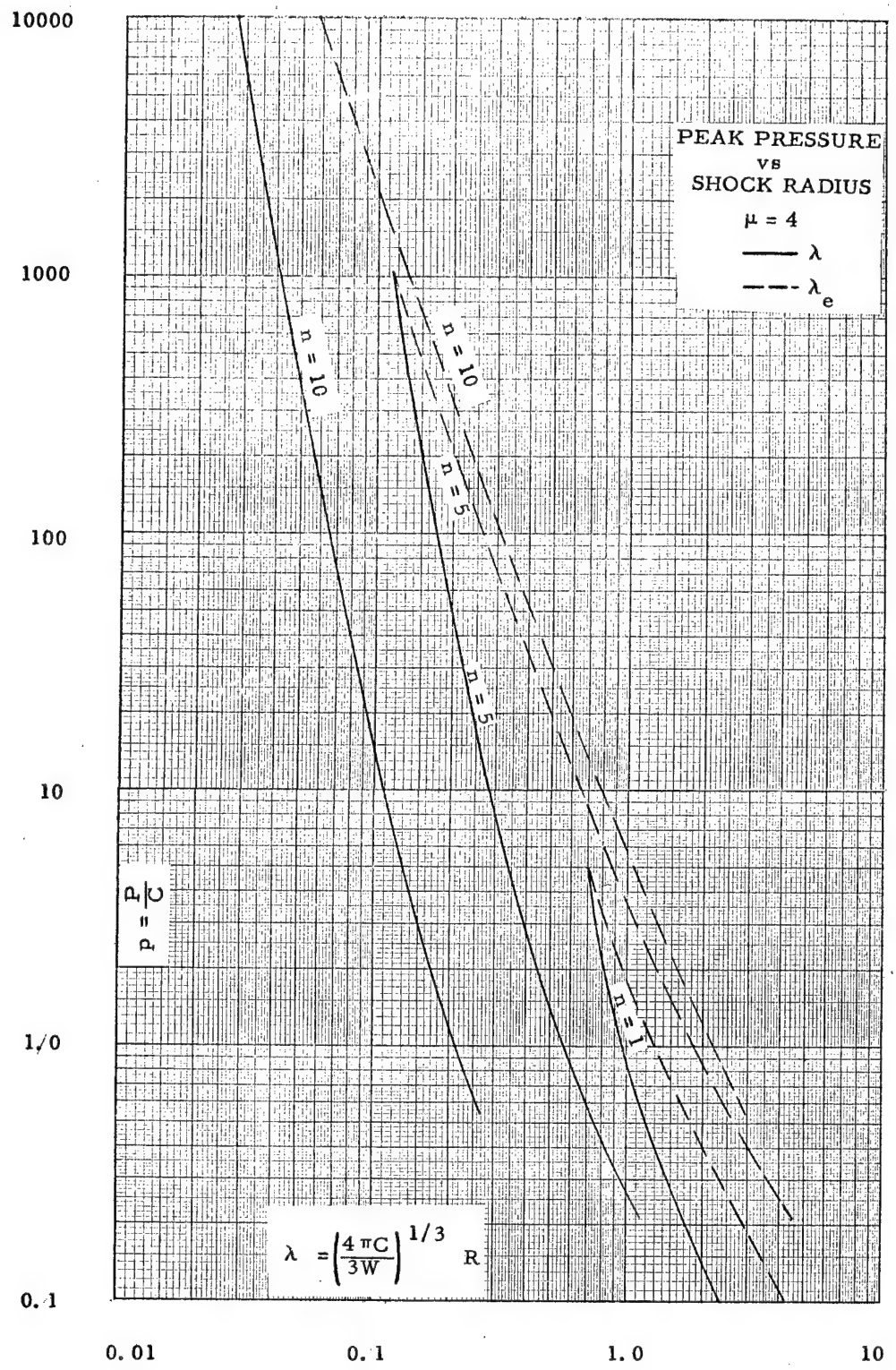

Fig. 3 PRESSURE-DISTANCE CURVES, $\mu = 4$

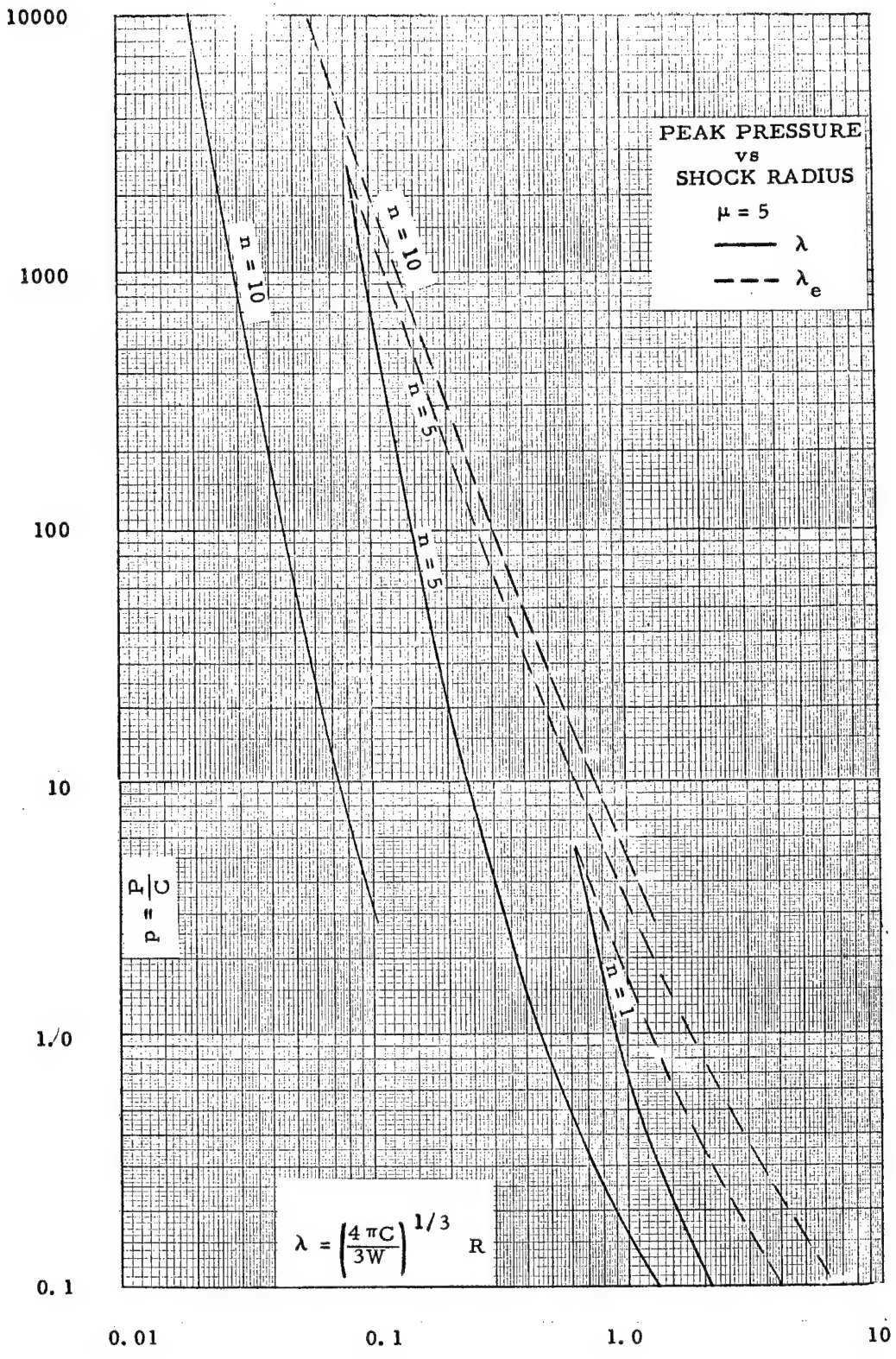

Fig. 4 PRESSURE-DISTANCE CURVES, $\mu = 5$

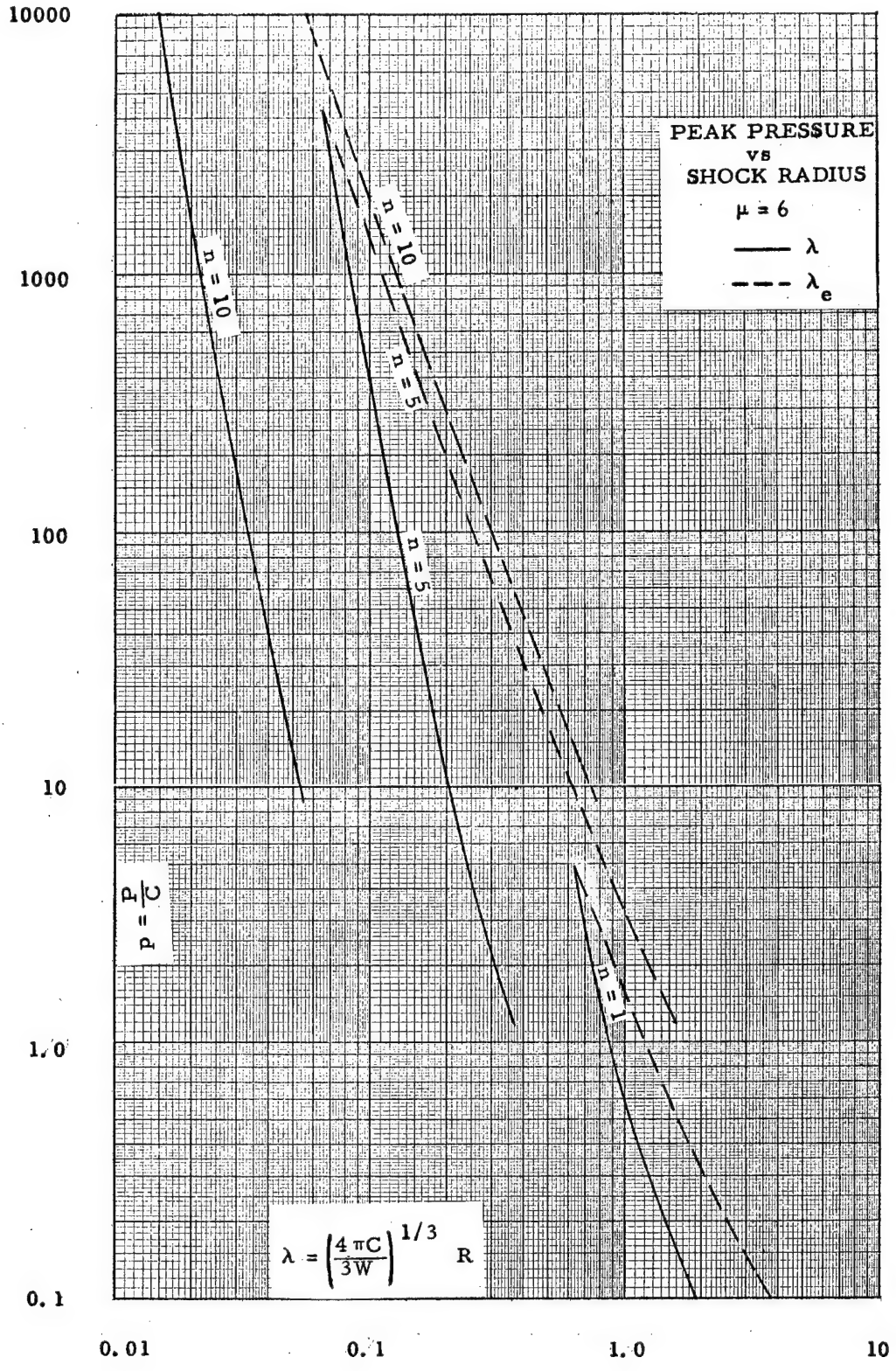

Fig. 5 PRESSURE-DISTANCE CURVES, $\mu = 6$

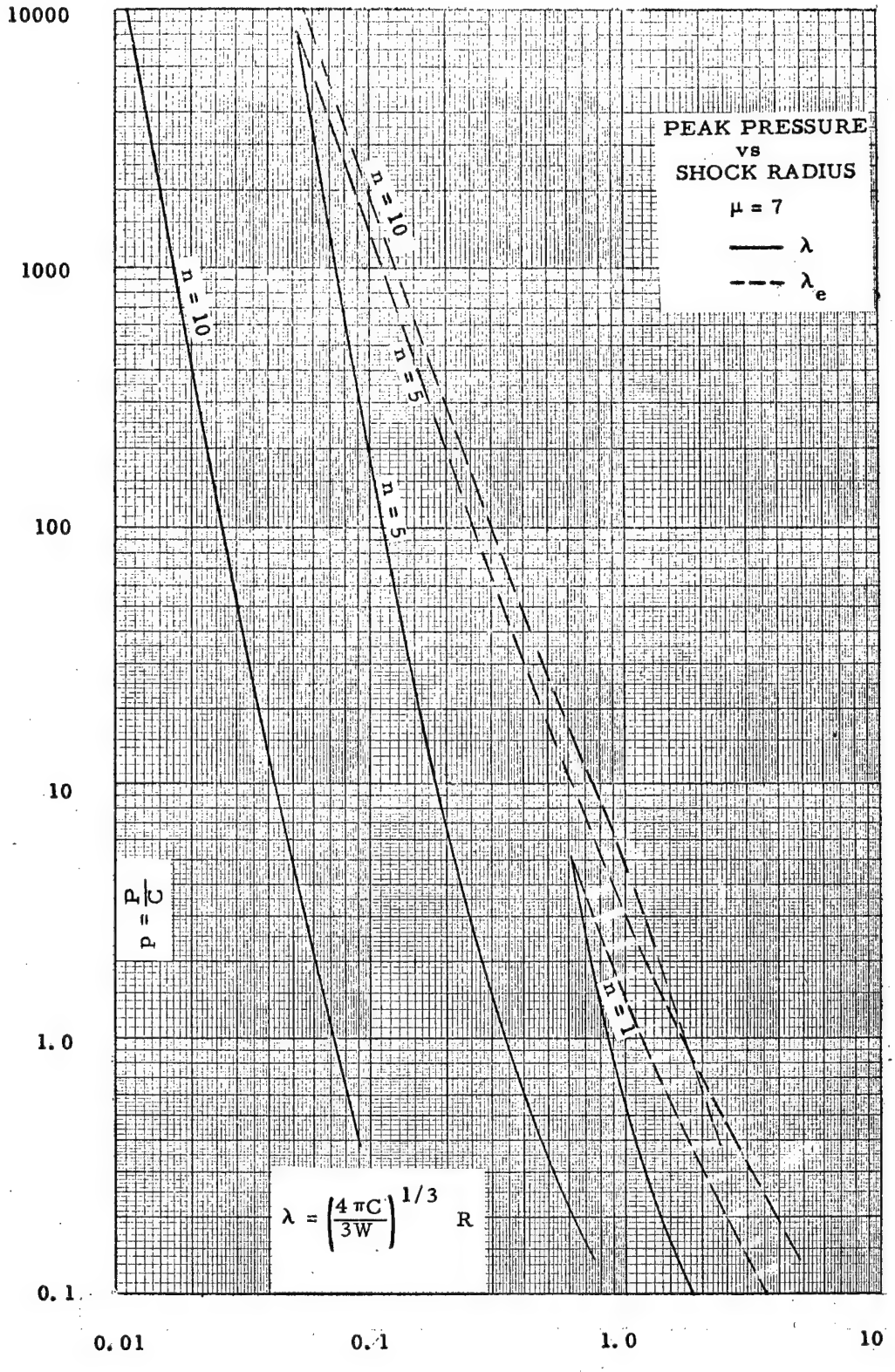

Fig. 6 PRESSURE-DISTANCE CURVES, $\mu = 7$

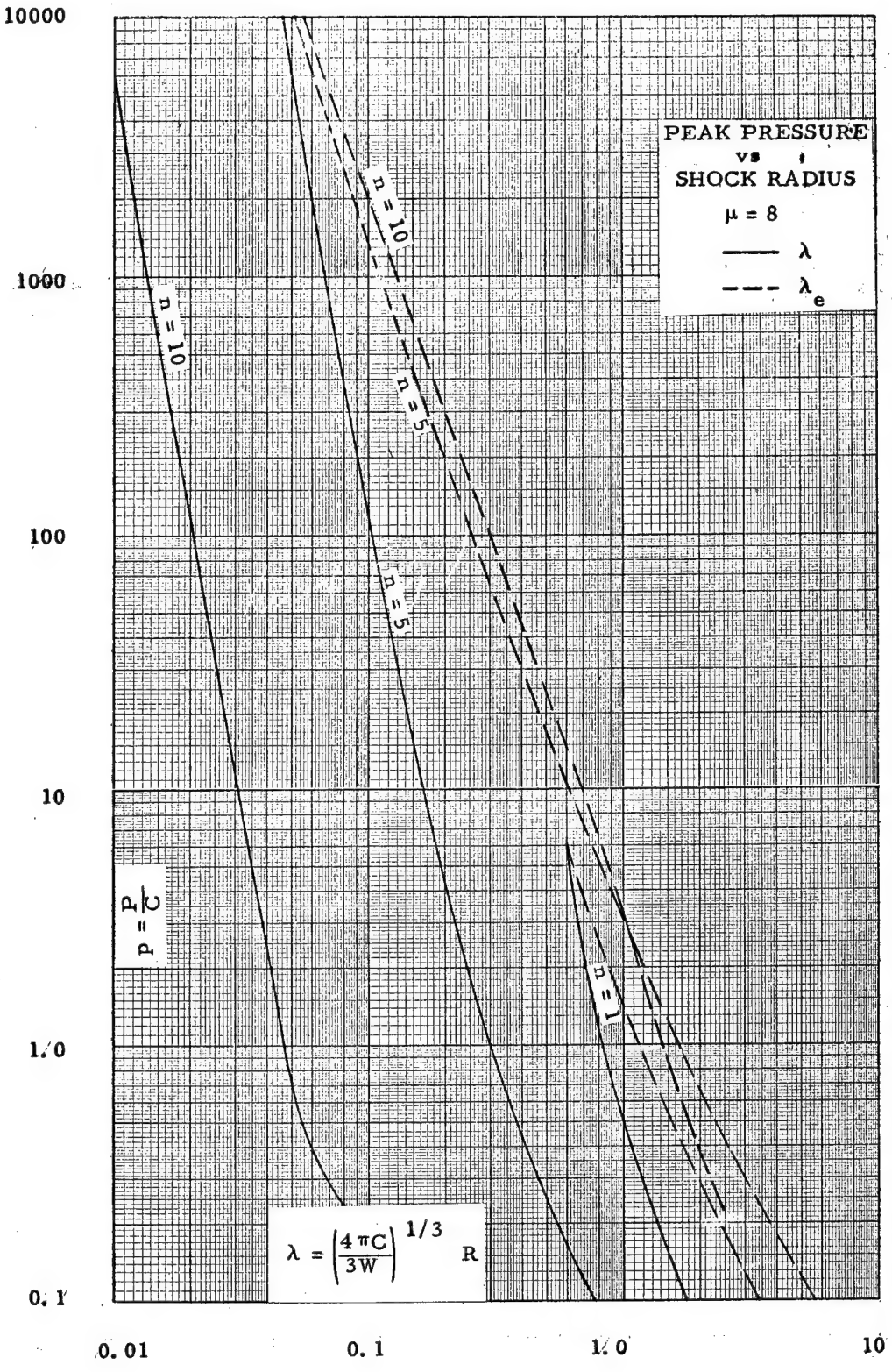

Fig. 7 PRESSURE-DISTANCE CURVES, $\mu = 8$

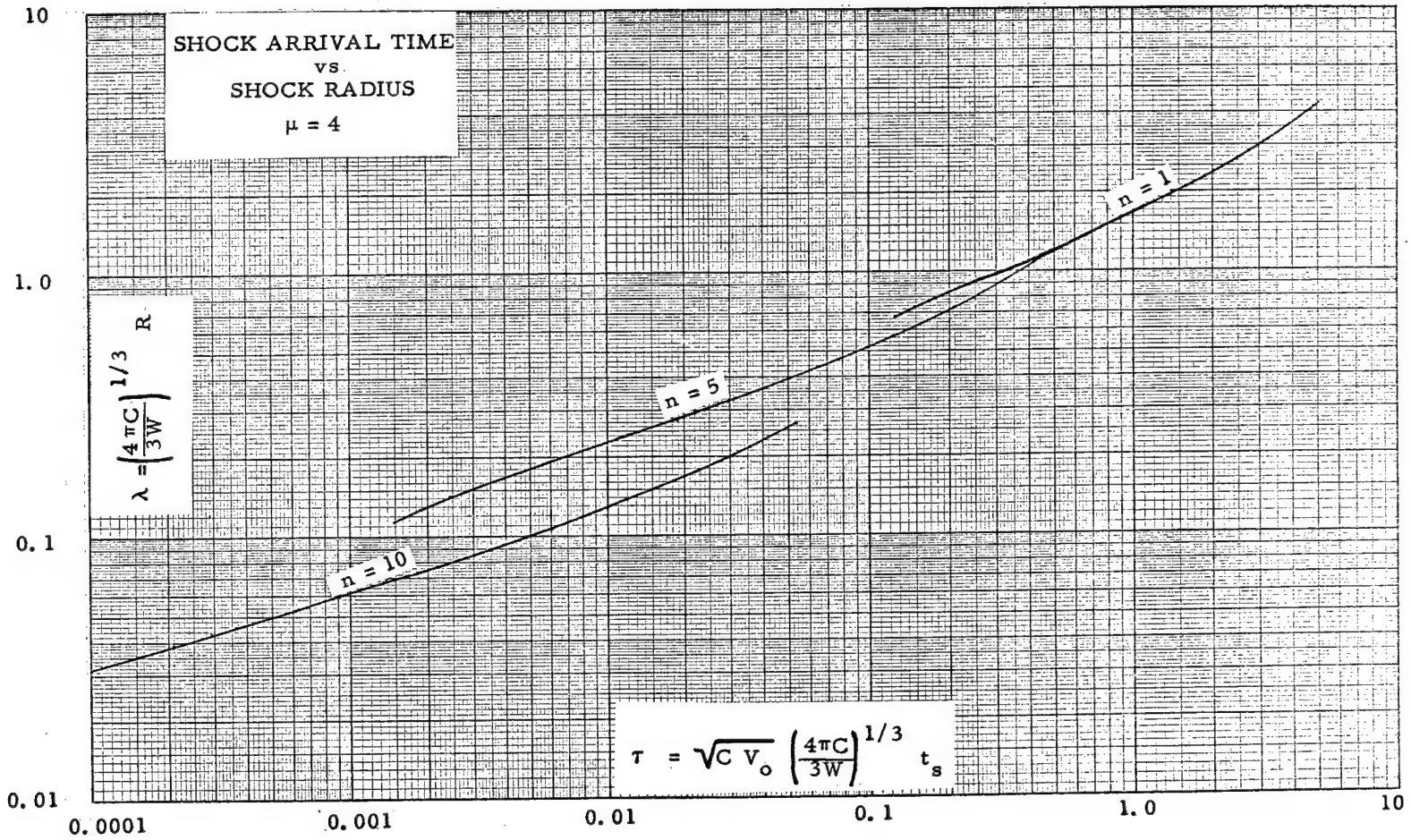

Fig. 8 ARRIVAL TIME CURVES, $\mu = 4$

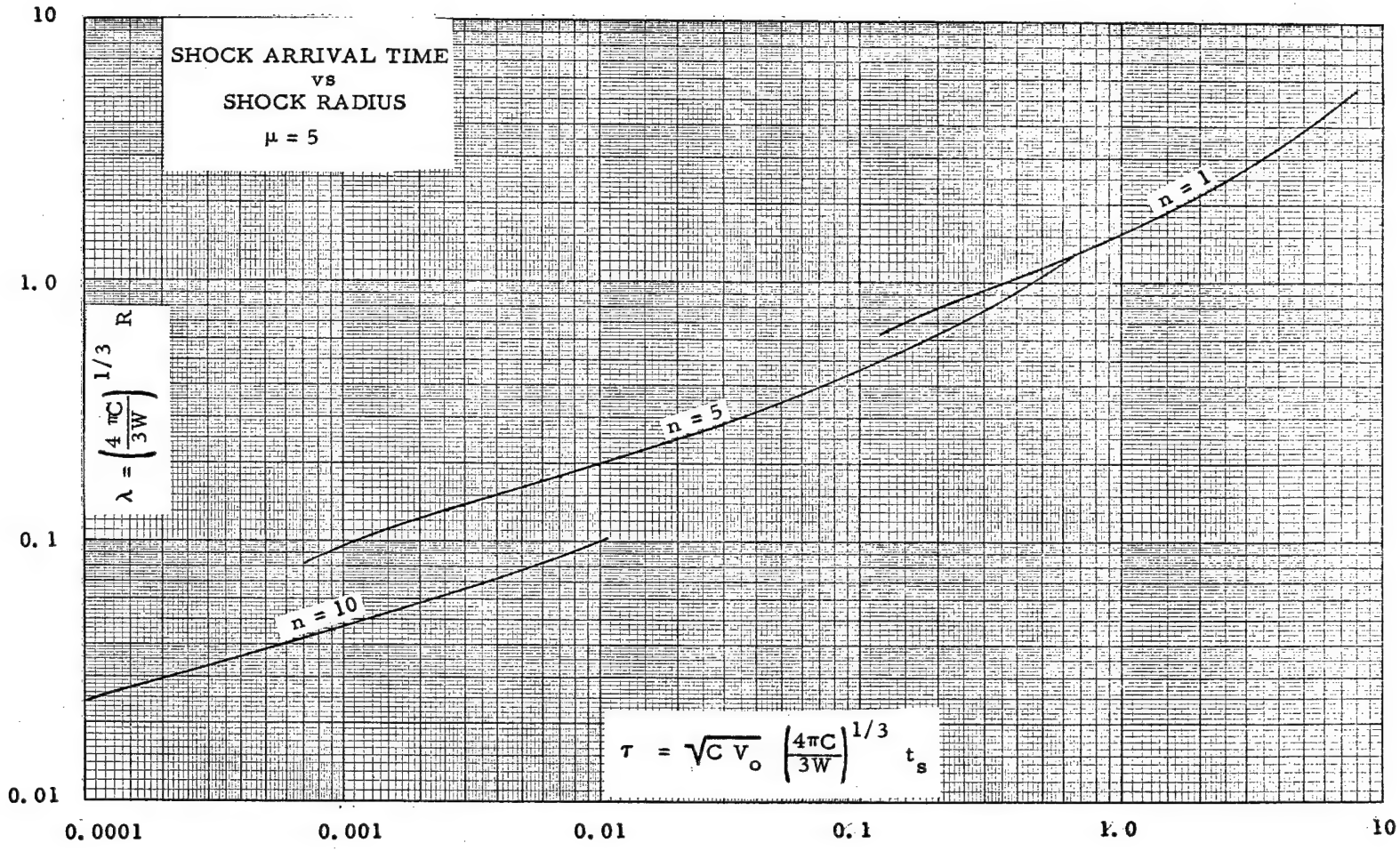

Fig. 9 ARRIVAL TIME CURVES, μ = 5

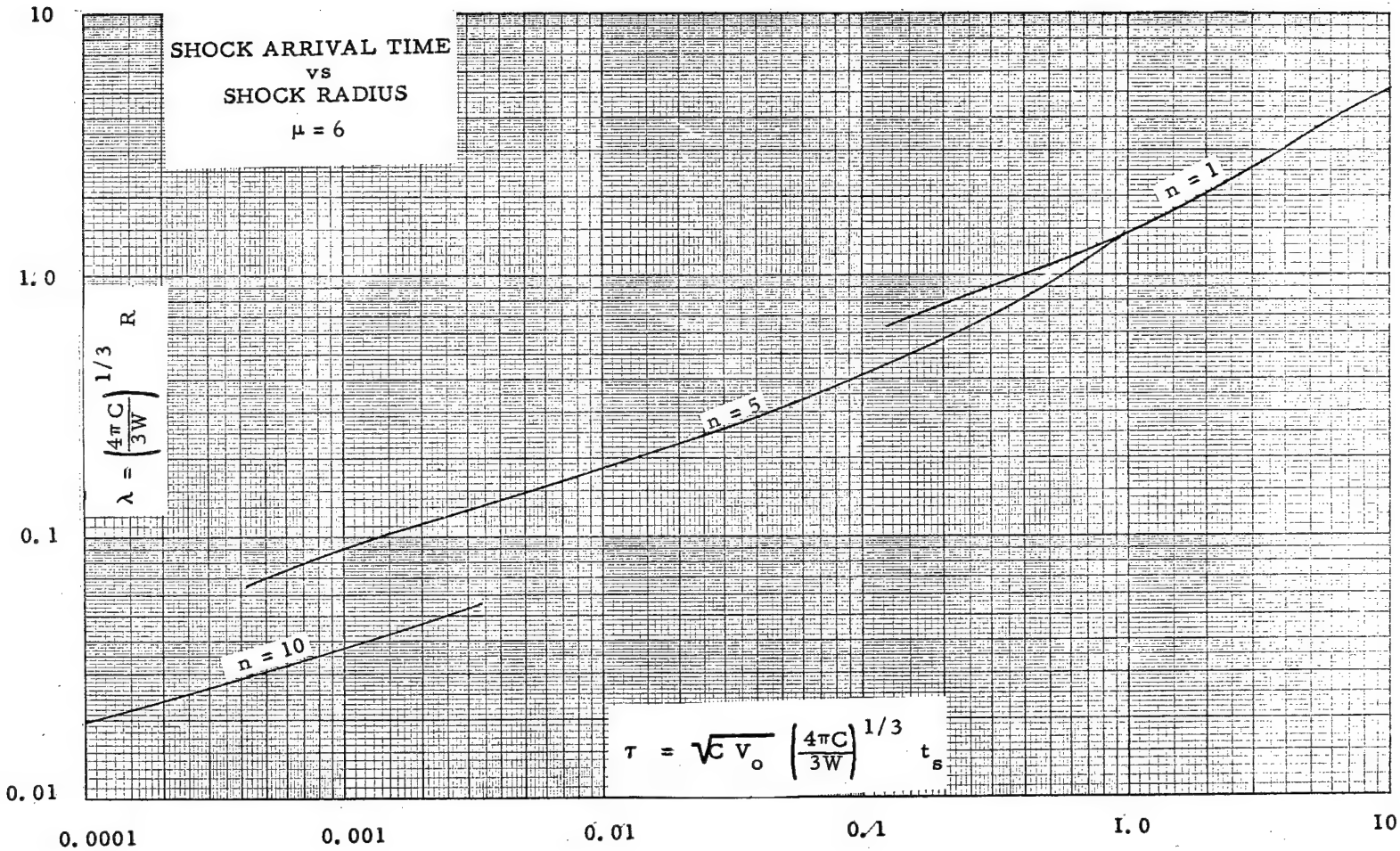

Fig. 10 ARRIVAL TIME CURVES, μ = 6

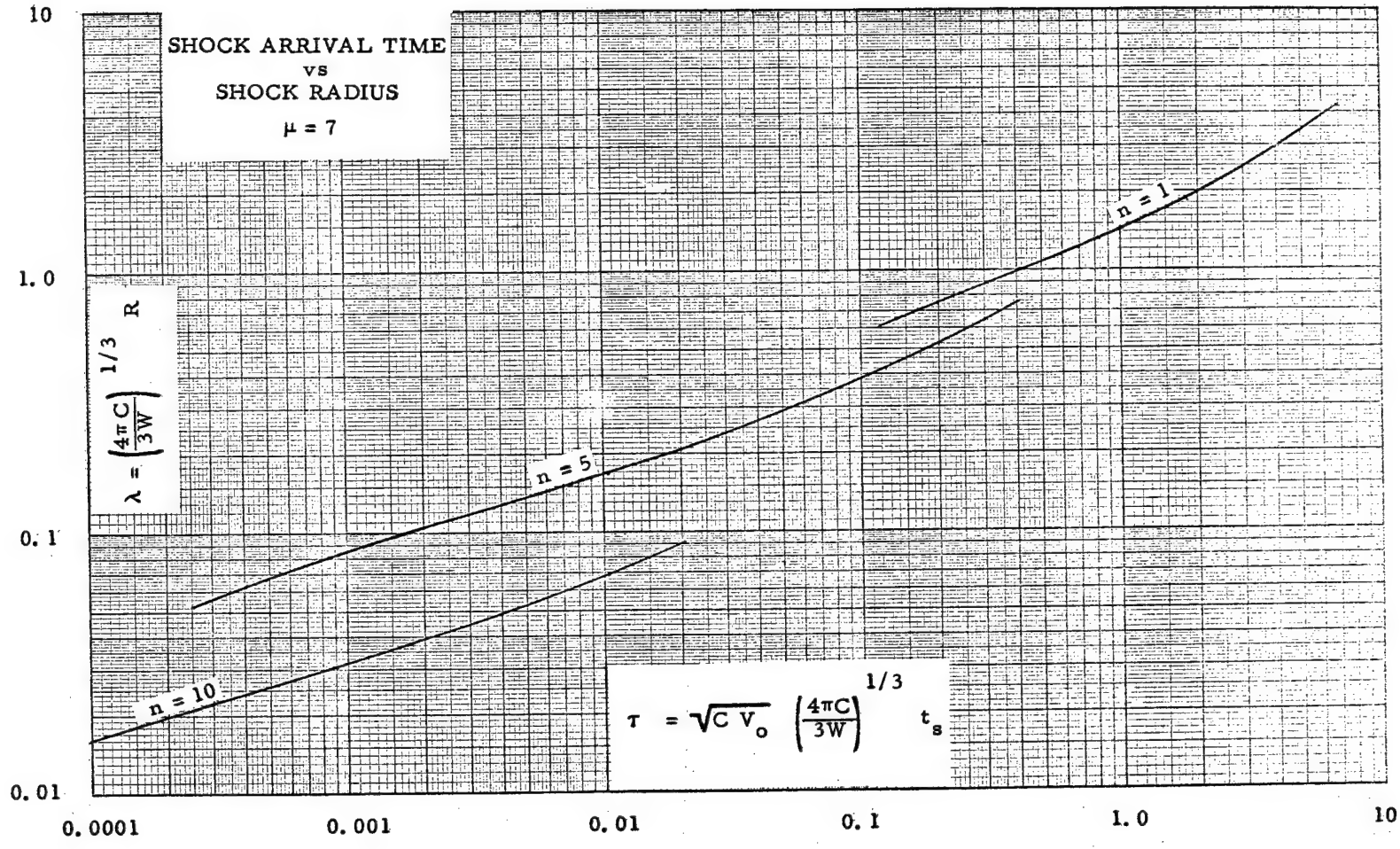

Fig. 11 ARRIVAL TIME CURVES, $\mu = 7$

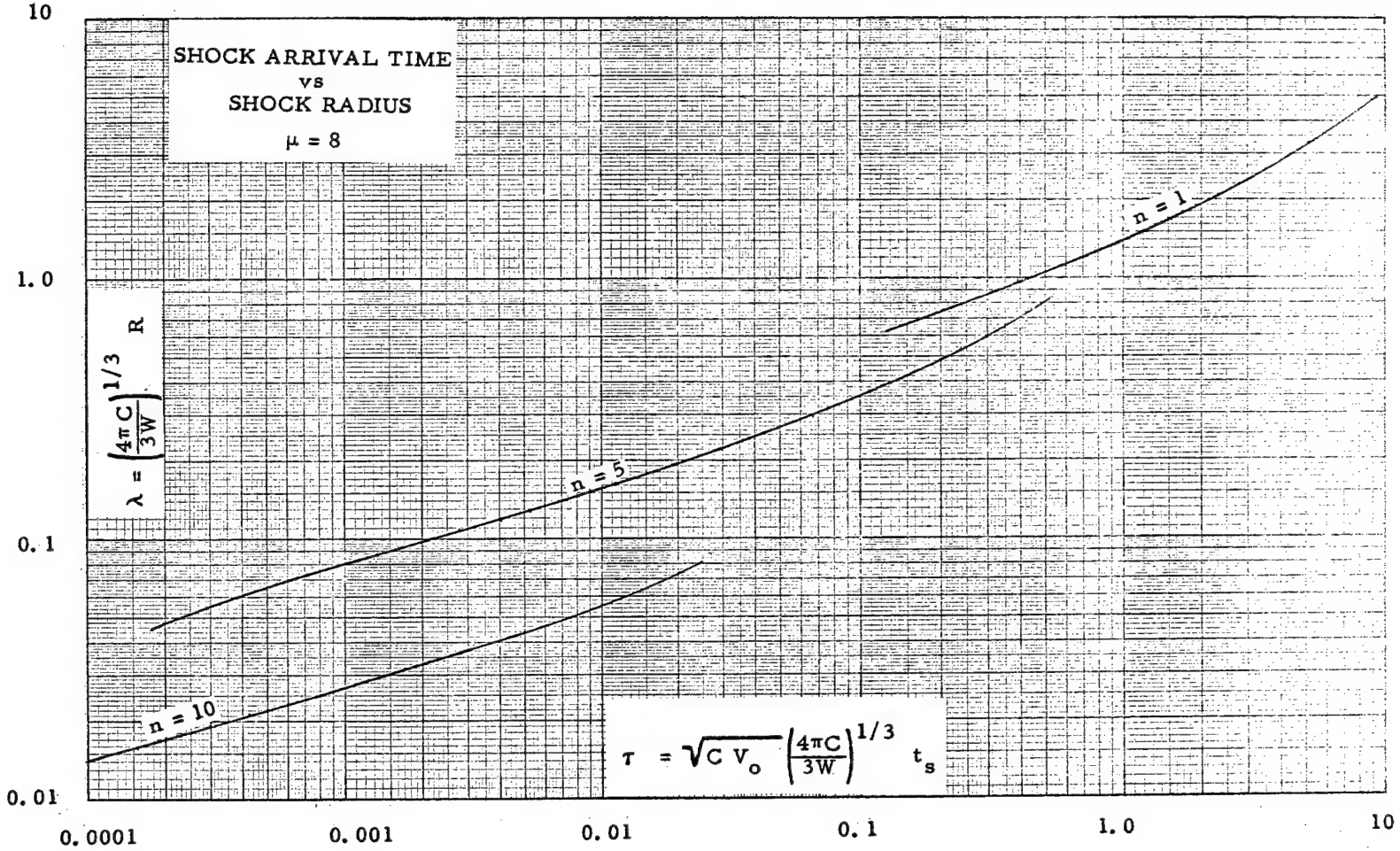

Fig. 12 ARRIVAL TIME CURVES, $\mu = 8$

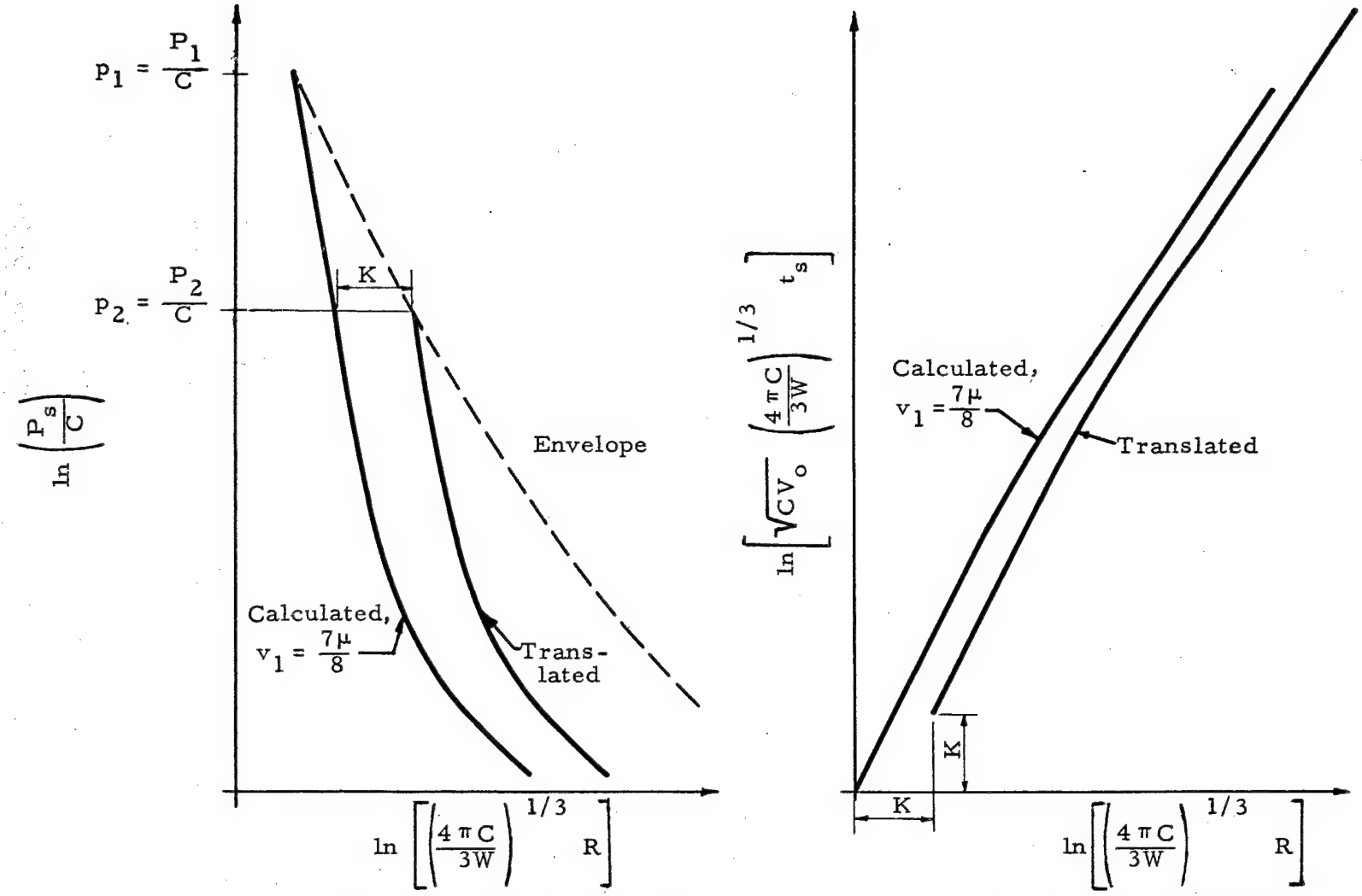

a. Pressure-Distance Curve b. Arrival Time Curve

Fig. 13 VARIATION OF INITIAL CONDITIONS

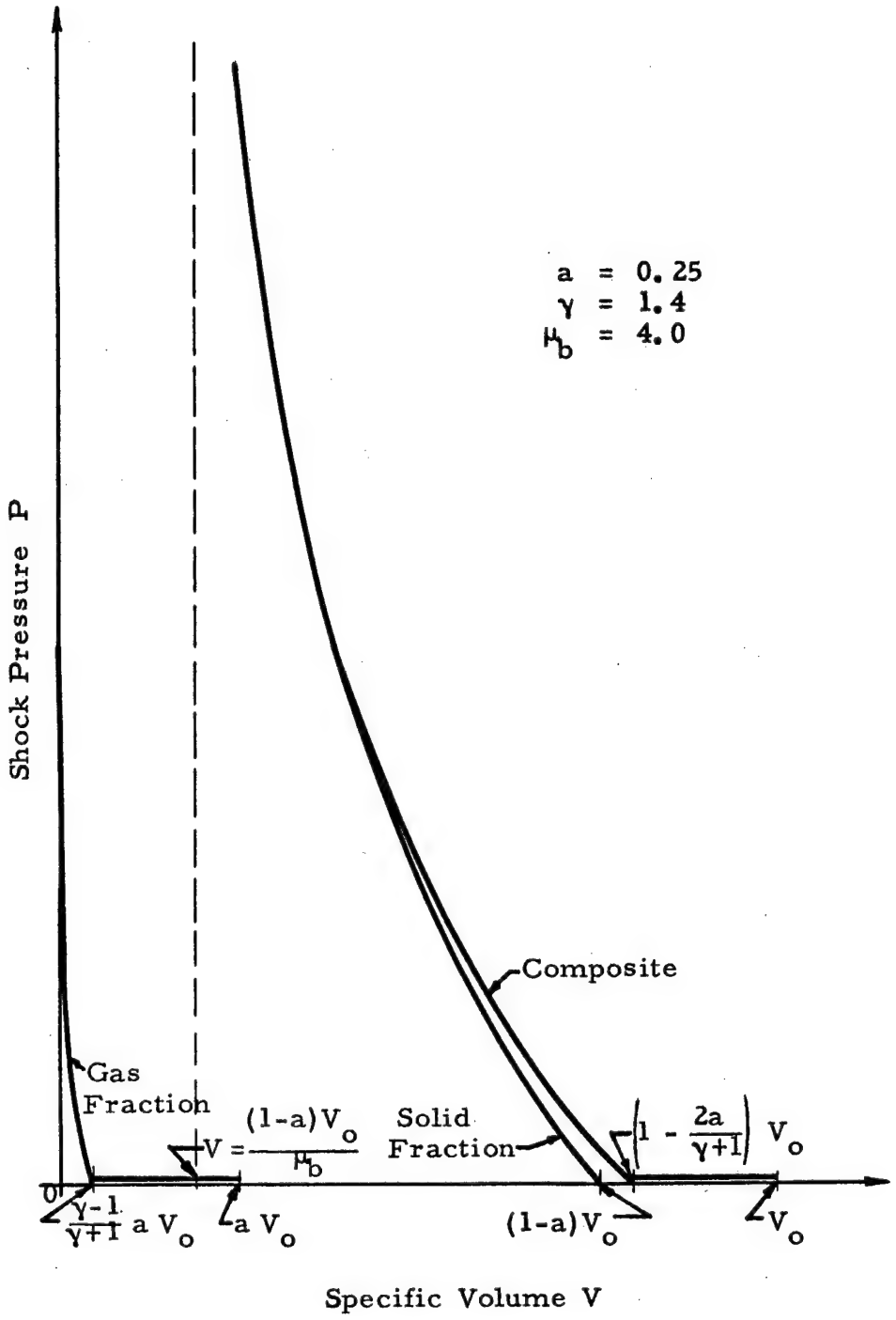

Fig. 14 HUGONIOT FOR A POROUS SOLID

TABLE 1

Values of p

$\mu = 4$

v \ n	1	2	3	4	5	6	7	8	9	10
1.100	0.0344	0.0724	0.1141	0.1600	0.211	0.266	0.327	0.394	0.468	0.550
1.200	0.0714	0.1571	0.260	0.383	0.532	0.709	0.923	1.179	1.486	1.854
1.300	0.1111	0.256	0.443	0.687	1.005	1.417	1.954	2.65	3.557	4.73
1.400	0.1538	0.369	0.671	1.093	1.684	2.51	3.67	5.29	7.56	10.74
1.500	0.200	0.500	0.950	1.625	2.64	4.15	6.43	9.85	14.97	22.6
1.600	0.250	0.650	1.290	2.31	3.95	6.57	10.77	17.48	28.2	45.4
1.700	0.304	0.822	1.701	3.20	5.74	10.06	17.41	29.8	51.1	87.2
1.800	0.364	1.018	2.20	4.32	8.13	15.01	27.4	49.6	89.7	161.8
1.900	0.429	1.243	2.79	5.73	11.31	21.9	42.1	80.4	153.2	292
2.000	0.500	1.500	3.50	7.50	15.50	31.5	63.5	127.5	256	512
2.100	0.579	1.795	4.35	9.71	21.0	44.6	94.3	198.5	418	877
2.200	0.667	2.13	5.36	12.46	28.1	62.4	138.0	304	670	1475
2.300	0.765	2.52	6.57	15.87	37.3	86.5	199.7	406	1059	2436
2.400	0.875	2.98	8.02	20.1	49.1	118.8	286	687	1651	3962
2.500	1.000	3.50	9.75	25.4	64.4	162.1	406	1017	2542	6357
2.600	1.143	4.11	11.84	31.9	84.2	220	573	1491	3878	10080
2.700	1.308	4.84	14.37	40.1	109.6	297	804	2170	5865	15840
2.800	1.500	5.70	17.46	50.4	142.6	401	1124	3150	8815	24700
2.900	1.727	6.74	21.3	63.4	185.6	540	1567	4550	13190	38200
3.000	2.00	8.00	26.0	80.0	242	728	2186	6560	19680	59000
3.100	2.33	9.57	32.0	101.5	317	985	3060	9480	29380	91100
3.200	2.75	11.55	39.7	129.8	418	1341	4290	13740	43980	140700
3.300	3.29	14.13	49.9	168.0	558	1844	6090	20090	66300	219000
3.400	4.00	17.60	63.8	221	756	2570	8750	29760	101200	344000
3.500	5.00	22.5	83.8	298	1048	3670	12870	45040	157600	552000

TABLE 2

Values of λ

$\mu = 4$

ν \ n	1	2	3	4	5	6	7	8	9	10
1.100	4.33	2.87	2.06	1.523	1.139	0.858	0.649	0.492	0.371	0.266
1.200	2.84	1.875	1.339	0.982	0.730	0.547	0.411	0.310	0.235	0.1770
1.300	2.25	1.476	1.048	0.764	0.564	0.419	0.314	0.325	0.1769	0.1332
1.400	1.919	1.252	0.884	0.641	0.470	0.348	0.258	0.1921	0.1434	0.1071
1.500	1.702	1.105	0.776	0.559	0.408	0.299	0.221	0.1632	0.1208	0.0896
1.600	1.548	1.000	0.698	0.500	0.363	0.265	0.1935	0.1420	0.1044	0.0768
1.700	1.430	0.919	0.639	0.455	0.328	0.238	0.1726	0.1257	0.0917	0.0692
1.800	1.336	0.856	0.591	0.419	0.300	0.216	0.1558	0.1127	0.0816	0.0591
1.900	1.260	0.803	0.552	0.389	0.277	0.1980	0.1420	0.1019	0.0733	0.0527
2.000	1.195	0.759	0.519	0.364	0.257	0.1829	0.1303	0.0929	0.0663	0.0474
2.100	1.139	0.720	0.491	0.342	0.241	0.1699	0.1202	0.0852	0.0604	0.0428
2.200	1.090	0.687	0.466	0.323	0.226	0.1585	0.1115	0.0785	0.0553	0.0390
2.300	1.046	0.657	0.443	0.306	0.213	0.1484	0.1038	0.0726	0.0508	0.0356
2.400	1.007	0.630	0.423	0.291	0.201	0.1394	0.0969	0.0674	0.0469	0.0326
2.500	0.971	0.605	0.405	0.277	0.1903	0.1313	0.0907	0.0627	0.0434	0.0300
2.600	0.937	0.582	0.388	0.264	0.1805	0.1239	0.0851	0.0585	0.0403	0.0277
2.700	0.906	0.561	0.372	0.252	0.1715	0.1171	0.0800	0.0547	0.0374	0.0256
2.800	0.876	0.541	0.357	0.241	0.1631	0.1108	0.0753	0.0513	0.0349	0.0237
2.900	0.848	0.521	0.343	0.230	0.1553	0.1049	0.0710	0.0480	0.0325	0.0220
3.000	0.820	0.503	0.330	0.220	0.1478	0.0994	0.0669	0.0451	0.0304	0.0205
3.100	0.793	0.485	0.317	0.211	0.1407	0.0942	0.0631	0.0423	0.0284	0.01901
3.200	0.766	0.467	0.304	0.201	0.1339	0.0892	0.0595	0.0397	0.0265	0.01767
3.300	0.739	0.449	0.291	0.1921	0.1273	0.0844	0.0561	0.0372	0.0247	0.01642
3.400	0.711	0.431	0.279	0.1830	0.1207	0.0797	0.0527	0.0348	0.0230	0.01523
3.500	0.682	0.412	0.265	0.1736	0.1141	0.0750	0.0494	0.0325	0.0214	0.01409

TABLE 3

Values of τ

$\mu = 4$

v \ n	1	2	3	4	5	6	7	8	9	10
1.100	5.07	2.21	1.213	0.727	0.457	0.296	0.1954	0.1307	0.0873	0.0537
1.200	2.72	1.141	0.600	0.345	0.208	0.1293	0.0821	0.0530	0.0344	0.0224
1.300	1.840	0.745	0.378	0.210	0.1218	0.0730	0.0447	0.0277	0.01741	0.01102
1.400	1.375	0.540	0.265	0.1423	0.0799	0.0462	0.0273	0.01632	0.00987	0.00602
1.500	1.088	0.416	0.1983	0.1030	0.0560	0.0313	0.01782	0.01029	0.00600	0.00352
1.600	0.893	0.333	0.1544	0.0778	0.0410	0.0222	0.01220	0.00680	0.00382	0.00217
1.700	0.753	0.274	0.1238	0.0606	0.0309	0.01621	0.00863	0.00465	0.00253	0.001380
1.800	0.647	0.230	0.1015	0.0483	0.0239	0.01216	0.00627	0.00327	0.001716	0.000906
1.900	0.564	0.1969	0.0846	0.0392	0.01889	0.00930	0.00465	0.00235	0.001193	0.000609
2.000	0.498	0.1704	0.0716	0.0323	0.01514	0.00724	0.00351	0.001717	0.000845	0.000418
2.100	0.443	0.1490	0.0612	0.0270	0.01230	0.00571	0.00269	0.001276	0.000610	0.000292
2.200	0.398	0.1314	0.0529	0.0227	0.01010	0.00457	0.00209	0.000962	0.000446	0.000208
2.300	0.359	0.1168	0.0461	0.01936	0.00838	0.00369	0.001640	0.000735	0.000331	0.000150
2.400	0.326	0.1044	0.0404	0.01661	0.00702	0.00301	0.001303	0.000568	0.000249	0.000109
2.500	0.297	0.0938	0.0356	0.01434	0.00592	0.00248	0.001045	0.000443	0.000189	0.000081
2.600	0.272	0.0846	0.0316	0.01247	0.00503	0.00206	0.000846	0.000350	0.000145	0.000060
2.700	0.250	0.0767	0.0282	0.01089	0.00430	0.001718	0.000691	0.000279	0.000113	0.000046
2.800	0.229	0.0696	0.0252	0.00957	0.00371	0.001448	0.000569	0.000224	0.000089	0.000035
2.900	0.211	0.0634	0.0226	0.00844	0.00321	0.001228	0.000472	0.000182	0.000070	0.000027
3.000	0.1949	0.0578	0.0203	0.00748	0.00279	0.001049	0.000396	0.000149	0.000056	0.000021
3.100	0.1798	0.0528	0.01834	0.00665	0.00244	0.000902	0.000334	0.000124	0.000046	0.000017
3.200	0.1658	0.0483	0.01657	0.00592	0.00215	0.000780	0.000284	0.000103	0.000037	0.000013
3.300	0.1528	0.0441	0.01499	0.00529	0.001892	0.000679	0.000244	0.000087	0.000031	0.000011
3.400	0.1405	0.0403	0.01356	0.00474	0.001676	0.000594	0.000211	0.000075	0.000026	0.000009
3.500	0.1289	0.0367	0.01226	0.00425	0.001488	0.000523	0.000183	0.000064	0.000022	0.000008

TABLE 4

Values of λ_e

$\mu = 1$

ν	1	2	3	4	5	6	7	8	9	10
1.100	8.41	6.53	5.59	4.97	4.52	4.16	3.86	3.60	3.34	2.91
1.200	5.32	4.05	3.40	2.97	2.64	2.39	2.17	1.992	1.831	1.680
1.300	4.07	3.05	2.51	2.15	1.882	1.667	1.488	1.337	1.206	1.091
1.400	3.36	2.48	2.01	1.692	1.453	1.263	1.106	0.974	0.861	0.763
1.500	2.89	2.10	1.680	1.391	1.174	1.002	0.861	0.743	0.644	0.559
1.600	2.56	1.835	1.443	1.176	0.976	0.818	0.691	0.585	0.497	0.423
1.700	2.30	1.630	1.264	1.015	0.828	0.683	0.566	0.471	0.392	0.327
1.800	2.10	1.467	1.122	0.888	0.714	0.578	0.471	0.385	0.315	0.258
1.900	1.928	1.333	1.007	0.785	0.622	0.496	0.397	0.319	0.257	0.207
2.000	1.785	1.221	0.911	0.701	0.547	0.429	0.339	0.268	0.212	0.1677
2.100	1.663	1.126	0.830	0.630	0.484	0.375	0.291	0.226	0.1764	0.1374
2.200	1.555	1.042	0.759	0.569	0.432	0.329	0.252	0.1931	0.1481	0.1137
2.300	1.459	0.968	0.698	0.516	0.387	0.291	0.219	0.1657	0.1253	0.0948
2.400	1.372	0.902	0.643	0.470	0.348	0.258	0.1920	0.1431	0.1067	0.0796
2.500	1.293	0.843	0.594	0.430	0.314	0.230	0.1688	0.1241	0.0913	0.0672
2.600	1.219	0.788	0.550	0.393	0.284	0.205	0.1489	0.1080	0.0785	0.0570
2.700	1.151	0.738	0.510	0.361	0.257	0.1838	0.1317	0.0944	0.0677	0.0486
2.800	1.087	0.691	0.473	0.331	0.233	0.1648	0.1167	0.0827	0.0586	0.0415
2.900	1.025	0.647	0.439	0.304	0.212	0.1480	0.1036	0.0725	0.0580	0.0360
3.000	0.966	0.605	0.407	0.279	0.1922	0.1329	0.0920	0.0637	0.0441	0.0306
3.100	0.909	0.565	0.376	0.255	0.1744	0.1193	0.0817	0.0560	0.0383	0.0263
3.200	0.853	0.526	0.348	0.234	0.1579	0.1069	0.0725	0.0491	0.0333	0.0226
3.300	0.797	0.488	0.320	0.213	0.1425	0.0955	0.0641	0.0430	0.0289	0.01939
3.400	0.740	0.450	0.293	0.1930	0.1280	0.0850	0.0565	0.0375	0.0249	0.01658
3.500	0.682	0.412	0.265	0.1736	0.1141	0.0750	0.0494	0.0325	0.0214	0.01409

TABLE 5

Values of p

μ =

v \ n	1	2	3	4	5	6	7	8	9	10
1.475	0.0191	0.0396	0.0617	0.0854	0.1109	0.1384	0.1679	0.1996	0.234	0.270
1.575	0.0457	0.0995	0.1626	0.237	0.324	0.427	0.547	0.688	0.855	1.050
1.675	0.0738	0.1679	0.288	0.441	0.636	0.885	1.202	1.606	2.12	2.78
1.775	0.1034	0.245	0.441	0.710	1.080	1.588	2.29	3.25	4.57	6.38
1.875	0.1347	0.333	0.626	1.059	1.697	2.64	4.03	6.07	9.09	13.54
1.975	0.1678	0.432	0.848	1.505	2.54	4.17	6.73	10.76	17.12	27.1
2.075	0.203	0.543	1.113	2.07	3.67	6.34	10.82	18.33	30.9	52.0
2.175	0.240	0.667	1.424	2.77	5.15	9.39	16.90	30.2	53.9	96.0
2.275	0.280	0.805	1.789	3.64	7.10	13.58	25.8	48.6	91.3	171.5
2.375	0.322	0.959	2.22	4.70	9.60	19.29	38.4	76.2	150.8	298
2.475	0.367	1.130	2.71	6.00	12.81	27.0	56.3	117.2	243	506
2.575	0.416	1.321	3.29	7.57	16.88	37.1	81.2	176.9	385	838
2.675	0.468	1.532	3.95	9.46	22.0	50.5	115.4	263	599	1362
2.775	0.524	1.768	4.72	11.74	28.4	68.0	162.0	385	916	2170
2.875	0.584	2.03	5.61	14.46	36.4	90.6	225	557	1380	3420
2.975	0.649	2.32	6.63	17.72	46.3	119.8	309	797	2050	5280
3.075	0.720	2.65	7.80	21.6	58.5	157.2	421	1127	3120	8068
3.175	0.798	3.01	9.16	26.2	73.5	205	569	1580	4390	12170
3.275	0.882	3.42	10.71	31.7	92.0	265	764	2200	6310	18160
3.375	0.975	3.88	12.51	38.2	114.6	342	1018	3030	9010	26800
3.475	1.078	4.39	14.58	45.9	142.3	439	1350	4150	12770	39300
3.575	1.192	4.98	16.99	55.1	176.2	561	1782	5660	17960	57000
3.675	1.319	5.64	19.78	66.1	218	715	2340	7670	25100	82300
3.775	1.462	6.39	23.0	79.2	269	909	3070	10360	35000	118000
3.875	1.623	7.26	26.9	95.0	332	1154	4010	13940	48500	168400
3.975	1.807	8.27	31.3	113.9	409	1464	5240	18720	67000	240000
4.075	2.02	9.44	36.7	136.9	505	1858	6830	25100	92300	339000
4.175	2.27	10.82	43.1	164.9	625	2360	8920	23670	127100	480000
4.275	2.56	12.46	50.8	199.5	776	3010	11660	45200	175100	679000
4.375	2.90	14.44	60.3	243	967	3850	15300	60800	242000	961000
4.475	3.32	16.87	72.1	297	1214	4950	20200	82000	335000	
4.575	3.85	19.92	87.0	367	1536	6420	26800	111900	467000	
4.675	4.52	23.8	106.4	459	1968	8420	36000	153900	658000	
4.775	5.40	29.0	132.4	585	2560	11220	49100	214800	940000	

TABLE 6

Values of λ

$\mu = 5$

ν \ n	1	2	3	4	5	6	7	8	9	10
1.075	5.44	3.49	2.42	1.721	1.238	0.897	0.650	0.464		
1.175	3.23	2.06	1.421	1.004	0.718	0.517	0.374	0.271	0.1928	
1.275	2.48	1.577	1.080	0.759	0.539	0.386	0.278	0.200	0.1442	0.1025
1.375	2.09	1.321	0.900	0.628	0.444	0.315	0.225	0.1614	0.1158	0.0829
1.475	1.844	1.159	0.785	0.545	0.382	0.270	0.1915	0.1362	0.0970	0.0692
1.575	1.671	1.045	0.704	0.485	0.339	0.238	0.1673	0.1181	0.0835	0.0591
1.675	1.541	0.960	0.643	0.441	0.305	0.213	0.1489	0.1043	0.0732	0.0515
1.775	1.440	0.892	0.594	0.405	0.279	0.1934	0.1343	0.0934	0.0651	0.0454
1.875	1.358	0.873	0.556	0.377	0.258	0.1774	0.1223	0.0845	0.0585	0.0405
1.975	1.290	0.792	0.522	0.352	0.240	0.1639	0.1123	0.0771	0.0529	0.0364
2.075	1.231	0.753	0.494	0.332	0.224	0.1524	0.1038	0.0707	0.0483	0.0329
2.175	1.181	0.719	0.490	0.314	0.211	0.1425	0.0964	0.0627	0.0442	0.0300
2.275	1.137	0.690	0.449	0.298	0.1992	0.1337	0.0899	0.0605	0.0407	0.0275
2.375	1.097	0.663	0.429	0.284	0.1887	0.1259	0.0842	0.0563	0.0377	0.0252
2.475	1.061	0.639	0.412	0.271	0.1792	0.1189	0.0703	0.0526	0.0350	0.0233
2.575	1.029	0.618	0.396	0.259	0.1706	0.1126	0.0744	0.0492	0.0326	0.0216
2.675	0.999	0.598	0.382	0.249	0.1628	0.1069	0.0703	0.0462	0.0304	0.0200
2.775	0.972	0.579	0.369	0.239	0.1556	0.1016	0.0665	0.0435	0.0285	0.01863
2.875	0.946	0.562	0.356	0.230	0.1490	0.0968	0.0630	0.0410	0.0267	0.01739
2.975	0.922	0.546	0.345	0.221	0.1428	0.0924	0.0598	0.0387	0.0251	0.01626
3.075	0.899	0.531	0.334	0.213	0.1371	0.0882	0.0568	0.0366	0.0236	0.01523
3.175	0.877	0.516	0.323	0.206	0.1317	0.0844	0.0541	0.0347	0.0223	0.01429
3.275	0.856	0.502	0.314	0.1988	0.1266	0.0807	0.0515	0.0329	0.0210	0.01342
3.375	0.836	0.489	0.304	0.1921	0.1218	0.0773	0.0491	0.0312	0.01986	0.01263
3.475	0.816	0.476	0.295	0.1856	0.1172	0.0741	0.0469	0.0297	0.01878	0.01189
3.575	0.797	0.464	0.286	0.1794	0.1128	0.0710	0.0448	0.0282		0.01121
3.675	0.778	0.452	0.278	0.1734	0.1086	0.0681	0.0427	0.0268	0.01684	0.01570
3.775	0.760	0.440	0.270	0.1677	0.1046	0.0653	0.0408	0.0255	0.01595	0.01000
3.875	0.741	0.428	0.262	0.1620	0.1007	0.0624	0.0390	0.0243	0.05112	0.00941
3.975	0.722	0.416	0.535	0.1565	0.0969	0.0600	0.0372	0.0231	0.01432	0.00888
4.075	0.703	0.404	0.245	0.1510	0.0931	0.0575	0.0355	0.0219	0.01356	0.00838
4.175	0.684	0.392	0.237	0.1455	0.0894	0.0550	0.0339	0.0208	0.01283	0.00790
4.275	0.664	0.379	0.229	0.1399	0.0857	0.0526	0.0322	0.01977	0.01212	0.00744
4.375	0.627	0.366	0.220	0.1343	0.0820	0.0501	0.0306	0.01870	0.01143	0.00699

TABLE 7

Values of τ

$\mu = 5$

n / ν	1	2	3	4	5	6	7	8	9	10
1.075	7.92	3.38	1.805	1.051	0.642	0.403	0.257	0.1616		0.0563
1.175	3.82	1.557	0.794	0.443	0.259	0.1561	0.0959	0.0595	0.0361	0.0521
1.275	2.51	0.985	0.484	0.260	0.1464	0.0850	0.0503	0.0303	0.01826	0.01075
1.375	1.852	0.705	0.335	0.1738	0.0945	0.0529	0.0302	0.01752	0.01024	0.00600
1.475	1.460	0.540	0.249	0.1249	0.0657	0.0355	0.01961	0.01097	0.00619	0.00353
1.575	1.198	0.431	0.1930	0.0940	0.0479	0.0251	0.01337	0.00722	0.00394	0.00217
1.675	1.011	0.355	0.1546	0.0731	0.0361	0.01832	0.00946	0.00494	0.00260	0.001385
1.775	0.872	0.299	0.1268	0.0583	0.0280	0.01375	0.00687	0.00347	0.001767	0.000913
1.875	0.763	0.256	0.1060	0.0474	0.0221	0.01054	0.00511	0.00250	0.001231	0.000618
1.975	0.677	0.223	0.0899	0.0392	0.01774	0.00822	0.00386	0.001833	0.000875	0.000429
2.075	0.606	0.1954	0.0771	0.0328	0.01445	0.00650	0.00297	0.001367	0.000633	0.000303
2.175	0.548	0.1732	0.0669	0.0277	0.01190	0.00521	0.00231	0.001035	0.000465	0.000219
2.275	0.498	0.1548	0.0585	0.0237	0.00990	0.00422	0.001822	0.000793	0.000347	0.000161
2.375	0.456	0.1392	0.0515	0.0204	0.00831	0.00345	0.001451	0.000614	0.000261	0.000120
2.475	0.419	0.1259	0.0457	0.01765	0.00703	0.00284	0.001166	0.000481	0.000199	0.000092
2.575	0.387	0.1443	0.0407	0.01540	0.00599	0.00237	0.000945	0.000380	0.000153	0.000071
2.675	0.358	0.1045	0.0365	0.01351	0.00514	0.001981	0.000772	0.000303	0.000119	0.000056
2.775	0.333	0.0957	0.0328	0.01191	0.00443	0.001670	0.000635	0.000243	0.000093	0.000045
2.875	0.311	0.0880	0.0297	0.01055	0.00383	0.001415	0.000526	0.000197	0.000074	0.000036
2.975	0.290	0.0811	0.0269	0.00939	0.00335	0.001207	0.000439	0.000160	0.000059	0.000030
3.075	0.272	0.0750	0.0245	0.00838	0.00293	0.001034	0.000368	0.000131	0.000047	0.000026
3.175	0.255	0.0695	0.0223	0.00751	0.00257	0.000891	0.000310	0.000108	0.000038	0.000022
3.275	0.239	0.0645	0.0204	0.00676	0.00227	0.000771	0.000263	0.000090	0.000031	0.000019
3.375	0.225	0.0600	0.01872	0.00609	0.00201	0.000670	0.000224	0.000075	0.000025	0.000017
3.475	0.212	0.0558	0.01720	0.00551	0.001790	0.000586	0.000192	0.000063	0.000021	0.000015
3.575	0.1992	0.0520	0.01583	0.00500	0.001597	0.000514	0.000166	0.000053		0.000014
3.675	0.1876	0.0485	0.01459	0.00454	0.001430	0.000452	0.000143	0.000045	0.000014	0.000013
3.775	0.1767	0.0453	0.01346	0.00414	0.001284	0.000400	0.000125	0.000039	0.000012	0.000012
3.875	0.1665	0.0423	0.01244	0.00378	0.001156	0.000355	0.000109	0.000033	0.000010	0.000012
3.975	0.1567	0.0395	0.01150	0.00345	0.001044	0.000317	0.000096	0.000029	0.000008	0.000011
4.075	0.1474	0.0369	0.01064	0.00316	0.000945	0.000283	0.000085	0.000025	0.000007	0.000011
4.175	0.1385	0.0344	0.00984	0.00290	0.000858	0.000254	0.000075	0.000022	0.000006	0.000010
4.275	0.1298	0.0321	0.00911	0.00266	0.000780	0.000229	0.000067	0.000019	0.000005	0.000010
4.375	0.1214	0.0298	0.00842	0.00243	0.000710	0.000207	0.000060	0.000017	0.000005	0.000009

TABLE 8

Values of λ_e

$\mu = 5$

v \ B	1	2	3	4	5	6	7	8	9	10
1.075	11.22	8.77	7.54	6.74	6.15	5.69	5.28	4.81		
1.175	6.43	4.93	4.15	3.64	3.26	2.95	2.70	2.47	2.225	
1.275	4.79	3.61	2.98	2.57	2.25	2.01	1.799	1.622	1.464	1.299
1.375	3.92	2.90	2.36	1.994	1.720	1.501	1.321	1.168	1.036	0.919
1.475	3.36	2.45	1.962	1.631	1.382	1.184	1.022	0.887	0.771	0.673
1.575	2.97	2.13	1.683	1.376	1.146	0.965	0.818	0.696	0.594	0.508
1.675	2.67	1.896	1.474	1.187	0.973	0.805	0.670	0.559	0.468	0.393
1.775	2.44	1.710	1.311	1.040	0.839	0.682	0.558	0.458	0.376	0.310
1.875	2.25	1.559	1.180	0.922	0.732	0.586	0.472	0.380	0.307	0.248
1.975	2.10	1.434	1.071	0.826	0.646	0.509	0.403	0.320	0.254	0.202
2.075	1.961	1.328	0.980	0.745	0.575	0.446	0.348	0.271	0.212	0.1660
2.175	1.844	1.236	0.901	0.677	0.515	0.394	0.302	0.232	0.1790	0.1379
2.275	1.742	1.156	0.833	0.618	0.464	0.350	0.265	0.201	0.1522	0.1155
2.375	1.651	1.085	0.773	0.566	0.420	0.313	0.233	0.1742	0.1303	0.0975
2.475	1.568	1.021	0.720	0.521	0.381	0.280	0.206	0.1522	0.1123	0.0829
2.575	1.494	0.964	0.673	0.482	0.348	0.252	0.1836	0.1336	0.0973	0.0709
2.675	1.425	0.912	0.630	0.446	0.318	0.228	0.1639	0.1178	0.0848	0.0610
2.775	1.362	0.864	0.591	0.414	0.292	0.207	0.1469	0.1044	0.0742	0.0527
2.875	1.303	0.820	0.556	0.385	0.269	0.1883	0.1321	0.0927	0.0651	0.0458
2.975	1.248	0.779	0.523	0.359	0.248	0.1717	0.1191	0.0827	0.0574	0.0399
3.075	1.196	0.741	0.493	0.335	0.229	0.1569	0.1076	0.0739	0.0508	0.0349
3.175	1.146	0.705	0.465	0.313	0.212	0.1436	0.0975	0.0662	0.0450	0.0306
3.275	1.099	0.671	0.439	0.294	0.1959	0.1316	0.0885	0.0595	0.0400	0.0269
3.375	1.054	0.639	0.415	0.274	0.1816	0.1208	0.0804	0.0535	0.0357	0.0237
3.475	1.010	0.609	0.392	0.256	0.1684	0.1109	0.0731	0.0482	0.0318	0.0210
3.575	0.968	0.579	0.370	0.240	0.1562	0.1019	0.0666	0.0435		0.01858
3.675	0.927	0.551	0.349	0.224	0.1449	0.0937	0.0606	0.0393	0.0254	0.01646
3.775	0.886	0.524	0.329	0.210	0.1343	0.0861	0.0552	0.0354	0.0228	0.01460
3.875	0.846	0.497	0.310	1.960	0.1244	0.0791	0.0503	0.0320	0.0204	0.01296
3.975	0.807	0.471	0.291	1.828	0.1151	0.0726	0.0458	0.0289	0.01822	0.01150
4.075	0.767	0.445	0.273	1.702	0.1063	0.0665	0.0416	0.0260	0.01628	0.01019
4.175	0.726	0.419	0.256	1.580	0.0979	0.0607	0.0377	0.0234	0.01452	0.00902
4.275	0.685	0.393	0.238	1.460	0.0898	0.0553	0.0340	0.0210	0.01291	0.00796
4.375	0.643	0.366	0.220	1.343	0.0820	0.0501	0.0306	0.01870	0.01143	0.00699

TABLE 9

Values of p

$\mu = 6$

v \ n	1	2	3	4	5	6	7	8	9	10
1.030	0.0101	0.0207	0.0318	0.0435	0.0558	0.0687	0.0822	0.0964	0.1113	
1.150	0.0309	0.0664	0.1073	0.1544	0.209	0.271	0.342	0.424	0.519	
1.250	0.0526	0.1184	0.201	0.303	0.432	0.593	0.793	1.044	1.358	
1.350	0.0752	0.1768	0.314	0.499	0.749	1.087	1.542	2.16	2.99	
1.450	0.0989	0.242	0.450	0.752	1.189	1.823	2.74	4.08	6.01	8.81
1.550	0.1235	0.315	0.612	1.072	1.786	2.89	4.61	7.26	11.38	17.76
1.650	0.1494	0.396	0.803	1.474	2.58	4.41	7.42	12.40	20.6	34.2
1.750	0.1764	0.485	1.026	1.972	3.63	6.52	11.59	20.5	36.0	63.2
1.850	0.205	0.584	1.285	2.58	4.98	9.42	17.63	32.8	60.9	112.9
1.950	0.235	0.692	1.584	3.32	6.72	13.3	26.2	51.4	100.4	196.0
2.050	0.266	0.811	1.928	4.22	8.91	18.5	38.3	78.7	161.6	332
2.150	0.299	0.941	2.32	5.29	11.67	25.4	54.9	118.3	255	548
2.250	0.333	1.083	2.77	6.57	15.11	34.3	77.6	174.9	394	887
2.350	0.370	1.239	3.28	8.08	19.36	45.9	108.2	255	599	1407
2.450	0.408	1.409	3.86	9.87	24.6	60.6	149.0	365	896	2190
2.550	0.449	1.595	4.52	11.97	30.1	79.4	203	518	1321	3370
2.650	0.493	1.798	5.26	14.42	38.7	103.1	274	726	1924	5010
2.750	0.538	2.02	6.09	17.29	48.1	132.8	336	1006	2770	7610
2.850	0.587	2.26	7.03	20.6	59.4	169.8	485	1381	3940	11220
2.950	0.639	2.53	8.09	24.5	72.9	216	637	1880	5550	16360
3.050	0.695	2.81	9.28	29.0	89.1	273	832	2540	7740	23600
3.150	0.754	3.13	10.62	34.2	108.5	342	1079	3400	10710	33700
3.250	0.818	3.48	12.12	40.2	131.5	428	1392	4530	14700	47800
3.350	0.887	3.86	13.81	47.2	158.8	533	1786	4990	20100	67200
3.450	0.961	4.28	15.71	55.2	191.3	661	2280	7870	27200	93700
3.550	1.041	4.74	17.85	64.4	230	817	2900	10300	36500	129800
3.650	1.128	5.24	20.3	75.1	275	1006	3670	13400	48900	178600
3.750	1.222	5.82	23.0	87.5	329	1236	4630	17380	65200	244000
3.850	1.326	6.43	26.1	101.7	393	1514	5830	22500	86400	333000
3.950	1.439	7.12	29.6	118.3	469	1852	7320	28900	114200	451000
4.050	1.564	7.90	33.6	137.5	558	2260	9160	37100	150300	609000
4.150	1.703	8.77	38.1	159.8	665	2760	11460	47600	197400	819000
4.250	1.857	9.75	43.3	185.9	792	3370	14310	60800	259000	
4.350	2.03	10.86	49.3	216	943	4110	17860	77700	33800	
4.450	2.23	12.13	56.2	252	1125	5010	22300	99200	441000	
4.550	2.25	13.59	64.3	295	1344	6120	27800	126700	576000	
4.650	2.70	15.28	73.7	346	1610	7490	34800	161900	753000	
4.750	3.00	17.25	84.9	407	1934	9190	43600	207000	985000	
4.850	3.35	19.59	98.3	480	2330	11320	54900	266000		
4.950	3.76	22.4	114.6	571	2830	14010	69300	343000		
5.050	4.26	25.8	134.5	684	3460	17460	88200	445000		
5.150	4.88	30.0	159.5	826	4260	21900	113000	582000		

TABLE 10

Values of λ

$\mu = 6$

ν \ r	1	2	3	4	5	6	7	8	9	10
1.050	7.31	4.57	3.08	2.12	1.482	1.045	0.749	0.571	0.434	
1.150	3.68	2.29	1.530	1.049	0.727	0.508	0.355	0.244		
1.250	2.72	1.685	1.121	0.763	0.526	0.365	0.254	0.1766	0.1133	
1.350	2.26	1.389	0.918	0.622	0.426	0.294	0.203	0.1411	0.0974	
1.450	1.974	1.208	0.794	0.535	0.364	0.249	0.1714	0.1182	0.0814	0.0553
1.550	1.781	1.084	0.709	0.474	0.321	0.218	0.1491	0.1020	0.0700	0.0480
1.650	1.638	0.992	0.645	0.429	0.289	0.1950	0.1322	0.0899	0.0612	0.0417
1.750	1.528	0.921	0.596	0.394	0.263	0.1767	0.1190	0.0803	0.0543	0.0367
1.850	1.439	0.864	0.556	0.366	0.243	0.1619	0.1083	0.0726	0.0487	0.0327
1.950	1.367	0.817	0.523	0.342	0.226	0.1496	0.0994	0.0661	0.0440	0.0294
2.050	1.305	0.777	0.495	0.322	0.211	0.1390	0.0918	0.0607	0.0401	0.0266
2.150	1.252	0.742	0.471	0.304	0.1985	0.1300	0.0852	0.0560	0.0368	0.0242
2.250	1.206	0.712	0.449	0.289	0.1875	0.1220	0.0795	0.0519	0.0339	0.0221
2.350	1.165	0.685	0.430	0.276	0.1777	0.1150	0.0745	0.0483	0.0314	0.0204
2.450	1.129	0.661	0.414	0.263	0.1690	0.1087	0.0700	0.0452	0.0291	0.01880
2.550	1.096	0.640	0.398	0.252	0.1611	0.1030	0.0660	0.0423	0.0272	0.01742
2.650	1.066	0.620	0.384	0.242	0.1539	0.0979	0.0624	0.0398	0.0254	0.01619
2.750	1.038	0.602	0.372	0.233	0.1473	0.0933	0.0591	0.0375	0.0238	0.01510
2.850	1.013	0.585	0.360	0.225	0.1413	0.0890	0.0561	0.0354	0.0223	0.01411
2.950	0.989	0.569	0.349	0.217	0.1357	0.0851	0.0534	0.0335	0.0210	0.01321
3.050	0.967	0.555	0.339	0.210	0.1305	0.0814	0.0508	0.0318	0.01985	0.01240
3.150	0.946	0.541	0.329	0.203	0.1257	0.0781	0.0485	0.0302	0.01875	0.01166
3.250	0.926	0.528	0.320	0.1965	0.1212	0.0749	0.0463	0.0287	0.01775	0.01099
3.350	0.908	0.516	0.311	0.1904	0.1170	0.0720	0.0443	0.0273	0.01683	0.01037
3.450	0.890	0.504	0.303	0.1847	0.1130	0.0692	0.0424	0.0260	0.01597	0.00980
3.550	0.873	0.493	0.295	0.1793	0.1092	0.0666	0.0407	0.0248	0.01518	0.00927
3.650	0.856	0.483	0.288	0.1741	0.1057	0.0642	0.0390	0.0237	0.01444	0.00878
3.750	0.840	0.472	0.281	0.1692	0.1023	0.0619	0.0375	0.0227	0.01375	0.00833
3.850	0.825	0.462	0.274	0.1645	0.0990	0.0597	0.0360	0.0217	0.01310	0.00791
3.950	0.810	0.453	0.268	0.1600	0.0959	0.0576	0.0346	0.0208	0.01250	0.00751
4.050	0.795	0.443	0.261	0.1556	0.0930	0.0556	0.0333	0.01993	0.01193	0.00714
4.150	0.781	0.434	0.255	0.1514	0.0901	0.0537	0.0320	0.01910	0.01139	0.00680
4.250	0.766	0.425	0.249	0.1473	0.0874	0.0519	0.0308	0.01832	0.01089	0.00647
4.350	0.752	0.416	0.243	0.1433	0.0847	0.0501	0.0297	0.01757	0.01041	0.00616
4.450	0.738	0.408	0.237	0.1394	0.0821	0.0484	0.0286	0.01686	0.01000	0.00587
4.550	0.724	0.399	0.231	0.1356	0.0796	0.0468	0.0275	0.01618	0.00952	0.00560
4.650	0.710	0.390	0.226	0.1318	0.0772	0.0452	0.0265	0.01553	0.00910	0.00533
4.750	0.696	0.382	0.220	0.1281	0.0748	0.0437	0.0255	0.01490	0.00870	0.00508
4.850	0.682	0.373	0.214	0.1244	0.0724	0.0421	0.0245	0.01429	0.00832	0.00484
4.950	0.667	0.364	0.209	0.1208	0.0700	0.0406	0.0236	0.01370	0.00795	0.00461
5.050	0.652	0.355	0.203	0.1171	0.0677	0.0392	0.0227	0.01311	0.00759	0.00439
5.150	0.636	0.345	0.1970	0.1133	0.0653	0.0377	0.0217	0.01254	0.00724	0.00417

TABLE 11

Values of τ

$\mu =$

ν \ n	1	2	3	4	5	6	7	8	9	10
1.050	12.81	5.39	2.829	1.616	0.968	0.599	0.384	0.271	0.1769	
1.150	5.14	2.06	1.029	0.561	0.321	0.1886	0.1128	0.0661	0.0944	
1.250	3.24	1.247	0.599	0.314	0.1726	0.0978	0.0564	0.0327	0.01594	
1.350	2.35	0.857	0.406	0.205	0.1090	0.0596	0.0332	0.01874	0.01054	
1.450	1.840	0.664	0.298	0.1460	0.0749	0.0396	0.0213	0.01161	0.00637	0.00337
1.550	1.504	0.528	0.230	0.1092	0.0543	0.0277	0.01443	0.00760	0.00406	0.00216
1.650	1.267	0.433	0.1836	0.0846	0.0408	0.0202	0.01016	0.00517	0.00267	0.001378
1.750	1.092	0.364	0.1504	0.0673	0.0315	0.01511	0.00737	0.00363	0.001819	0.000907
1.850	0.957	0.312	0.1256	0.0547	0.0249	0.01157	0.00547	0.00261	0.001271	0.000613
1.950	0.850	0.271	0.1065	0.0452	0.0200	0.00902	0.00414	0.001916	0.000908	0.000424
2.050	0.763	0.238	0.0914	0.0378	0.01626	0.00715	0.00318	0.001430	0.000662	0.000299
2.150	0.691	0.212	0.0794	0.0320	0.01340	0.00573	0.00248	0.001083	0.000491	0.000216
2.250	0.630	0.1895	0.0695	0.0274	0.01117	0.00465	0.001958	0.000832	0.000371	0.000158
2.350	0.578	0.1708	0.0613	0.0236	0.00939	0.00381	0.001562	0.000646	0.000284	0.000118
2.450	0.534	0.1549	0.0545	0.0205	0.00795	0.00315	0.001258	0.000507	0.000221	0.000089
2.550	0.495	0.1412	0.0487	0.01790	0.00679	0.00262	0.001022	0.000401	0.000174	0.000069
2.650	0.460	0.1293	0.0437	0.01573	0.00583	0.00220	0.000836	0.000320	0.000139	0.000053
2.750	0.430	0.1189	0.0945	0.01390	0.00504	0.001855	0.000690	0.000258	0.000112	0.000042
2.850	0.403	0.1097	0.0357	0.01234	0.00438	0.001575	0.000572	0.000209	0.000092	0.000034
2.950	0.378	0.1016	0.0325	0.01100	0.00382	0.001345	0.000478	0.000171	0.000077	0.000028
3.050	0.356	0.0943	0.0297	0.00985	0.00335	0.001154	0.000401	0.000140	0.000065	0.000023
3.150	0.336	0.0877	0.0272	0.00885	0.00295	0.000995	0.000339	0.000116	0.000055	0.000019
3.250	0.317	0.0819	0.0249	0.00797	0.00261	0.000862	0.000287	0.000096	0.000048	0.000017
3.350	0.300	0.0766	0.0229	0.00721	0.00231	0.000749	0.000245	0.000080	0.000042	0.000015
3.450	0.285	0.0717	0.0212	0.00654	0.00206	0.000654	0.000210	0.000067	0.000037	0.000013
3.550	0.270	0.0673	0.0196	0.00594	0.001836	0.000573	0.000180	0.000057	0.000033	0.000011
3.650	0.257	0.0632	0.0181	0.00542	0.001645	0.000504	0.000155	0.000048	0.000030	0.000010
3.750	0.244	0.0595	0.0168	0.00495	0.001478	0.000445	0.000135	0.000041	0.000028	0.000010
3.850	0.235	0.0560	0.0156	0.00453	0.001331	0.000394	0.000117	0.000035	0.000026	0.000009
3.950	0.221	0.0528	0.0146	0.00416	0.001202	0.000350	0.000102	0.000030	0.000024	0.000008
4.050	0.211	0.0499	0.0136	0.00382	0.001088	0.000312	0.000090	0.000026	0.000023	0.000008
4.150	0.201	0.0471	0.0127	0.00352	0.000988	0.000279	0.000079	0.000022	0.000022	0.000008
4.250	0.1919	0.0445	0.0118	0.00325	0.000899	0.000250	0.000070	0.000019	0.000021	0.000007
4.350	0.1830	0.0421	0.0111	0.00300	0.000820	0.000225	0.000062	0.000017	0.000020	0.000006
4.450	0.1745	0.0398	0.0104	0.00278	0.000749	0.000203	0.000055	0.000015	0.000019	0.000006
4.550	0.1665	0.0377	0.00972	0.00257	0.000686	0.000183	0.000049	0.000013	0.000019	0.000006
4.650	0.1587	0.0357	0.00911	0.00239	0.000629	0.000166	0.000044	0.000011	0.000018	0.000005
4.750	0.1512	0.0337	0.00854	0.00222	0.000578	0.000151	0.000039	0.000010	0.000018	0.000005
4.850	0.1440	0.0319	0.00802	0.00206	0.000532	0.000137	0.000035	0.000009	0.000017	0.000005
4.950	0.1370	0.0302	0.00752	0.001917	0.000491	0.000126	0.000032	0.000008	0.000017	0.000004
5.050	0.1302	0.0285	0.00706	0.001785	0.000453	0.000115	0.000029	0.000007	0.000016	0.000004
5.150	0.1235	0.0269	0.00662	0.001662	0.000419	0.000105	0.000026	0.000006	0.000016	0.000004

TABLE 12

Values of λ_e

$\mu = 6$

ν	1	2	3	4	5	6	7	8	9	10
1.100	15.82	12.42	10.74	9.65	8.86	8.27	7.84	7.74		
1.150	7.69	5.92	5.01	4.41	3.97	3.61	3.31	2.96		
1.200	5.52	4.17	3.47	3.00	2.64	2.36	2.13	1.909	1.563	
1.300	4.45	3.31	2.70	2.29	1.985	1.740	1.538	1.364	1.204	
1.400	3.79	2.77	2.23	1.858	1.581	1.361	1.180	1.028	0.896	0.769
1.500	3.33	2.40	1.902	1.561	1.306	1.104	0.940	0.803	0.688	0.591
1.600	3.00	2.13	1.663	1.343	1.105	0.918	0.767	0.643	0.541	0.456
1.700	2.74	1.922	1.477	1.176	0.951	0.777	0.638	0.526	0.434	0.359
1.800	2.53	1.752	1.329	1.042	0.831	0.667	0.539	0.436	0.354	0.288
1.900	2.35	1.613	1.208	0.934	0.733	0.580	0.461	0.367	0.293	0.234
2.000	2.21	1.496	1.106	0.844	0.653	0.508	0.398	0.312	0.245	0.1920
2.100	2.08	1.395	1.019	0.767	0.585	0.449	0.346	0.267	0.206	0.1596
2.200	1.969	1.307	0.944	0.702	0.528	0.400	0.303	0.231	0.1757	0.1338
2.300	1.872	1.203	0.879	0.645	0.479	0.358	0.268	0.201	0.1507	0.1132
2.400	1.784	1.162	0.821	0.595	0.436	0.322	0.238	0.1758	0.1301	0.0964
2.500	1.705	1.100	0.769	0.551	0.399	0.291	0.212	0.1547	0.1130	0.0826
2.600	1.634	1.045	0.723	0.512	0.367	0.264	0.1899	0.1369	0.0987	0.0713
2.700	1.568	0.994	0.681	0.477	0.338	0.240	0.1708	0.1216	0.0867	0.0618
2.800	1.507	0.948	0.643	0.446	0.312	0.219	0.1541	0.1085	0.0764	0.0538
2.900	1.451	0.905	0.608	0.418	0.289	0.201	0.1396	0.0972	0.0677	0.0471
3.000	1.398	0.866	0.576	0.392	0.268	0.1843	0.1268	0.0873	0.0601	0.0414
3.100	1.349	0.829	0.547	0.368	0.250	0.1697	0.1155	0.0787	0.0536	0.0365
3.200	1.302	0.794	0.520	0.346	0.233	0.1565	0.1054	0.0711	0.0479	0.0323
3.300	1.258	0.762	0.494	0.327	0.217	0.1446	0.0965	0.0644	0.0430	0.0287
3.400	1.216	0.732	0.471	0.308	0.203	0.1339	0.0885	0.0585	0.0387	0.0256
3.500	1.177	0.703	0.448	0.291	0.1899	0.1241	0.0812	0.0532	0.0348	0.0228
3.600	1.138	0.675	0.427	0.275	0.1779	0.1153	0.0747	0.0485	0.0315	0.0204
3.700	1.101	0.649	0.408	0.260	0.1668	0.1071	0.0689	0.0443	0.0285	0.01832
3.800	1.066	0.624	0.389	0.246	0.1566	0.0997	0.0635	0.0405	0.0258	0.01646
3.900	1.031	0.600	0.371	0.233	0.1470	0.0928	0.0587	0.0371	0.0234	0.01482
4.000	0.998	0.577	0.355	0.221	0.1382	0.0865	0.0542	0.0340	0.0213	0.01336
4.100	0.965	0.555	0.339	0.209	0.1299	0.0807	0.0501	0.0312	0.01939	0.01206
4.200	0.933	0.534	0.323	0.1983	0.1221	0.0753	0.0464	0.0286	0.01767	0.01090
4.300	0.902	0.513	0.308	0.1878	0.1148	0.0702	0.0430	0.0263	0.01611	0.00986
4.400	0.871	0.492	0.294	0.1779	0.1079	0.0655	0.0398	0.0242	0.01469	0.00893
4.500	0.840	0.472	0.280	0.1863	0.1014	0.0611	0.0368	0.0222	0.01340	0.00809
4.600	0.809	0.452	0.267	0.1592	0.0952	0.0570	0.0341	0.0204	0.01223	0.00732
4.700	0.779	0.433	0.254	0.1504	0.0893	0.0531	0.0315	0.01876	0.01115	0.00663
4.800	0.748	0.414	0.241	0.1418	0.0837	0.0494	0.0292	0.01721	0.01017	0.00600
4.900	0.717	0.394	0.228	0.1335	0.0782	0.0459	0.0269	0.01578	0.00925	0.00543
5.000	0.685	0.375	0.216	0.1254	0.0730	0.0425	0.0248	0.01443	0.00841	0.00490
5.100	0.653	0.355	0.203	0.1174	0.0679	0.0393	0.0228	0.01317	0.00762	0.00441

$\mu = 7$ TABLE 13 Values of p

v \ n	1	2	3	4	5	6	7	8	9	10
1.125	0.0212	0.0452	0.0721	0.1024	0.1365	0.1748	0.218	0.267	0.321	0.383
1.225	0.0389	0.0866	0.1451	0.217	0.305	0.412	0.544	0.705	0.902	1.145
1.325	0.0572	0.1331	0.234	0.367	0.543	0.777	1.087	1.498	2.04	2.76
1.425	0.0762	0.1848	0.340	0.560	0.875	1.323	1.961	2.87	4.17	6.01
1.525	0.0958	0.242	0.465	0.805	1.324	2.112	3.32	5.16	7.97	12.24
1.625	0.1162	0.305	0.612	1.111	1.922	3.24	5.38	8.86	14.51	23.7
1.725	0.1374	0.375	0.783	1.489	2.71	4.81	8.43	14.67	25.5	44.0
1.825	0.1594	0.450	0.981	1.950	3.72	6.95	12.84	23.6	43.2	79.0
1.925	0.1822	0.533	1.209	2.51	5.01	9.83	19.10	37.0	71.3	137.5
2.025	0.206	0.623	1.468	3.18	6.64	13.66	27.9	56.6	114.9	233
2.125	0.231	0.721	1.763	3.98	8.68	18.68	39.9	85.1	181.0	385
2.225	0.257	0.827	2.10	4.92	11.21	25.2	56.3	125.6	280	623
2.325	0.283	0.942	2.47	6.04	14.32	33.6	78.3	182.4	424	987
2.425	0.311	1.067	2.90	7.34	18.11	44.2	107.6	261	634	1537
2.525	0.341	1.201	3.37	8.86	22.7	57.7	146.0	369	932	2350
2.625	0.371	1.346	3.91	10.62	28.3	74.6	196.1	515	1352	3550
2.725	0.404	1.503	4.50	12.66	34.9	95.5	261	711	1938	5280
2.825	0.437	1.672	5.16	15.02	42.9	121.5	344	971	2740	7750
2.925	0.472	1.854	5.90	17.72	52.3	153.4	449	1315	3850	11250
3.025	0.509	2.05	6.71	20.8	63.5	192.5	583	1764	5340	16140
3.125	0.548	2.26	7.62	24.4	76.7	240	751	2350	7330	22900
3.225	0.589	2.49	8.62	28.4	92.2	298	961	3010	10000	32200
3.325	0.633	2.74	9.73	33.0	110.3	367	1222	4060	13520	44900
3.425	0.678	3.00	10.96	38.2	131.6	451	1546	5300	18140	62100
3.525	0.727	3.29	12.32	44.1	156.3	552	1946	6860	24200	85200
3.625	0.778	3.60	13.82	50.9	185.2	672	2440	8830	32000	116100
3.725	0.832	3.93	15.48	58.5	219	815	3040	11320	42200	157100
3.825	0.890	4.29	17.31	67.1	258	986	3770	14430	55200	211100
3.925	0.951	4.69	19.34	76.9	303	1189	4670	18320	71900	282200
4.025	1.017	5.11	21.6	87.9	355	1429	5750	23200	93200	375000
4.125	1.087	5.57	24.1	100.4	415	1713	7070	29200	120300	496000
4.225	1.162	6.07	26.8	114.5	485	2050	8660	36600	155000	653000
4.325	1.243	6.62	29.9	130.4	565	2450	10580	45800	198000	856000
4.425	1.330	7.22	33.3	148.5	659	2920	12900	57100	253000	
4.525	1.424	7.87	37.0	169.0	766	3470	15690	71000	321000	
4.625	1.526	8.59	41.2	192.2	891	4120	19060	88200	408000	
4.725	1.637	9.37	45.9	219	1035	4890	23100	109200	516000	
4.825	1.759	10.24	51.2	249	1202	5800	28000	135000	652000	
4.925	1.892	11.21	57.1	283	1396	6880	33900	167000	822000	
5.025	2.04	12.28	63.7	322	1622	8150	41000	206000		
5.125	2.20	13.48	71.3	367	1885	9660	49500	254000		
5.225	2.38	14.82	79.8	419	2190	11460	59900	313000		
5.325	2.58	16.33	89.6	479	2560	13610	72500	386000		
5.425	2.81	18.05	100.7	549	2980	16180	87800	476000		
5.525	3.07	20.0	113.7	631	3490	19280	106500	589000		
5.625	3.36	22.3	128.7	727	4090	23000	129600	729000		
5.725	3.71	24.9	146.4	842	4820	27600	158100	905000		
5.825	4.11	28.0	167.4	979	5710	33200	193700			
5.925	4.58	31.7	192.6	1145	6790	40200	238500			
6.025	5.15	36.2	223	1350	8140	49100	295600			

$\mu = 7$ TABLE 14 Values of λ

ν	1	2	3	4	5	6	7	8	9	1
1.125	4.23	2.58	1.682	1.124	0.759	0.516	0.346			0.0911
1.225	2.99	1.806	1.172	0.778	0.523	0.353	0.239	0.1571		0.0692
1.325	2.43	1.460	0.942	0.622	0.415	0.279	0.1881	0.1262		0.0574
1.425	2.10	1.257	0.806	0.529	0.351	0.234	0.1570	0.1052	0.0686	0.0488
1.525	1.884	1.121	0.715	0.467	0.308	0.204	0.1358	0.0906	0.0633	0.0374
1.625	1.727	1.023	0.649	0.421	0.276	0.1816	0.1200	0.0795	0.0527	0.0347
1.725	1.607	0.947	0.598	0.385	0.251	0.1642	0.1078	0.0709	0.0467	0.0307
1.825	1.512	0.887	0.557	0.357	0.231	0.1501	0.0979	0.0639	0.0418	0.0274
1.925	1.434	0.837	0.523	0.333	0.214	0.1385	0.0897	0.0582	0.0378	0.0246
2.025	1.369	0.796	0.495	0.313	0.200	0.1286	0.0828	0.0533	0.0344	0.0222
2.125	1.313	0.760	0.470	0.296	0.1884	0.1202	0.0768	0.0492	0.0315	0.0202
2.225	1.265	0.729	0.449	0.281	0.1779	0.1128	0.0717	0.0456	0.0290	0.01849
2.325	1.222	0.702	0.430	0.268	0.1686	0.1063	0.0671	0.0424	0.0269	0.01700
2.425	1.184	0.678	0.413	0.256	0.1603	0.1005	0.0631	0.0397	0.0249	0.01569
2.525	1.150	0.656	0.398	0.246	0.1529	0.0953	0.0595	0.0372	0.0232	0.01454
2.625	1.120	0.636	0.384	0.236	0.1461	0.0906	0.0563	0.0350	0.0217	0.01352
2.725	1.092	0.618	0.372	0.227	0.1400	0.0863	0.0533	0.0330	0.0204	0.01260
2.825	1.066	0.601	0.360	0.219	0.1343	0.0824	0.0507	0.0311	0.01915	0.01178
2.925	1.042	0.586	0.350	0.212	0.1291	0.0789	0.0482	0.0295	0.01804	0.01104
3.025	1.020	0.571	0.340	0.205	0.1243	0.0756	0.0460	0.0280	0.01703	0.01037
3.125	1.000	0.558	0.330	0.1985	0.1199	0.0725	0.0439	0.0266	0.01611	0.00976
3.225	0.980	0.545	0.322	0.1925	0.1157	0.0697	0.0420	0.0253	0.01527	0.00921
3.325	0.961	0.533	0.313	0.1868	0.1118	0.0670	0.0402	0.0241	0.01449	0.00870
3.425	0.944	0.522	0.306	0.1815	0.1081	0.0645	0.0385	0.0230	0.01377	0.00823
3.525	0.927	0.511	0.298	0.1765	0.1047	0.0622	0.0370	0.0220	0.01310	0.00780
3.625	0.911	0.501	0.291	0.1716	0.1014	0.0600	0.0356	0.0210	0.01248	0.00740
3.725	0.896	0.492	0.285	0.1671	0.0984	0.0580	0.0342	0.0202	0.01191	0.00703
3.825	0.882	0.482	0.279	0.1628	0.0955	0.0560	0.0329	0.01935	0.01137	0.00668
3.925	0.868	0.473	0.272	0.1586	0.0927	0.0542	0.0317	0.01857	0.01087	0.00636
4.025	0.854	0.465	0.267	0.1547	0.0900	0.0525	0.0306	0.01783	0.01040	0.00606
4.125	0.841	0.456	0.261	0.1509	0.0875	0.0508	0.0295	0.01714	0.00996	0.00579
4.225	0.828	0.448	0.256	0.1473	0.0851	0.0492	0.0285	0.01649	0.00954	0.00553
4.325	0.816	0.440	0.250	0.1438	0.0828	0.0477	0.0275	0.01587	0.00915	0.00528
4.425	0.804	0.433	0.245	0.1404	0.0806	0.0463	0.0266	0.01528	0.00878	0.00505
4.525	0.792	0.425	0.240	0.1371	0.0784	0.0449	0.0257	0.01472	0.00843	0.00483
4.625	0.780	0.418	0.236	0.1340	0.0764	0.0436	0.0249	0.01419	0.00810	0.00463
4.725	0.769	0.411	0.231	0.1309	0.0744	0.0423	0.0241	0.01369	0.00779	0.00443
4.825	0.757	0.404	0.226	0.1279	0.0724	0.0411	0.0233	0.01320	0.00740	0.00425
4.925	0.746	0.397	0.222	0.1250	0.0706	0.0399	0.0225	0.01274	0.00720	0.00407
5.025	0.735	0.390	0.217	0.1221	0.0687	0.0387	0.0218	0.01229	0.00693	0.00391
5.125	0.724	0.383	0.213	0.1193	0.0670	0.0376	0.0211	0.01187	0.00667	0.00375
5.225	0.712	0.377	0.209	0.1166	0.0652	0.0365	0.0205	0.01146	0.00642	0.00360
5.325	0.701	0.370	0.204	0.1139	0.0635	0.0355	0.01981	0.01106	0.00618	0.00345
5.425	0.690	0.363	0.200	0.1112	0.0619	0.0344	0.01918	0.01068	0.00595	0.00331
5.525	0.678	0.356	0.1959	0.1085	0.0602	0.0334	0.01856	0.01031	0.00572	0.00318
5.625	0.667	0.350	0.1917	0.1059	0.0586	0.0324	0.01796	0.00995	0.00551	0.00305
5.725	0.655	0.343	0.1874	0.1033	0.0570	0.0315	0.01737	0.00959	0.00530	0.00293
5.825	0.643	0.336	0.1831	0.1006	0.0554	0.0305	0.01679	0.00925	0.00500	0.00281
5.925	0.630	0.328	0.1787	0.0980	0.0538	0.0295	0.01622	0.00891	0.00489	0.00269
6.025	0.617	0.321	0.1742	0.0953	0.0522	0.0286	0.01565	0.00857	0.00470	0.00257

$\mu = 7$ TABLE 15 Values of τ .

n / v	1	2	3	4	5	6	7	8	9	10
1.125	6.86	2.710	1.332	0.714	0.401	0.231	0.1329	0.1349	0.0332	0.0206
1.225	4.08	1.546	0.729	0.375	0.203	0.1126	0.0635	0.0340	0.01315	0.01034
1.325	2.89	1.059	0.482	0.239	0.1246	0.0668	0.0365	0.01989	0.0278	0.00620
1.425	2.23	0.792	0.349	0.1676	0.0843	0.0437	0.0230	0.01225	0.00609	0.00398
1.525	1.817	0.625	0.267	0.1243	0.0605	0.0303	0.01548	0.00800	0.00414	0.001747
1.625	1.525	0.511	0.212	0.0958	0.0452	0.0220	0.01084	0.00542	0.00272	0.001350
1.725	1.311	0.428	0.1731	0.0760	0.0348	0.01638	0.00783	0.00379	0.001848	0.000904
1.825	1.148	0.366	0.1442	0.0616	0.0274	0.01251	0.00580	0.00272	0.001285	0.000610
1.925	1.020	0.318	0.1221	0.0508	0.0220	0.00974	0.00438	0.001994	0.000914	0.000423
2.025	0.915	0.280	0.1048	0.0425	0.01789	0.00771	0.00337	0.001489	0.000663	0.000298
2.125	0.830	0.248	0.0909	0.0359	0.01475	0.00618	0.00262	0.001129	0.000489	0.000214
2.225	0.758	0.222	0.0797	0.0307	0.01228	0.00501	0.00207	0.000868	0.000366	0.000157
2.325	0.696	0.200	0.0703	0.0265	0.01033	0.00411	0.001652	0.000675	0.000278	0.000116
2.425	0.644	0.1820	0.0625	0.0230	0.00876	0.00340	0.001332	0.000532	0.000214	0.000088
2.525	0.598	0.1662	0.0560	0.0201	0.00748	0.00283	0.001083	0.000423	0.000167	0.000067
2.625	0.557	0.1524	0.0503	0.01170	0.00643	0.00238	0.000887	0.000339	0.000131	0.000053
2.725	0.522	0.1403	0.0454	0.01566	0.00556	0.00201	0.000733	0.000275	0.000104	0.000042
2.825	0.490	0.1297	0.0412	0.01392	0.00484	0.001708	0.000609	0.000224	0.000084	0.000033
2.925	0.461	0.1203	0.0375	0.01242	0.00423	0.001460	0.000509	0.000184	0.000068	0.000027
3.025	0.435	0.1120	0.0343	0.01113	0.00371	0.001255	0.000428	0.000153	0.000056	0.000022
3.125	0.412	0.1045	0.0315	0.01001	0.00327	0.001083	0.000362	0.000127	0.000046	0.000019
3.225	0.391	0.0977	0.0289	0.00904	0.00289	0.000939	0.000307	0.000107	0.000039	0.000016
3.325	0.371	0.0916	0.0267	0.00818	0.00257	0.000818	0.000262	0.000090	0.000033	0.000014
3.425	0.353	0.0860	0.0247	0.00743	0.00229	0.000715	0.000225	0.000077	0.000028	0.000012
3.525	0.336	0.0809	0.0228	0.00677	0.00205	0.000627	0.000193	0.000066	0.000024	0.000011
3.625	0.321	0.0763	0.0212	0.00618	0.001836	0.000552	0.000167	0.000057	0.000021	0.000010
3.725	0.306	0.0720	0.01973	0.00565	0.001651	0.000488	0.000145	0.000049	0.000018	0.000009
3.825	0.293	0.0681	0.01839	0.00518	0.001489	0.000432	0.000126	0.000043	0.000016	0.000008
3.925	0.280	0.0644	0.01717	0.00476	0.001345	0.000384	0.000110	0.000037	0.000015	0.000008
4.025	0.269	0.0610	0.01605	0.00439	0.001219	0.000342	0.000096	0.000033	0.000013	0.000007
4.125	0.257	0.0579	0.01503	0.00405	0.001107	0.000306	0.000085	0.000029	0.000012	0.000007
4.225	0.247	0.0550	0.01409	0.00374	0.001008	0.000274	0.000075	0.000026	0.000011	0.000006
4.325	0.237	0.0523	0.01323	0.00346	0.000919	0.000246	0.000066	0.000023	0.000010	0.000006
4.425	0.228	0.0497	0.01244	0.00321	0.000840	0.000221	0.000058	0.000021	0.000009	0.000006
4.525	0.219	0.0473	0.01170	0.00298	0.000769	0.000200	0.000052	0.000019	0.000009	0.000005
4.625	0.210	0.0451	0.01102	0.00277	0.000706	0.000180	0.000046	0.000018	0.000008	0.000005
4.725	0.202	0.0430	0.01039	0.00258	0.000649	0.000164	0.000041	0.000016	0.000008	0.000005
4.825	0.1944	0.0410	0.00980	0.00241	0.000597	0.000149	0.000037	0.000015	0.000008	0.000005
4.925	0.1869	0.0391	0.00926	0.00225	0.000551	0.000135	0.000033	0.000014	0.000007	0.000004
5.025	0.1798	0.0373	0.00875	0.00210	0.000509	0.000123	0.000030	0.000013	0.000007	0.000003
5.125	0.1729	0.0356	0.00827	0.001967	0.000471	0.000113	0.000027	0.000012	0.000006	0.000003
5.225	0.1662	0.0340	0.00783	0.001842	0.000436	0.000103	0.000024	0.000011	0.000005	0.000003
5.325	0.1598	0.0325	0.00741	0.001727	0.000405	0.000095	0.000022	0.000011	0.000005	0.000003
5.425	0.1536	0.0310	0.00702	0.001621	0.000376	0.000087	0.000020	0.000010	0.000004	0.000002
5.525	0.1476	0.0296	0.00665	0.001522	0.000350	0.000080	0.000018	0.000010	0.000004	0.000002
5.625	0.1417	0.0282	0.00630	0.001430	0.000326	0.000074	0.000017	0.000009	0.000003	0.000002
5.725	0.1359	0.0269	0.00597	0.001345	0.000304	0.000069	0.000015	0.000009	0.000003	0.000001
5.825	0.1303	0.0257	0.00565	0.001265	0.000284	0.000063	0.000014	0.000008	0.000002	0.000001
5.925	0.1248	0.0245	0.00535	0.001191	0.000265	0.000059	0.000013	0.000008	0.000002	0.000001
6.025	0.1194	0.0233	0.00507	0.001121	0.000248	0.000055	0.000012	0.000007	0.000002	0.000001

$\mu = 7$ TABLE 16 Values of λ_e

v \ n	1	2	3	4	5	6	7	8	9	10
1.125	9.22	7.13	6.07	5.37	4.85	4.43	4.00			2.33
1.225	6.30	4.78	3.99	3.47	3.07	2.76	2.48	2.15		1.643
1.325	4.98	3.72	3.05	2.60	2.26	1.990	1.764	1.556		1.222
1.425	4.20	3.09	2.49	2.08	1.781	1.540	1.340	1.168	0.986	0.916
1.525	3.68	2.66	2.11	1.741	1.461	1.241	1.061	0.910	0.780	0.614
1.625	3.30	2.35	1.840	1.492	1.232	1.028	0.863	0.727	0.613	0.514
1.725	3.01	2.12	1.632	1.303	1.059	0.868	0.716	0.592	0.491	0.408
1.825	2.77	1.928	1.467	1.154	0.923	0.744	0.603	0.491	0.400	0.326
1.925	2.58	1.774	1.332	1.033	0.814	0.646	0.515	0.412	0.330	0.265
2.025	2.42	1.645	1.219	0.933	0.724	0.566	0.444	0.350	0.275	0.217
2.125	2.29	1.535	1.124	0.848	0.649	0.500	0.387	0.300	0.232	0.1804
2.225	2.17	1.440	1.042	0.776	0.586	0.445	0.339	0.259	0.1977	0.1512
2.325	2.06	1.356	0.970	0.714	0.532	0.398	0.299	0.225	0.1696	0.1278
2.425	1.968	1.282	0.907	0.660	0.485	0.359	0.266	0.1973	0.1465	0.1089
2.525	1.884	1.216	0.851	0.612	0.444	0.324	0.237	0.1738	0.1274	0.0934
2.625	1.808	1.157	0.802	0.569	0.409	0.295	0.213	0.1539	0.1113	0.0806
2.725	1.739	1.103	0.756	0.532	0.377	0.269	0.1916	0.1369	0.0978	0.0700
2.825	1.675	1.054	0.716	0.498	0.349	0.246	0.1733	0.1223	0.0864	0.0610
2.925	1.617	1.009	0.679	0.467	0.324	0.225	0.1572	0.1097	0.0766	0.0535
3.025	1.562	0.967	0.644	0.439	0.301	0.207	0.1431	0.0988	0.0682	0.0471
3.125	1.511	0.928	0.613	0.413	0.281	0.1914	0.1306	0.0892	0.0609	0.0416
3.225	1.464	0.892	0.584	0.390	0.262	0.1770	0.1195	0.0808	0.0546	0.0369
3.325	1.419	0.859	0.557	0.369	0.246	0.1641	0.1097	0.0734	0.0491	0.0329
3.425	1.377	0.827	0.532	0.349	0.230	0.1523	0.1009	0.0668	0.0443	0.0294
3.525	1.336	0.798	0.509	0.331	0.216	0.1417	0.0930	0.0610	0.0400	0.0263
3.625	1.298	0.770	0.487	0.314	0.203	0.1321	0.0858	0.0558	0.0363	0.0236
3.725	1.262	0.743	0.467	0.298	0.1916	0.1233	0.0794	0.0512	0.0330	0.0213
3.825	1.227	0.718	0.448	0.284	0.1806	0.1152	0.0736	0.0470	0.0300	0.01918
3.925	1.194	0.694	0.429	0.270	0.1705	0.1078	0.0683	0.0432	0.0274	0.01734
4.025	1.161	0.671	0.412	0.257	0.1610	0.1010	0.0634	0.0398	0.0250	0.01572
4.125	1.130	0.649	0.396	0.245	0.1523	0.0947	0.0590	0.0368	0.0229	0.01427
4.225	1.100	0.628	0.380	0.234	0.1441	0.0890	0.0550	0.0340	0.0210	0.01298
4.325	1.071	0.608	0.366	0.223	0.1364	0.0836	0.0512	0.0314	0.01927	0.01182
4.425	1.043	0.588	0.352	0.213	0.1292	0.0786	0.0478	0.0291	0.01772	0.01079
4.525	1.015	0.570	0.338	0.203	0.1225	0.0740	0.0447	0.0270	0.01630	0.00985
4.625	0.988	0.551	0.325	0.1941	0.1162	0.0696	0.0418	0.0250	0.01502	0.00901
4.725	0.961	0.534	0.313	0.1854	0.1102	0.0656	0.0391	0.0233	0.01385	0.00825
4.825	0.935	0.516	0.301	0.1771	0.1046	0.0618	0.0365	0.0216	0.01278	0.00756
4.925	0.910	0.500	0.289	0.1692	0.0992	0.0583	0.0342	0.0201	0.01181	0.00694
5.025	0.884	0.483	0.278	0.1616	0.0942	0.0549	0.0320	0.01869	0.01091	0.00636
5.125	0.859	0.467	0.267	0.1543	0.0894	0.0518	0.0300	0.01740	0.01008	0.00585
5.225	0.834	0.451	0.257	0.1474	0.0848	0.0488	0.0281	0.01619	0.00933	0.00537
5.325	0.809	0.436	0.246	0.1406	0.0804	0.0460	0.0263	0.01507	0.00862	0.00494
5.425	0.785	0.420	0.236	0.1341	0.0762	0.0433	0.0246	0.01402	0.00798	0.00454
5.525	0.760	0.405	0.227	0.1278	0.0722	0.0408	0.0231	0.01304	0.00737	0.00417
5.625	0.735	0.390	0.217	0.1216	0.0683	0.0384	0.0216	0.01212	0.00681	0.00383
5.725	0.710	0.375	0.274	0.1156	0.0645	0.0361	0.0201	0.01126	0.00629	0.00352
5.825	0.684	0.360	0.1979	0.1097	0.0609	0.0338	0.01880	0.01044	0.00580	0.00322
5.925	0.658	0.344	0.1885	0.1039	0.0574	0.0317	0.01751	0.00967	0.00534	0.00295
6.025	0.631	0.329	0.1791	0.0982	0.0539	0.0296	0.01627	0.00894	0.00491	0.00270

TABLE 17

μ = 0

Values of p

v \ n	1	2	3	4	5	6	7	8	9	10
1.100	0.0144	0.0304	0.0479	0.0672	0.0884	0.1118	0.1374	0.166	0.1968	0.231
1.200	0.0294	0.0647	0.1079	0.1578	0.219	0.292	0.380	0.485	0.612	0.763
1.300	0.0447	0.1029	0.1786	0.277	0.405	0.571	0.787	1.068	1.434	1.908
1.400	0.0606	0.1454	0.264	0.431	0.663	0.989	1.446	2.09	2.98	4.23
1.500	0.0769	0.1923	0.365	0.625	1.014	1.599	2.48	3.79	5.76	8.72
1.600	0.0937	0.244	0.484	0.868	1.482	2.47	4.04	6.56	10.58	17.02
1.700	0.1111	0.300	0.621	1.167	2.10	3.67	6.36	10.91	18.66	31.8
1.800	0.1290	0.361	0.779	1.532	2.89	5.33	9.71	17.61	31.8	57.4
1.900	0.1475	0.428	0.960	1.972	3.90	7.55	14.49	27.7	52.7	100.4
2.000	0.1666	0.500	1.167	2.50	5.17	10.50	21.17	42.5	85.2	170.5
2.100	0.1864	0.578	1.400	3.13	6.75	14.37	30.4	63.9	134.5	283
2.200	0.207	0.662	1.663	3.87	8.71	19.38	42.8	94.4	208	458
2.300	0.228	0.753	1.959	4.73	11.17	25.8	59.6	137.2	316	727
2.400	0.250	0.850	2.29	5.75	14.04	34.0	81.7	196.4	472	1132
2.500	0.273	0.955	2.66	6.92	17.57	44.2	110.8	277	693	1734
2.600	0.296	1.067	3.07	8.28	21.8	57.0	148.6	387	1005	2610
2.700	0.321	1.187	3.53	9.84	26.9	72.9	197.2	533	1439	3880
2.800	0.346	1.315	4.03	11.63	32.9	92.5	259	726	2030	5700
2.900	0.373	1.453	4.59	13.67	40.0	116.4	338	981	2840	8250
3.000	0.400	1.600	5.20	16.00	48.4	145.6	437	1312	3940	11810
3.100	0.429	1.757	5.88	18.64	58.2	180.9	561	1740	5400	16730
3.200	0.458	1.925	6.62	21.6	69.7	224	716	2290	7330	23500
3.300	0.489	2.10	7.43	25.0	83.1	275	907	2990	9870	32600
3.400	0.522	2.30	8.33	28.8	98.6	336	1141	3880	13200	44900
3.500	0.556	2.50	9.31	33.1	116.5	408	1430	5000	17510	61300
3.600	0.591	2.72	10.38	38.0	137.2	495	1781	6410	23100	83100
3.700	0.628	2.95	11.55	43.3	161.0	596	2210	8170	30200	11180
3.800	0.667	3.20	12.83	49.4	188.4	717	2720	10350	39300	149500
3.900	0.707	3.47	14.22	56.2	220	858	3350	13050	50900	198500
4.000	0.750	3.75	15.75	63.8	256	1024	4100	16380	65500	262000
4.100	0.795	4.05	17.42	72.2	297	1218	4990	20500	83900	344000
4.200	0.842	4.38	19.23	81.6	364	1444	6070	25500	107000	449000
4.300	0.892	4.73	21.2	92.1	397	1708	7350	31600	135800	584000
4.400	0.944	5.10	23.4	103.8	458	2020	8870	39000	171700	755000
4.500	1.000	5.50	25.8	116.9	527	2370	10680	48000	216000	973000
4.600	1.059	5.93	28.3	131.4	606	2790	12820	59000	271000	
4.700	1.121	6.39	31.2	147.6	695	3270	15350	72200	339000	
4.800	1.188	6.89	34.3	165.6	796	3820	18350	88000	423000	
4.900	1.258	7.42	37.6	185.6	911	4460	21900	107200	525000	
5.000	1.333	8.00	41.3	208	1041	5210	26000	130200	651000	
5.100	1.414	8.62	45.4	233	1189	6070	30900	157800	805000	
5.200	1.500	9.30	49.9	261	1358	7060	36700	190900	993000	
5.300	1.593	10.03	54.8	292	1549	8210	43500	231000		
5.400	1.692	10.83	60.2	327	1766	9540	51500	278000		
5.500	1.800	11.70	66.2	366	2010	11070	60900	335000		
5.600	1.917	12.65	72.8	409	2290	12850	72000	403000		
5.700	2.04	13.69	80.1	459	2620	14910	85000	484000		
5.800	2.18	14.84	88.2	514	2980	17300	100400	582000		
5.900	2.33	16.10	97.3	577	3400	20100	118500	699000		
6.000	2.50	17.50	107.5	648	3890	23300	140000	840000		
6.100	2.68	19.06	118.9	728	4440	27100	165400			
6.200	2.89	20.8	131.8	820	5090	31600	195600			
6.300	3.12	22.8	146.5	926	5840	36800	232000			
6.400	3.38	25.0	163.2	1048	6710	42900	275000			
6.500	3.67	27.5	182.4	1189	7730	50300	327000			
6.600	4.00	30.4	205	1355	8940	59000	390000			
6.700	4.38	33.8	231	1549	10380	69600	466000			

TABLE 18 Values of λ

$\mu = .8$

ν \ n	1	2	3	4	5	6	7	8	9	10
1.100	4.98	2.98	1.902	1.244	0.822	0.546	0.356		0.1696	0.0808
1.200	3.28	1.947	1.237	0.804	0.528	0.349	0.229		0.1035	0.0488
1.300	2.61	1.537	0.971	0.627	0.410	0.269	0.1771	0.1105	0.0834	0.0420
1.400	2.30	1.308	0.821	0.527	0.342	0.224	0.1464	0.0949	0.0709	0.0365
1.500	1.985	1.159	0.724	0.462	0.298	0.1933	0.1258	0.0817	0.0444	0.0322
1.600	1.812	1.052	0.653	0.415	0.266	0.1713	0.1108	0.0718	0.0462	0.0295
1.700	1.681	0.972	0.600	0.379	0.241	0.1544	0.0992	0.0638	0.0411	0.0259
1.800	1.579	0.908	0.558	0.350	0.221	0.1409	0.0899	0.0575	0.0367	0.0234
1.900	1.495	0.856	0.523	0.326	0.205	0.1298	0.0823	0.0522	0.0332	0.0211
2.000	1.426	0.813	0.494	0.307	0.1917	0.1204	0.0758	0.0478	0.0302	0.01906
2.100	1.367	0.776	0.470	0.290	0.1801	0.1124	0.0703	0.0440	0.0276	0.01734
2.200	1.316	0.744	0.448	0.275	0.1699	0.1054	0.0655	0.0408	0.0254	0.01585
2.300	1.272	0.716	0.429	0.262	0.1610	0.0993	0.0614	0.0380	0.0235	0.01456
2.400	1.233	0.691	0.412	0.250	0.1531	0.0939	0.0577	0.0355	0.0218	0.01343
2.500	1.197	0.669	0.397	0.240	0.1459	0.0890	0.0544	0.0332	0.0203	0.01244
2.600	1.166	0.649	0.384	0.231	0.1395	0.0846	0.0514	0.0312	0.01901	0.01156
2.700	1.137	0.630	0.371	0.222	0.1337	0.0806	0.0487	0.0295	0.01782	0.01078
2.800	1.110	0.613	0.360	0.214	0.1283	0.0770	0.0463	0.0278	0.01675	0.01008
2.900	1.086	0.598	0.349	0.207	0.1234	0.0737	0.0441	0.0264	0.01578	0.00945
3.000	1.063	0.584	0.339	0.200	0.1188	0.0706	0.0420	0.0250	0.01490	0.00888
3.100	1.042	0.570	0.330	0.1941	0.1146	0.0678	0.0402	0.0238	0.01410	0.00836
3.200	1.023	0.558	0.322	0.1883	0.1107	0.0652	0.0384	0.0227	0.01336	0.00788
3.300	1.004	0.546	0.314	0.1829	0.1070	0.0627	0.0368	0.0216	0.01269	0.00745
3.400	0.987	0.535	0.306	0.1778	0.1036	0.0605	0.0353	0.0206	0.01206	0.00705
3.500	0.971	0.524	0.299	0.1730	0.1004	0.0583	0.0339	0.01974	0.01149	0.00669
3.600	0.955	0.514	0.293	0.1684	0.0973	0.0563	0.0326	0.01890	0.01095	0.00635
3.700	0.940	0.505	0.286	0.1641	0.0945	0.0544	0.0314	0.01812	0.01046	0.00604
3.800	0.926	0.496	0.280	0.1600	0.0917	0.0527	0.0303	0.01739	0.01000	0.00575
3.900	0.912	0.487	0.274	0.1561	0.0892	0.0510	0.0292	0.01670	0.00956	0.00548
4.000	0.899	0.479	0.269	0.1524	0.0867	0.0494	0.0282	0.01606	0.00916	0.00522
4.100	0.887	0.471	0.263	0.1489	0.0844	0.0479	0.0272	0.01545	0.00878	0.00499
4.200	0.874	0.463	0.258	0.1455	0.0822	0.0465	0.0263	0.01488	0.00842	0.00477
4.300	0.863	0.456	0.253	0.1422	0.0801	0.0451	0.0254	0.01434	0.00809	0.00456
4.400	0.851	0.449	0.249	0.1391	0.0780	0.0438	0.0246	0.01383	0.00777	0.00437
4.500	0.840	0.442	0.244	0.1361	0.0761	0.0426	0.0238	0.01335	0.00748	0.00419
4.600	0.829	0.435	0.240	0.1332	0.0742	0.0414	0.0231	0.01289	0.00719	0.00402
4.700	0.819	0.428	0.235	0.1304	0.0724	0.0403	0.0224	0.01245	0.00693	0.00385
4.800	0.808	0.422	0.231	0.1277	0.0707	0.0392	0.0217	0.01204	0.00668	0.00370
4.900	0.798	0.416	0.227	0.1250	0.0690	0.0381	0.0211	0.01164	0.00644	0.00356
5.000	0.788	0.410	0.223	0.1225	0.0674	0.0371	0.0204	0.01126	0.00621	0.00342
5.100	0.779	0.404	0.219	0.1200	0.0658	0.0361	0.01985	0.01090	0.00599	0.00329
5.200	0.769	0.398	0.215	0.1176	0.0643	0.0352	0.01928	0.01056	0.00578	0.00317
5.300	0.759	0.392	0.212	0.1153	0.0629	0.0343	0.01873	0.01023	0.00558	0.00305
5.400	0.750	0.386	0.208	0.1130	0.0614	0.0334	0.01820	0.00991	0.00539	0.00294
5.500	0.741	0.381	0.205	0.1108	0.0601	0.0326	0.01769	0.00960	0.00521	0.00283
5.600	0.731	0.375	0.201	0.1086	0.0587	0.0318	0.01719	0.00931	0.00504	0.00273
5.700	0.722	0.370	0.1976	0.1064	0.0574	0.0310	0.01672	0.00902	0.00487	0.00263
5.800	0.713	0.364	0.1942	0.1043	0.0561	0.0302	0.01625	0.00875	0.00471	0.00254
5.900	0.703	0.359	0.1908	0.1022	0.0548	0.0294	0.01580	0.00848	0.00456	0.00245
6.000	0.694	0.353	0.1875	0.1002	0.0536	0.0287	0.01537	0.00823	0.00441	0.00236
6.100	0.685	0.348	0.1842	0.0982	0.0524	0.0280	0.01494	0.00798	0.00426	0.00228
6.200	0.675	0.342	0.1808	0.0962	0.0520	0.0273	0.01452	0.00774	0.00412	0.00220
6.300	0.666	0.337	0.1775	0.0942	0.0500	0.0266	0.01412	0.00750	0.00399	0.00212
6.400	0.656	0.331	0.1742	0.0922	0.0488	0.0259	0.01372	0.00727	0.00385	0.00204
6.500	0.646	0.326	0.1709	0.0902	0.0477	0.0252	0.01332	0.00705	0.00373	0.001971
6.600	0.636	0.320	0.1675	0.0882	0.0465	0.0245	0.01294	0.00683	0.00360	0.001900
6.700	0.626	0.314	0.1641	0.0862	0.0454	0.0239	0.01256	0.00661	0.00348	0.001831

TABLE 19

μ =

Values of τ

β / α	1	2	3	4	5	6	7	8	9	10
1.100	9.24	3.61	1.756	0.930	0.516	0.294	0.1652	0.1937	0.0685	0.0247
1.200	5.07	1.897	0.883	0.482	0.238	0.1304	0.0711	0.0855	0.0288	0.00721
1.300	3.50	1.261	0.566	0.277	0.1419	0.0749	0.0401	0.01926	0.01949	0.00445
1.400	2.66	0.929	0.403	0.1905	0.0944	0.0481	0.0249	0.01272	0.01505	0.00277
1.500	2.14	0.726	0.305	0.1398	0.0670	0.0331	0.01659	0.00834	0.01667	0.001796
1.600	1.791	0.590	0.241	0.1071	0.0498	0.0238	0.01155	0.00567	0.00275	0.001325
1.700	1.535	0.493	0.1958	0.0845	0.0381	0.01764	0.00830	0.00395	0.001886	0.000859
1.800	1.341	0.420	0.1626	0.0683	0.0299	0.01343	0.00612	0.00283	0.001311	0.000605
1.900	1.189	0.364	0.1374	0.0562	0.0239	0.01043	0.00461	0.00207	0.000931	0.000422
2.000	1.067	0.320	0.1177	0.0469	0.01943	0.00824	0.00354	0.001540	0.000674	0.000298
2.100	0.967	0.284	0.1021	0.0396	0.01600	0.00660	0.00275	0.001166	0.000497	0.000214
2.200	0.883	0.254	0.0893	0.0339	0.01332	0.00535	0.00217	0.000895	0.000371	0.000156
2.300	0.812	0.229	0.0789	0.0292	0.01120	0.00438	0.001732	0.000696	0.000282	0.000116
2.400	0.751	0.208	0.0701	0.0254	0.00949	0.00362	0.001396	0.000548	0.000217	0.000088
2.500	0.698	0.1899	0.0627	0.0222	0.00811	0.00302	0.001135	0.000436	0.000169	0.000067
2.600	0.651	0.1743	0.0564	0.01952	0.00697	0.00253	0.000931	0.000350	0.000133	0.000052
2.700	0.610	0.1606	0.0510	0.01727	0.00603	0.00214	0.000769	0.000283	0.000106	0.000041
2.800	0.574	0.1486	0.0463	0.01535	0.00525	0.001823	0.000639	0.000231	0.000085	0.000033
2.900	0.541	0.1380	0.0422	0.01371	0.00459	0.001560	0.000535	0.000190	0.000069	0.000027
3.000	0.512	0.1285	0.0386	0.01230	0.00403	0.001341	0.000450	0.000158	0.000057	0.000022
3.100	0.485	0.1200	0.0354	0.01107	0.00356	0.001159	0.000381	0.000132	0.000047	0.000019
3.200	0.461	0.1124	0.0326	0.01000	0.00315	0.001006	0.000324	0.000111	0.000039	0.000016
3.300	0.438	0.1055	0.0301	0.00906	0.00280	0.000877	0.000277	0.000094	0.000033	0.000014
3.400	0.418	0.0992	0.0278	0.00824	0.00250	0.000767	0.000238	0.000080	0.000028	0.000012
3.500	0.399	0.0935	0.0258	0.00751	0.00234	0.000674	0.000205	0.000068	0.000024	0.000011
3.600	0.381	0.0883	0.0240	0.00686	0.00201	0.000594	0.000177	0.000059	0.000021	0.000010
3.700	0.365	0.0835	0.0224	0.00629	0.001805	0.000525	0.000154	0.000051	0.000018	0.000009
3.800	0.350	0.0791	0.0209	0.00577	0.001629	0.000465	0.000134	0.000044	0.000016	0.000008
3.900	0.336	0.0750	0.01951	0.00531	0.001474	0.000414	0.000117	0.000039	0.000015	0.000008
4.000	0.323	0.0712	0.01827	0.00489	0.001337	0.000369	0.000102	0.000034	0.000013	0.000007
4.100	0.310	0.0677	0.01714	0.00452	0.001215	0.000330	0.000090	0.000030	0.000012	0.000007
4.200	0.298	0.0645	0.01610	0.00418	0.001107	0.000296	0.000079	0.000027	0.000011	0.000006
4.300	0.287	0.0614	0.01514	0.00388	0.001010	0.000266	0.000070	0.000024	0.000010	0.000006
4.400	0.277	0.0586	0.01425	0.00360	0.000924	0.000239	0.000062	0.000022	0.000009	0.000006
4.500	0.267	0.0559	0.01344	0.00335	0.000846	0.000216	0.000055	0.000020	0.000009	0.000006
4.600	0.258	0.0534	0.01269	0.00312	0.000777	0.000195	0.000049	0.000018	0.000008	0.000006
4.700	0.249	0.0511	0.01199	0.00291	0.000714	0.000177	0.000044	0.000017	0.000008	0.000005
4.800	0.240	0.0489	0.01134	0.00271	0.000658	0.000161	0.000039	0.000015	0.000007	0.000005
4.900	0.232	0.0468	0.01073	0.00254	0.000607	0.000146	0.000035	0.000014	0.000007	0.000004
5.000	0.224	0.0448	0.01017	0.00237	0.000561	0.000133	0.000032	0.000013	0.000007	0.000004
5.100	0.217	0.0430	0.00965	0.00223	0.000519	0.000122	0.000028	0.000012	0.000007	0.000004
5.200	0.209	0.0412	0.00915	0.00209	0.000481	0.000111	0.000026	0.000012	0.000006	0.000004
5.300	0.203	0.0395	0.00869	0.001961	0.000446	0.000102	0.000023	0.000011	0.000006	0.000003
5.400	0.1959	0.0379	0.00826	0.001843	0.000415	0.000093	0.000021	0.000010	0.000006	0.000003
5.500	0.1895	0.0364	0.00786	0.001743	0.000386	0.000086	0.000019	0.000010	0.000006	0.000003
5.600	0.1834	0.0350	0.00748	0.001634	0.000359	0.000079	0.000017	0.000009	0.000005	0.000003
5.700	0.1774	0.0336	0.00712	0.001540	0.000335	0.000073	0.000016	0.000009	0.000005	0.000003
5.800	0.1716	0.0323	0.00678	0.001453	0.000313	0.000067	0.000014	0.000009	0.000005	0.000002
5.900	0.1660	0.0310	0.00646	0.001372	0.000293	0.000062	0.000013	0.000008	0.000005	0.000002
6.000	0.1605	0.0298	0.00616	0.001296	0.000274	0.000058	0.000012	0.000008	0.000004	0.000002
6.100	0.1552	0.0286	0.00587	0.001226	0.000257	0.000054	0.000011	0.000007	0.000004	0.000002
6.200	0.1500	0.0275	0.00560	0.001160	0.000241	0.000050	0.000010	0.000005	0.000003	0.000002
6.300	0.1449	0.0264	0.00535	0.001098	0.000226	0.000046	0.000009	0.000005	0.000003	0.000002
6.400	0.1400	0.0254	0.00510	0.001040	0.000213	0.000043	0.000008	0.000005	0.000003	0.000002
6.500	0.1351	0.0244	0.00487	0.000986	0.000200	0.000040	0.000008	0.000004	0.000003	0.000001
6.600	0.1303	0.0234	0.00464	0.000934	0.000188	0.000038	0.000007	0.000004	0.000003	0.000001
6.700	0.1256	0.0225	0.00443	0.000886	0.000177	0.000035	0.000007	0.000004	0.000002	0.000001

TABLE 20

$\mu = 8$

Values of λ_e

v \ n	1	2	3	4	5	6	7	8	9	10
1.100	11.24	8.74	7.47	6.64	6.03	5.53	4.93		4.11	2.45
1.200	7.17	5.47	4.59	4.00	3.56	3.20	2.85		2.25	1.429
1.300	5.54	4.15	3.42	2.92	2.55	2.26	2.00	1.659	1.617	1.168
1.400	4.62	3.40	2.76	2.32	1.989	1.726	1.507	1.298	1.214	0.935
1.500	4.02	2.91	2.32	1.921	1.620	1.381	1.185	1.015		0.745
1.600	3.59	2.57	2.01	1.639	1.359	1.138	0.959	0.811	0.681	0.605
1.700	3.26	2.30	1.780	1.427	1.163	0.958	0.793	0.659	0.548	0.447
1.800	3.00	2.09	1.597	1.261	1.012	0.819	0.667	0.545	0.445	0.363
1.900	2.79	1.923	1.448	1.127	0.891	0.710	0.568	0.456	0.367	0.295
2.000	2.62	1.782	1.325	1.017	0.792	0.621	0.490	0.387	0.306	0.243
2.100	2.47	1.663	1.221	0.924	0.710	0.549	0.426	0.331	0.258	0.201
2.200	2.34	1.560	1.131	0.846	0.640	0.488	0.373	0.286	0.219	0.1683
2.300	2.23	1.470	1.054	0.778	0.581	0.437	0.329	0.249	0.1879	0.1421
2.400	2.13	1.390	0.986	0.719	0.530	0.393	0.292	0.218	0.1622	0.1210
2.500	2.04	1.320	0.926	0.667	0.486	0.356	0.261	0.1917	0.1410	0.1037
2.600	1.961	1.256	0.872	0.621	0.447	0.323	0.234	0.1698	0.1232	0.0895
2.700	1.888	1.199	0.824	0.580	0.413	0.295	0.211	0.1511	0.1083	0.0777
2.800	1.821	1.147	0.780	0.543	0.382	0.270	0.1908	0.1351	0.0957	0.0678
2.900	1.760	1.099	0.740	0.510	0.355	0.248	0.1732	0.1212	0.0849	0.0594
3.000	1.703	1.055	0.704	0.480	0.331	0.228	0.1578	0.1092	0.0756	0.0524
3.100	1.650	1.014	0.671	0.453	0.309	0.211	0.1442	0.0987	0.0676	0.0463
3.200	1.601	0.976	0.640	0.428	0.289	0.1952	0.1321	0.0895	0.0607	0.0411
3.300	1.555	0.941	0.612	0.405	0.271	0.1811	0.1214	0.0814	0.0546	0.0366
3.400	1.511	0.908	0.585	0.384	0.254	0.1684	0.1118	0.0742	0.0493	0.0328
3.500	1.470	0.877	0.561	0.365	0.239	0.1570	0.1032	0.0679	0.0446	0.0294
3.600	1.431	0.848	0.538	0.347	0.225	0.1465	0.0954	0.0622	0.0405	0.0264
3.700	1.394	0.821	0.516	0.330	0.213	0.1370	0.0884	0.0571	0.0369	0.0238
3.800	1.359	0.795	0.496	0.315	0.201	0.1283	0.0821	0.0525	0.0336	0.0215
3.900	1.325	0.770	0.477	0.300	0.1899	0.1204	0.0763	0.0484	0.0308	0.01952
4.000	1.293	0.747	0.459	0.287	0.1799	0.1130	0.0711	0.0447	0.0282	0.01773
4.100	1.262	0.724	0.442	0.274	0.1705	0.1063	0.0663	0.0414	0.0258	0.01614
4.200	1.232	0.703	0.426	0.262	0.1618	0.1001	0.0619	0.0384	0.0238	0.01471
4.300	1.204	0.683	0.411	0.251	0.1537	0.0943	0.0579	0.0360	0.0219	0.01344
4.400	1.176	0.663	0.396	0.240	0.1461	0.0890	0.0542	0.0331	0.0202	0.01230
4.500	1.149	0.644	0.383	0.230	0.1390	0.0840	0.0508	0.0308	0.01862	0.01128
4.600	1.123	0.626	0.369	0.221	0.1323	0.0794	0.0477	0.0287	0.01722	0.01035
4.700	1.098	0.609	0.357	0.212	0.1261	0.0751	0.0448	0.0267	0.01595	0.00951
4.800	1.073	0.592	0.345	0.203	0.1202	0.0711	0.0421	0.0249	0.01478	0.00876
4.900	1.049	0.575	0.333	0.1951	0.1146	0.0674	0.0396	0.0233	0.01372	0.00807
5.000	1.025	0.560	0.322	0.1874	0.1093	0.0638	0.0330	0.0218	0.01274	0.00745
5.100	1.002	0.544	0.311	0.1800	0.1043	0.0605	0.0351	0.0204	0.01185	0.00688
5.200	0.980	0.529	0.301	0.1730	0.0996	0.0574	0.0331	0.01911	0.01102	0.00636
5.300	0.957	0.515	0.291	0.1662	0.0951	0.0545	0.0312	0.01790	0.01026	0.00588
5.400	0.936	0.501	0.281	0.1598	0.0909	0.0517	0.0295	0.01679	0.00957	0.00545
5.500	0.914	0.487	0.272	0.1536	0.0868	0.0491	0.0278	0.01575	0.00892	0.00505
5.600	0.893	0.473	0.263	0.1476	0.0830	0.0467	0.0263	0.01478	0.00832	0.00468
5.700	0.871	0.460	0.254	0.1418	0.0793	0.0443	0.0248	0.01388	0.00777	0.00435
5.800	0.850	0.447	0.246	0.1363	0.0757	0.0421	0.0234	0.01303	0.00725	0.00403
5.900	0.830	0.434	0.237	0.1309	0.0724	0.0400	0.0221	0.01224	0.00677	0.00375
6.000	0.809	0.421	0.229	0.1258	0.0691	0.0380	0.0209	0.01150	0.00633	0.00348
6.100	0.788	0.408	0.221	0.1207	0.0660	0.0361	0.01974	0.01080	0.00591	0.00323
6.200	0.767	0.396	0.213	0.1158	0.0630	0.0343	0.01864	0.01014	0.00552	0.00300
6.300	0.746	0.383	0.206	0.1111	0.0601	0.0325	0.01759	0.00952	0.00515	0.00279
6.400	0.725	0.371	0.1981	0.1064	0.0573	0.0308	0.01660	0.00893	0.00481	0.00259
6.500	0.704	0.359	0.1906	0.1019	0.0545	0.0292	0.01565	0.00838	0.00449	0.00241
6.600	0.683	0.346	0.1831	0.0974	0.0519	0.0277	0.01474	0.00785	0.00419	0.00223
6.700	0.661	0.334	0.1757	0.0930	0.0493	0.0261	0.01386	0.00735	0.00390	0.00207

APPENDICES

APPENDIX A

FLUID DYNAMIC MODEL

Experience has shown that useful results for the behavior of solids under high stress intensities can be obtained under the assumption of stress isotropy and thermodynamic equilibrium[9]. This is equivalent to assuming that the material behaves as an ideal compressible fluid. Such behavior in a blast absorber can be approximately insured by suitable selection of material. In this appendix, we indicate the character of the approximations involved in a fluid dynamic model of a non-linear solid.

Generally, one expects that a complete thermodynamic description of a material would involve a highly complex equation of state comprising a relation among many variables such as density, temperature, internal energy, stress, and deformation rate. Alternatively the stress is regarded as a function of a number of other state variables, thus defining a stress-deformation law involving variables in addition to density or strain. This would be the general "stress-strain" law, different approximations to which would be expected to hold in various applications. We can, however, discuss properties of the stress without regard to a general law, in order to define what is meant by a fluid dynamic approximation.

In Cartesian coordinates x_1, x_2, x_3 the stress condition at a point in a body is represented by the tensor σ_{ij}, a set of nine numbers ($i, j = 1, 2, 3$) which are the stress components:

$$\sigma_{ij} = \begin{pmatrix} \sigma_{11} & \sigma_{12} & \sigma_{13} \\ \sigma_{21} & \sigma_{22} & \sigma_{23} \\ \sigma_{31} & \sigma_{32} & \sigma_{33} \end{pmatrix}.$$

The components are interpreted as tensile and shear forces per unit area acting on the sides of an infinitesimal cubical element. Thus σ_{12} is the force in the x_2 - direction per unit area acting on a plane whose normal is in the positive x_1 - direction. The stress tensor can be shown to have the symmetry property $\sigma_{ij} = \sigma_{ji}$; thus there are in general only six independent stress components.

We can separate the stress tensor into so-called isotropic and deviatoric parts by writing

$$\sigma_{ij} = - P \delta_{ij} + \sigma'_{ij} ,$$

where δ_{ij} is the Kronecker delta, and the mean normal pressure P is defined by $P = - \sigma_{kk}/3$. Here the repeated subscript indicates summation over the values 1, 2, 3 of the index, and P is therefore the negative average normal stress.[14]

A hydrostatic state of stress in any material is by definition such that all components of the stress deviator σ'_{ij} vanish; in such a case $\sigma_{11} = \sigma_{22} = \sigma_{33} = P$, and P is simply referred to as the hydrostatic pressure. We are interested in materials which behave so that, as the magnitude of a general stress state is increased, the magnitude of the stress deviator becomes and remains small compared to the mean normal pressure. Then the state of stress at sufficiently high stress magnitudes becomes nearly hydrostatic. The stress magnitude is evaluated in terms of the scalar invariant $\sigma_{ij} \sigma_{ji}$:

$$\sigma_{ij}\sigma_{ji} = 3 P^2 + \sigma'_{ij}\sigma'_{ji} ,$$

since by definition $\sigma'_{kk} = 0$. This invariant of σ_{ij} is therefore the sum

of the invariants of the isotropic and deviatoric parts of σ_{ij}. For a linear elastic material, $\sigma'_{ij}\sigma'_{ji}$ can be shown to be proportional to the energy of distortion or change of shape of the material[15]. An approximately isotropic state of stress is defined by $\sigma'_{ij}\,\sigma'_{ji} \ll 3P^2$.

In many applications, one is interested in material behavior in a state of uniaxial strain such as one-dimensional fully confined compression in, say, the x_1 - direction. For example, the uniaxial strain condition is approached at large distances from a point-source explosion. Referred to principal axes of deformation, the (symmetric) strain tensor ϵ_{ij} is such that $\epsilon_{11} \neq 0$ while all other components $\epsilon_{ij} = 0$. Then by symmetry $\sigma_{22} = \sigma_{33}$, and $\sigma_{ij} = 0$ for $i \neq j$. For this case

$$\sigma'_{ij}\sigma'_{ji} = \frac{2}{3}\,(\sigma_{22} - \sigma_{11})^2.$$

Now it is easily shown[3] that $(\sigma_{22} - \sigma_{11})$ is twice the maximum shear stress in the material for this stress state. If the shear stress is limited by some maximum value $\bar{\sigma}$, a property of the material, then $\sigma'_{ij}\sigma'_{ji} = 8\bar{\sigma}^2/3$ for sufficiently high σ_{11}. The mean normal pressure for this case is

$$P = -\frac{1}{3}\,(\sigma_{11} + 2\,\sigma_{22}) = -\sigma_{11} - \frac{2}{3}\,(\sigma_{22} - \sigma_{11}),$$

and $P = -\sigma_{11} - 4\bar{\sigma}/3$ when the maximum shear stress is reached. Therefore $P \cong -\sigma_{11}$ for sufficiently high compressions, and the state of stress becomes nearly hydrostatic.

Unfortunately, both $\bar{\sigma}$ and P are likely to be rate-dependent quantities. For easily crushable solids it is plausible to assume that the rate dependence of $\bar{\sigma}$ is not serious. In order to make possible the formulation of an ideal fluid-type equation of state applicable at high stress magnitudes, it is also necessary to assume that the rate dependence of P

is embodied solely in changes of, say, temperature and internal energy, and to discard any explicit dependence of P on rate of strain. To illustrate this point, consider a stress-strain-strain rate relation of the following type:

$$\sigma_{ij} - (\sigma_{ij})_o = \lambda \epsilon_{kk} \delta_{ij} + 2 \mu \epsilon_{ij} + \lambda' \dot{\epsilon}_{kk} \delta_{ij} + 2 \mu' \dot{\epsilon}_{ij} \quad \text{(A-1)}$$

where the strain rate tensor $\dot{\epsilon}_{ij}$ is defined by

$$\dot{\epsilon}_{ij} = \frac{1}{2} (u_{i,j} + u_{j,i}),$$

u_i being the velocity vector. The subscript zero indicates a reference state of rest at zero strain. Subscripts following a comma denote partial differentiation with respect to the indicated coordinate, and the overhead dot denotes total differentiation with respect to time following the motion. The natural strain ϵ_{ij}, so defined in terms of its derivative following the motion, is not restricted to infinitesimal values. For the moment, the four quantitites λ, μ, λ', μ' are assumed to be constant properties of the material. Equation (A-1) above represents the simplest possible such relation for an isotropic material, since the strain and strain-rate dependencies are linear and additive. For infinitesimal strains in the absence of rate effects, λ and μ would be the Lame constants for an isotropic elastic solid. If the material were an ideal fluid which cannot support shear stress statically, $\lambda \epsilon_{kk} \delta_{ij} + 2 \mu \epsilon_{ij} = - (P - P_o) \delta_{ij}$ necessarily, and λ' and μ' would be the viscosity coefficients for a Newtonian fluid. Equation (A-1) may be interpreted as a possible approximate relation describing a material at stress levels and loading rates somewhat greater than those at which a rate-independent linear law would apply. The mean normal pressure for this case is

$$P - P_o = -\frac{1}{3}\left[\sigma_{kk} - (\sigma_{kk})_o\right] = -(\lambda + \frac{2}{3}\mu)\,\epsilon_{kk} - (\lambda' + \frac{2}{3}\mu')\,\dot{\epsilon}_{kk} \,. \quad (A\text{-}2)$$

From kinematic (continuity) considerations alone, it can be shown that $\dot{\epsilon}_{kk} = -\dot{\rho}/\rho$ and $\epsilon_{kk} = -\ln(\rho/\rho_o)$, where ρ is the mass density. Equation (A-2) thus represents a relation among pressure, density, and rate of change of density. Now, to discard the explicit rate of dependence of P at this point would be equivalent to the assumption $\lambda' + \frac{2}{3}\mu' = 0$; however, P can still be considered as implicitly rate-dependent if λ and μ are allowed to be functions of state (e.g., of temperature and internal energy) rather than constants. This is exactly analogous to the Stokes hypothesis, which assumes that $\lambda' + \frac{2}{3}\mu' = 0$ for an ideal fluid; only under this condition can the thermodynamic pressure in a moving fluid be identified with the thermostatic pressure, i.e., that which obtains when the same state is reached quasi-statically. Assumptions of this general nature are implicit in the characterization of a solid at high pressures by a fluid equation of state.

To recapitulate, the approximations involved in a fluid dynamic model of a solid at high pressures are

1. The stress tensor is nearly isotropic; that is, the magnitude of the stress deviator is small compared to the square of the mean normal pressure.

2. States of the material under consideration are states of thermodynamic equilibrium; the thermodynamic pressure is identified with the pressure when the same state is reached quasi-statically.

Returning to the case of confined compression (uniaxial strain) discussed earlier, consider a change of state of the material by, say, an

adiabatic process. Assume that, at stress conditions such that $\sigma_{22} - \sigma_{11} < 2\bar{\sigma}$, strains are small and the material is linearly elastic and rate-independent. Given a reference state of low hydrostatic stress $(\sigma_{ij})_o = -P_o \delta_{ij}$, the stress-strain relations at low stress magnitudes are

$$\sigma_{ij} + P_o \delta_{ij} = \lambda \epsilon_{kk} \delta_{ij} + 2\mu \epsilon_{ij} ,$$

and $\epsilon_{kk} = \epsilon_{11} \cong -(\rho - \rho_o)/\rho_o$. Denote conditions when $\sigma_{22} - \sigma_{11} = 2\bar{\sigma}$ by the subscript 1. It is readily verified that the isotropic, longitudinal and transverse normal stress components at this point are given by

$$P_1 - P_o = \left(\frac{\lambda}{\mu} + \frac{2}{3}\right)\bar{\sigma} ,$$

$$(-\sigma_{11})_1 - P_o = \left(\frac{\lambda}{\mu} + 2\right)\bar{\sigma} ,$$

$$(-\sigma_{22})_1 - P_o = \frac{\lambda}{\mu}\,\bar{\sigma} ,$$

and the density is given approximately by

$$\rho_1 = \rho_o \left(1 + \frac{\bar{\sigma}}{\mu}\right) .$$

The linear stress-density relations up to this point are shown schematically in Fig. A-1. The absolute maximum normal stress at state 1 thus differs from the mean normal pressure by the amount $4\bar{\sigma}/3$. Now for higher compressions the maximum stress difference is assumed to have at most the value $2\bar{\sigma}$. In materials such as metals it has been conjectured[11] that the rigidity modulus actually decreases; this is certainly plausible in the case of easily crushable porous solids. In such a case the absolute maximum normal stress and the mean normal pressure approach each other at high compressions as sketched in Fig. A-1; in addition, there must be a cusp in

the $-\sigma_{11}$ curve. In normal shock impingement experiments on crushable solids in a shock tube[16], the axial normal stress component in the solid is equal to the pressure measured in the gas upstream of the specimen, and a cusp is indeed observed in the curve of stress-density states reached by shock in the solid.

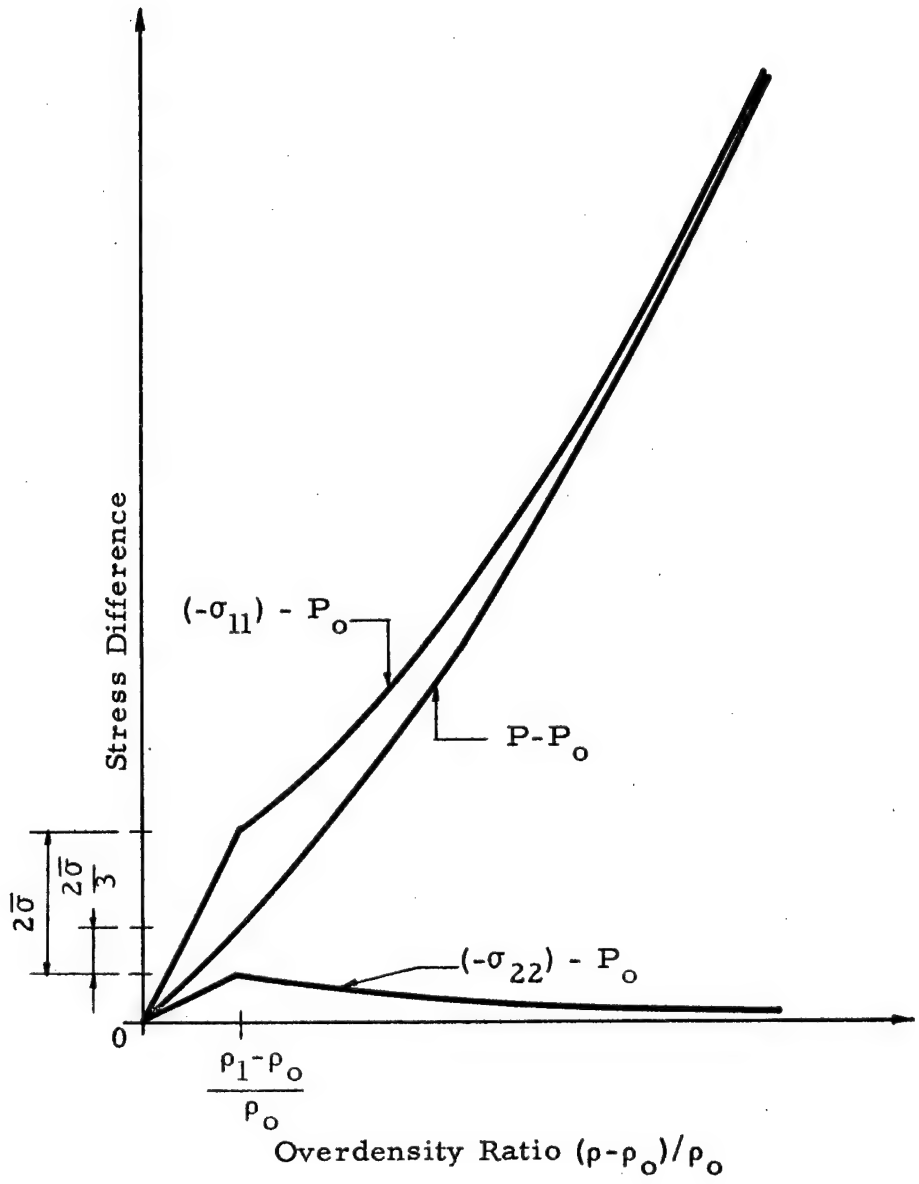

Fig. A-1 ASSUMED BEHAVIOR OF SOLID IN CONFINED COMPRESSION

APPENDIX B

WASTE HEAT CALCULATION

The approximate theory of explosion growth described in this report requires a simple method of estimating the so-called waste heat in shock. To do this, it is assumed that we are dealing with condensed matter whose thermal equation of state is approximated by the form $P = f(V)$, where P is absolute pressure and V is specific volume; a third variable, such as the absolute temperature T, is absent. The assumption is a reasonable one for pure solids and liquids in the absence of phase changes.

The constant-pressure and constant-volume specific heats (c_p and c_v) of typical condensed matter are very nearly equal. The difference of specific heats of any pure substance is given by

$$c_p - c_v = T \left(\frac{\partial P}{\partial T}\right)_V \left(\frac{\partial V}{\partial T}\right)_P .$$

If $c_p - c_v = 0$, then either $(\partial P/\partial T)_V = 0$ or $(\partial V/\partial T)_P = 0$; both cases lead to the result that the equation of state of the material is of the form $P = f(V)$. By use of the identity

$$\left(\frac{\partial P}{\partial T}\right)_V = - \left(\frac{\partial P}{\partial V}\right)_T \left(\frac{\partial V}{\partial T}\right)_P ,$$

we can write

$$c_p - c_v = - T \left(\frac{\partial P}{\partial V}\right)_T \left(\frac{\partial V}{\partial T}\right)_P^2 = VTG\beta^2 ,$$

where G and β are respectively the isothermal bulk modulus and isobaric volume expansivity of the substance. For water at standard conditions, for example, we have $G = 2.1 \times 10^{10}$ dynes/cm^2, $\beta = 2.1 \times 10^{-4}$°K^{-1},

$V = 1.0\ cm^3/gm$, $T = 20°C = 293°K$, and $c_p = 1.0$ cal/gm-°K. Hence $c_p - c_v = 0.0065$ cal/gm-°K, and the equation of state of water in the absence of phase changes is approximately of the form $P = f(V)$.

An equation of state of the form $P = f(V)$ implies that all states which the material can attain lie on a single curve in the P-V plane (Fig. B-1). In the present approximate theory, the Hugoniot is assumed to be given by the form

$$\frac{P-P_o}{C} = \frac{\left(\frac{V_o}{V}\right)^n - 1}{\mu - \frac{V_o}{V}}, \qquad \text{(B-1)}$$

where C, μ, and n are empirical constants to be determined by fitting to experimental shock compressibility data[11]. The initial pressure P_o was neglected in comparison to the pressures of interest. If the equation of state is of the form $P = f(V)$, then Eq. (B-1), in addition to being the locus of states which can be attained by shock from the initial state (P_o, V_o), is also the equation of any process involving pressure and volume changes. After passage of a shock pressure P, a particle of material expands nearly adiabatically to the initial pressure P_o, the path of expansion necessarily coinciding with the Hugoniot in the P-V plane.

It is pertinent to explore the implications of these assumptions. From thermodynamics, we have the reciprocity relation for any pure substance.

$$\left(\frac{\partial E}{\partial V}\right)_T = T\left(\frac{\partial P}{\partial T}\right)_V - P,$$

where E is specific internal energy. Hence for this case

$$\left(\frac{\partial E}{\partial V}\right)_T = -f(V).$$

From the definition of the constant-volume specific heat

$$\left(\frac{\partial E}{\partial T}\right)_V = c_v ,$$

but for this case $c_p = c_v = c$. Since E is a state variable and therefore its total differential is exact, we must have

$$\left(\frac{\partial c}{\partial V}\right)_T = -\left(\frac{\partial f}{\partial T}\right)_V = 0;$$

thus c is at most a function of temperature only.

We therefore write the total differential

$$dE = c(T)\, dT - f(V)\, dV. \tag{B-2}$$

Assuming c = constant, integration gives

$$E - E_o = c(T - T_o) + F(V), \tag{B-3}$$

where we define

$$F(V) = \int_V^{V_o} f(V)\, dV ,$$

and the subscript zero denotes conditions at the state (P_o, V_o). Evidently the internal energy consists of additive thermal energy and deformation (or strain) energy fractions.

By combination of the conservation laws for mass, momentum, and energy flux through a shock, one obtains

$$E - E_o = \frac{1}{2}\,(P + P_o)(V_o - V). \tag{B-4}$$

Thus the specific internal energy jump in shock is represented by the trapezoid below the chord of the Hugoniot in Fig. B-1. The fraction of specific internal energy which is recovered mechanically as expansion work in the

adiabatic expansion to (P_o, V_o) is precisely $F(V)$; the lens-shaped area between the Hugoniot and its chord is therefore unrecovered specific internal energy, equal to $c(T - T_o)$. This "waste heat" is evidenced as a residual temperature rise in the material. Eventually the temperature gradients are equalized by heat transfer processes at constant pressure, and none of the shock-induced thermal energy is mechanically recoverable.

If the equation of state of the material is of the form $P = f(V)$ and the Hugoniot is given by Eq. (B-1), then Eq. (B-1) is evidently also the thermal equation of state of the material. Equation (B-3) is the corresponding caloric equation of state. Writing the first law of thermodynamics for any reversible process, we have

$$TdS = dE + PdV = c(T)\, dT + \left[P - f(V)\right] dV,$$

where S is specific entropy and Eq. (B-2) has been used. Thus

$$dS = c(T)\, \frac{dT}{T},$$

and entropy is a function of temperature only. Assuming c = constant and integrating,

$$S - S_o = c \ln \left(\frac{T}{T_o}\right). \qquad \text{(B-5)}$$

We can also write the canonical equation of state $E = E(V, S)$ by substitution into Eq. (B-3):

$$E - E_o = cT_o \left[\exp\left(\frac{S - S_o}{c}\right) - 1\right] + F(V). \qquad \text{(B-6)}$$

The state surface (P-V-T surface) for the class of condensed matter having a thermal equation of state of the form $P = f(V)$ is therefore a ruled surface with generators parallel to the T-axis. Such a surface is shown in Fig. B-2. The temperature scale can also be regarded as a non-linear

entropy scale in view of Eq. (B-5). If the material is raised from the state (P_o, V_o, T_o) to the state (P_s, V_s, T_s) by a shock process, the temperature difference $(T_s - T_o)$ is given by QV_o/c, where QV_o denotes the lens-shaped area between the Hugoniot and its chord. The adiabatic (isentropic) expansion following shock is also isothermal in view of Eq. (B-5). As the state point moves to (P_o, V_o, T_s) in the adiabatic expansion, a unit mass of the material performs on its surroundings an amount of mechanical work equal to $F(V_s)$. No work is done in the constant-pressure (and hence constant-volume) process through which the material returns to its initial state.

It may be concluded that the lens-shaped area between the Hugoniot and its chord furnishes an estimate of the energy made mechanically unavailable by the shock process; the estimate is accurate to the extent that phase changes are absent and the ratio of specific heats for the condensed matter considered is close to unity.

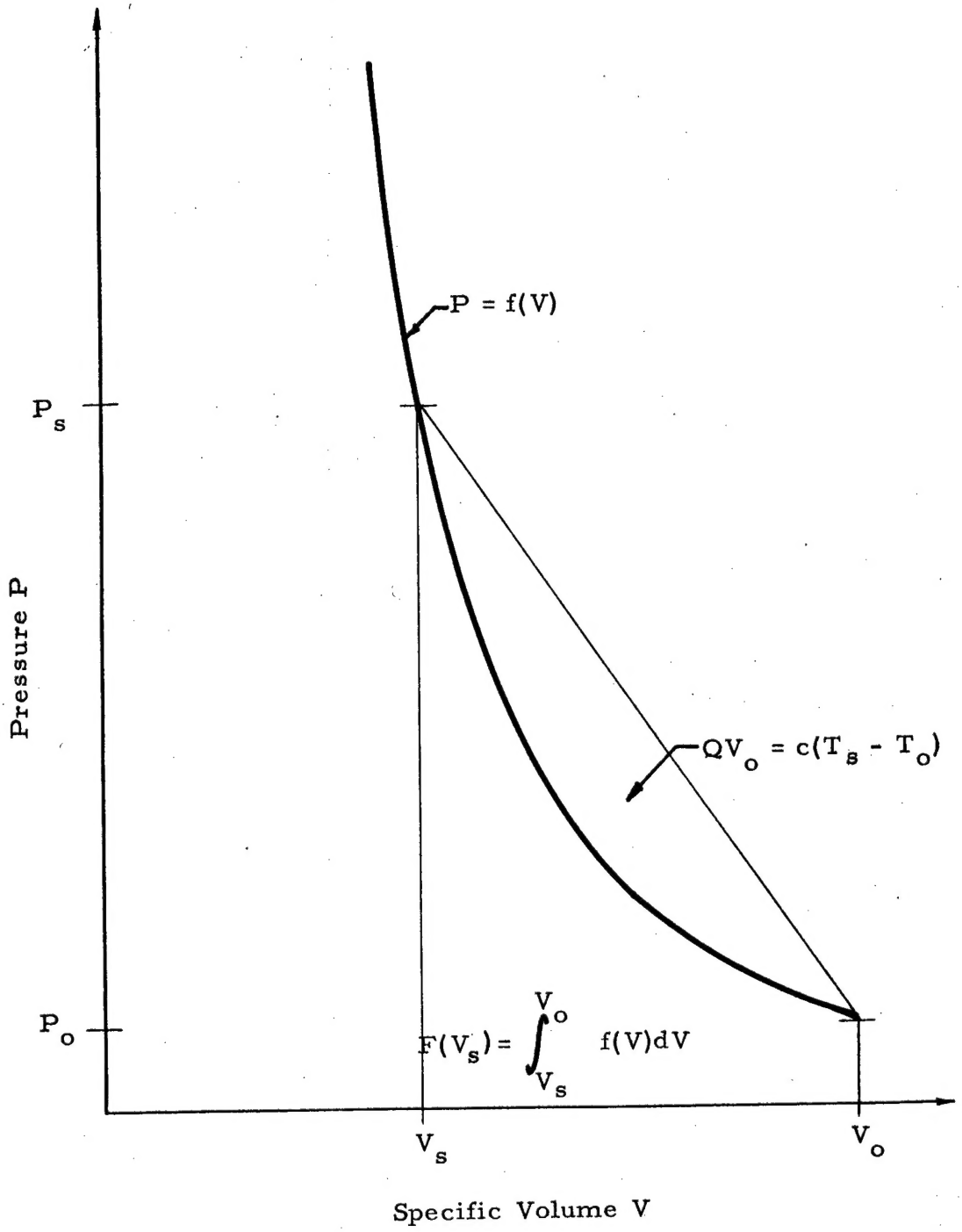

Fig. B-1 PRESSURE-VOLUME RELATIONS IN CONDENSED MATTER

entropy scale in view of Eq. (B-5). If the material is raised from the state (P_o, V_o, T_o) to the state (P_s, V_s, T_s) by a shock process, the temperature difference $(T_s - T_o)$ is given by QV_o/c, where QV_o denotes the lens-shaped area between the Hugoniot and its chord. The adiabatic (isentropic) expansion following shock is also isothermal in view of Eq. (B-5). As the state point moves to (P_o, V_o, T_s) in the adiabatic expansion, a unit mass of the material performs on its surroundings an amount of mechanical work equal to $F(V_s)$. No work is done in the constant-pressure (and hence constant-volume) process through which the material returns to its initial state.

It may be concluded that the lens-shaped area between the Hugoniot and its chord furnishes an estimate of the energy made mechanically unavailable by the shock process; the estimate is accurate to the extent that phase changes are absent and the ratio of specific heats for the condensed matter considered is close to unity.

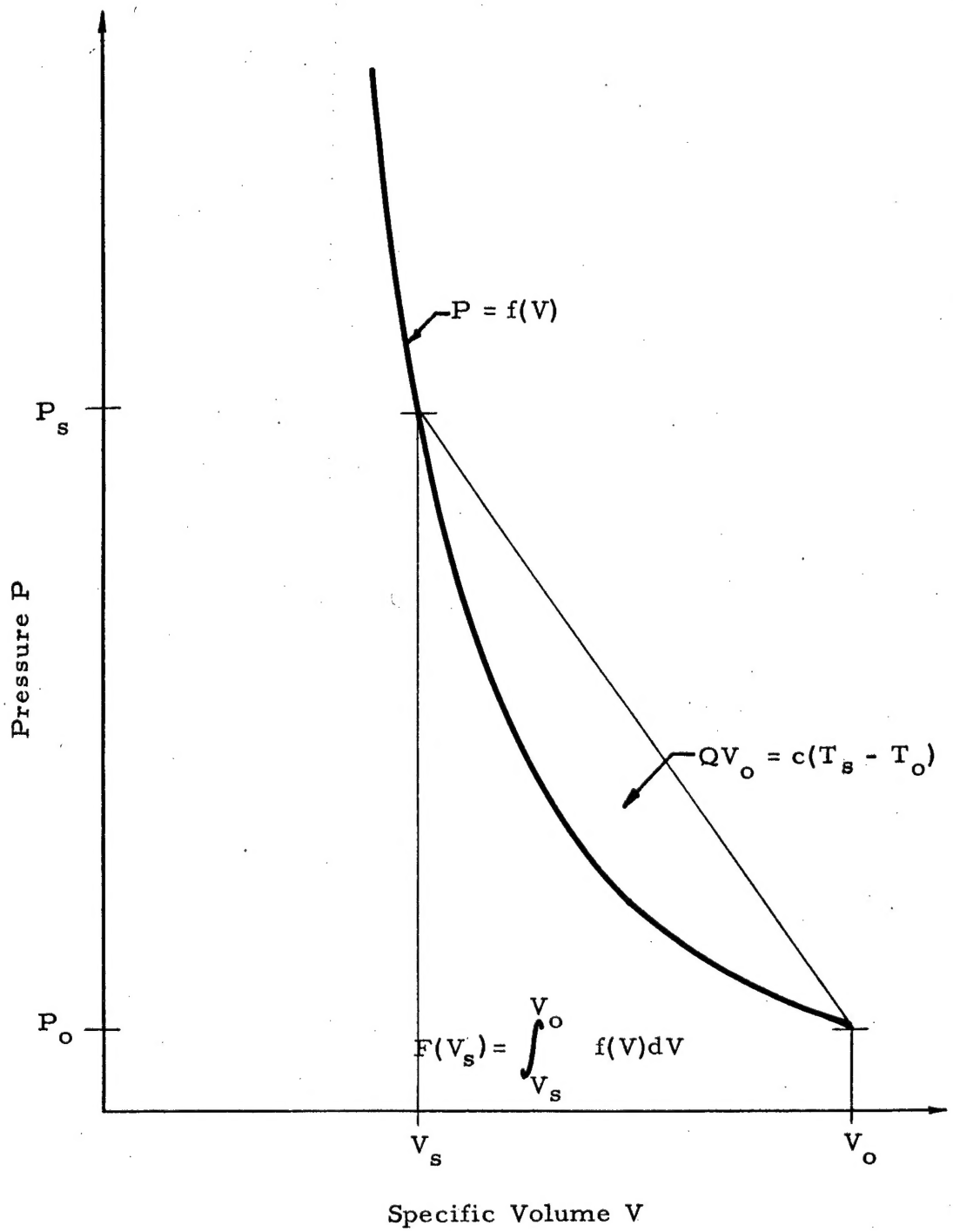

Fig. B-1 PRESSURE-VOLUME RELATIONS IN CONDENSED MATTER

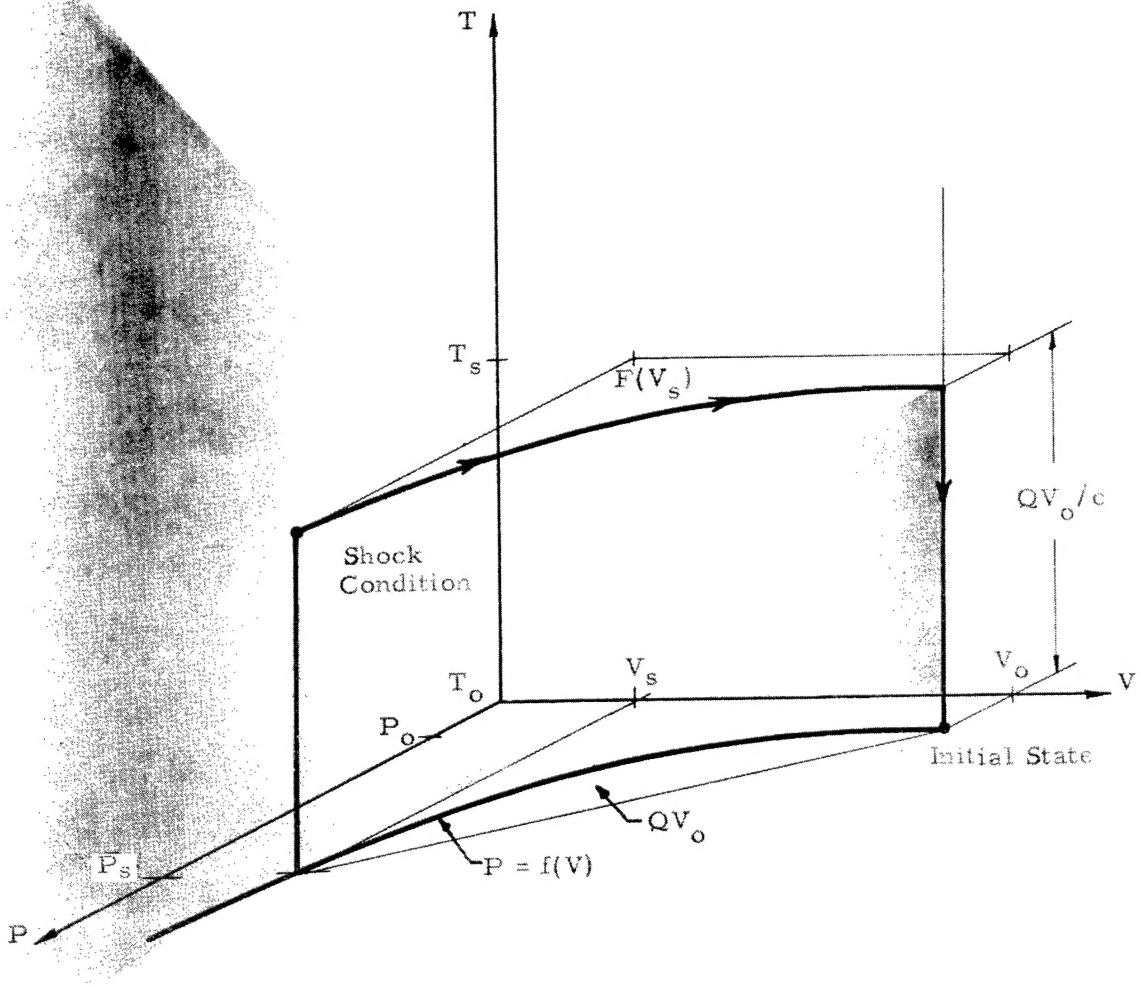

Fig. B-2 P-V-T SURFACE AND SHOCK COMPRESSION-EXPANSION CYCLE